INVESTIGATION OF SEISMIC ISOLATED STRUCTURES WITH ADDITIONAL ENERGY DISSIPATION DEVICES AT ISOLATION LEVEL

SİSMİK İZOLASYONLU YAPILARIN YALITIM KATINDA İLAVE ENERJİ SÖNÜMLEYİCİ CİHAZLAR İLE İNCELENMESİ

AHMET DEMİRHAN SEVER

ASSOC. PROF. DR ALPER ALDEMİR

Supervisor

PROF. DR UĞURHAN AKYÜZ

Co-Supervisor

Submitted to

Graduate School of Science and Engineering of Hacettepe University

as a Partial Fulfillment to the Requirements

for the Award of the Degree of Master of Science

in Civil Engineering

2024

ABSTRACT

INVESTIGATION OF SEISMIC ISOLATED STRUCTURES WITH ADDITIONAL ENERGY DISSIPATION DEVICES AT ISOLATION LEVEL

Ahmet Demirhan SEVER

Master of Science, Department of Civil Engineering

Supervisor: Assoc. Prof. Dr. Alper ALDEMİR

Co- Supervisor: Prof. Dr. Uğurhan AKYÜZ

June 2024, 108 pages

In this thesis study, the changes in the behavior of buildings designed with seismic isolation by adding additional energy dissipation devices used in the seismic isolation floor to the system were examined. Eleven ground motions were selected for each structure and nonlinear analyzes were performed in the two-dimensional time domain; vertical components of ground motions did not included. The main motivation for using additional dampers is to reduce the displacement demands of the isolators and observe the changes in the superstructure. It was aimed to control the isolator demands at different points and to ensure similar demands as much as possible, and the hysteretic behavior of the isolators was shown. In the superstructure, comparisons were made considering story accelerations, interstorey drifts and total shear force. The number of dampers was increased according to the center of mass and center of rigidity of the structure, and each analysis result was compared with the initial state of the structure. According to the results obtained, adding additional dampers in certain quantities and at appropriate positions based on centers of the structure to the isolators structure did not negatively affect the superstructure behavior. Interstorey drifts and story accelerations were kept within certain limits, and the total shear force remained at reasonable levels. Isolator displacement demands for structures subject to torsional behavior due to the center of rigidity and center of mass not overlapping are brought closer together and a more uniform behavior was achieved.

Keywords: Seismic Isolated Structures, Energy Dissipation Devices, Friction Pendulum Isolator, Metallic Damper, Fluid Viscous Damper

ÖZET

SİSMİK İZOLASYONLU YAPILARIN YALITIM KATINDA İLAVE ENERJİ SÖNÜMLEYİCİ CİHAZLAR İLE İNCELENMESİ

Ahmet Demirhan SEVER

Yüksek Lisans, İnşaat Mühendisliği Bölümü

Tez Danışmanı: Doç. Dr. Alper ALDEMİR

Eş Danışman: Prof. Dr. Uğurhan Akyüz

Haziran 2024, 108 sayfa

Bu tez çalışmasında, sismik izolasyonlu olarak tasarlanan yapıların, sismik izolasyon katında kullanılan ilave enerji sönümleyicilerin sisteme eklenmesiyle yapının davranışındaki değişimler incelenmiştir. Her yapı için 11 yer hareketi seçilmiş ve iki boyutlu zaman tanım alanında doğrusal olmayan analizler yapılmıştır, yer hareketlerinin düşey bileşenleri analizlere dahil edilmemiştir. İlave sönümleyici kullanmaktaki temel motivasyon izolatörlerin deplasman taleplerini azaltmak ve bu sırada üst yapıdaki değişimleri gözlemlemektir. Farklı noktalardaki izolatör taleplerini kontrol etmek ve olabildiğince benzer taleplerin sağlanması amaçlanmış, izolatörlerin histeretik davranışları gösterilmiştir. Üst yapıda ise kat ivmeleri, göreli kat ötelenmeleri ve toplam kesme kuvveti göz önünde bulundurularak karşılaştırmalar yapılmıştır. Yapının kütle ve rijitlik merkezlerine göre damper sayıları arttırılmış ve her analiz sonucu yapının ilk hali ile karşılaştırılmıştır. Elde edilen sonuçlara göre izolatörlü yapıya belirli adetlerde ve uygun konumlarda ilave damper eklenmesi üst yapı davranışını olumsuz etkilememiştir. Kat ötelenmeleri ve kat ivmeleri belirli limitler içinde tutulmuş, toplam kesme kuvveti makul seviyelerde kalmıştır. Merkezlerin tutmamasından ötürü burkulmaya maruz kalan yapılar için izolatör deplasman talepleri birbirine yaklaştırılmış ve daha tekdüze bir davranış elde edilmiştir.

Anahtar Kelimeler: Sismik İzolasyonlu Yapılar, Enerji Sönümleyici Cihazlar, Sürtünmeli Sarkaç İzolatör, Metalik Damper, Viskoz Damper

ACKNOWLEDGMENTS

First of all, I would like to thank and express my appreciation to my supervisor Assoc. Prof. Dr. Alper Aldemir. Without his support, guidance and comments, this work would not have been completed in such a short time span. I would also like to express my deep thankfulness to my co-supervisor Prof. Dr. Uğurhan Akyüz, for his guidance, patience, and support throughout this study. He offered valuable opportunities to develop my structural engineering skills in academic and professional life and self-development.

I want to express my deepest gratitude to the Prof. Dr Gökhan Özdemir, Dr. Kaan Kaatsız, Dr. Fırat Soner Alıcı, Dr. Abdullah Sandıkkaya, Dr. Bahadır Şadan, Dr. Cüneyt Tüzün, Mehmet Emre Özcanlı, Ömer Ülker, Barış Şahin and Mustafa Görkem Yıldız for their insightful feedback for this thesis work, also which I will make use of in my future research career.

I would like to sincerely thank my directors Uğurcan Özçamur and Sadun Tanışer, for their faith and support throughout my engineering career and for giving me the chance to work on my thesis along with my job. They were always there for me whenever I had a hard time working.

I'm grateful to my parents Sibel Karabulut and Sedat Sever. They have always been the most encouraging people in my life, and I never would have thought of completing my master's degree without their support. They have shown me a great deal of patience and understanding throughout these trying times. I will always be thankful to them.

Lastly, I would like to thank my friends Sude Çebi, Baran Can Özartaç, Zeynep Karabıyık Özartaç, Efe Sercan Özçam, Alperen Yaman, Emre Çelik, Serkan Nuri Taştekin, Ayşegül Özçelik, Mehmet Fahri Yılmaz and Mehmet Kaplan. This thesis would not have been possible without the support of my friends.

Ahmet Demirhan SEVER

June 2024, Ankara

TABLE OF CONTENTS

ABSTRACT i

ACKNOWLEDGMENTS v

TABLE OF CONTENTS vi

LIST OF TABLES ix

LIST OF FIGURES xi

ABBREVIATONS xvi

1. INTRODUCTION 1

1.1 Seismic Isolation 3

1.1.1 Rubber (Elastomeric) Isolators 5

1.1.2 Curved Surface Sliders 6

1.2 Dampers 8

1.2.1 Metallic Dampers 8

1.2.2 Friction Dampers 10

1.2.3 Fluid Viscous Dampers 12

1.2.4 Viscoelastic Solid Damper 13

1.2.5 Buckling Restrained Braces (BRB) 14

1.3 Motivation for this Dissertation 15

1.4 Scope of the Work 15

2. STRUCTURAL MODELLING AND ANALYSIS 17

2.1 Building 1: Kahramanmaraş State Hospital (B1) 17

2.1.1 Building Model Information 17

2.1.2 Seismicity and Selected Ground Motions 23

2.1.3 Isolator and Damper Design 24

2.2 Adıyaman Residential Building 32

2.2.1 Building Information Modelling 32

2.2.2 Seismicity and Selected Ground Motions 37
2.2.3 Isolator and Damper Design 39
2.3 Bolu PMR Hospital 42
2.3.1 Building Model Information 42
2.3.2 Seismicity and Selected Ground Motions 46
2.3.3 Isolator and Damper Design 48
3. ANALYSIS RESULTS 53
3.1 Kahramanmaraş State Hospital (B1) 53
3.1.1 Modal Analysis – Participating Mass Ratios 53
3.1.2 Maximum Isolator Displacements 56
3.1.3 Story Accelerations 59
3.1.4 Interstorey Drift Ratios 61
3.1.5 Base Shear Ratio 63
3.2 Adıyaman Kahta Residential Project (B2) 65
3.2.1 Modal Analysis – Participating Mass Ratios 65
3.2.2 Maximum Isolator Displacements 67
3.2.3 Story Accelerations 69
3.2.4 Interstorey Drift Ratios 70
3.2.5 Base Shear Ratio 72
3.3 Bolu PMR Hospital (B3) 73
3.3.1 Modal Analysis – Participating Mass Ratios 73
3.3.2 Maximum Isolator Displacements 74
3.3.3 Story Acceleration 75
3.3.4 Interstorey Drift Ratios 77
3.3.5 Base Shear Ratio 78
3.4 Comparison of Results 79
3.4.1 Kahramanmaraş State Hospital Results (B1) 79

3.4.2 Adıyaman Residential Building (B2) 89

3.4.3 Bolu PMR Hospital (B3) 95

4. SUMMARY AND CONCLUSIONS 103

REFERENCES 105

APPENDICES 109

CURRICULUM VITAE 111

LIST OF TABLES

Table 2.1 Conducted Numerical Analyses for B1 and their used abbreviations 21

Table 2.2 Selected ground motions for B1 24

Table 2.3 Characteristic Strength of Devices (kN/m).. 30

Table 2.4 Conducted Numerical Analyses for B2 and their used abbreviations 36

Table 2.5 Selected ground motions for B2 38

Table 2.6 Characteristic Strength of Devices (kN/m).. 41

Table 2.7 Conducted Numerical Analyses for B3 and their used abbreviations 45

Table 2.8 Selected ground motions for B3 48

Table 3.1 Modal analysis results for all cases – DBE UB... 54

Table 3.2 Modal analysis results for all cases – MCE LB... 55

Table 3.3 Maximum resultant displacements of selected link for each analysis -MCE LB 56

Table 3.4 Base shear ratios of all cases and change compared to FPS........................... 64

Table 3.5 Modal analysis results of all cases – DBE UB 65

Table 3.6 Modal analysis results of all cases – MCE LB 66

Table 3.7 Maximum resultant displacements of selected links for each case – MCE LB 67

Table 3.8 Base shear ratios of all cases and change compared to FPS........................... 73

Table 3.9 Modal analysis results of all cases... 73

Table 3.10 Maximum displacement of different links for each case – MCE LB 74

Table 3.11 Base shear ratios of all cases and change compared to FPS......................... 78

Table 3.12 Comparison of resultant accelerations for each story for U Damper – Kahramanmaraş (B1) (g) 80

Table 3.13 Comparison of resultant accelerations for each story for U Damper-Stiffer – Kahramanmaraş (B1) (g) 81

Table 3.14 Comparison of interstorey drifts for each story for U Damper – Kahramanmaraş (B1) (%) 82

Table 3.15 Comparison of interstorey drift ratios for U Damper-Stiffer – Kahramanmaraş (B1) (%)..83

Table 3.16 Comparison of all results for FPS and UD4 - Kahramanmaraş 89

Table 3.17 Comparison of story accelerations for all stories – Adıyaman UD (g).........90

Table 3.18 Comparison of story accelerations for all stories – Adıyaman UDs (g) 91

Table 3.19 Comparison of interstorey drifts for all story – Adıyaman U Damper (%) ..91

Table 3.20 Comparison of interstorey drifts for all story – Adıyaman U Damper-Stiffer (%)..91

Table 3.21 Comparison of all results of FPS and UD1 – Adıyaman 95

Table 3.22 Comparison of story accelerations for all stories – Bolu (g) 96

Table 3.23 Comparison of interstorey drifts for all story – Bolu (%).............................97

Table 3.24 Comparison of all results for FPS and VD4 - Bolu 101

LIST OF FIGURES

Figure 1.1 Typical performance curve for the structure (adapted from Ghobarah, 2001) 1

Figure 1.2 Building Performance Levels 2

Figure 1.3 Base-isolated structure and conventional structure (adapted from Nakamura & Okada, 2019).. 4

Figure 1.4 Effects of Base Isolation (adapted from Buckle et al., 2006).......................... 4

Figure 1.5 NRB and LRB (adapted from Cho et al., 2020)... 6

Figure 1.6 Geometry of pendulum isolators (adapted from Barrera-Vargas et al., 2020) 7

Figure 1.7 Pendulum type of isolators (adapted from Barrera-Vargas et al., 2020)......... 7

Figure 1.8 Double pendulum type of isolator at maximum displacement........................ 7

1.9 Hysteretic behaviors of dampers (adapted from Constantinou & Whittaker, 2005) .. 8

Figure 1.10 Metallic damper types (adapted from Javanmardi et al., 2019) 9

Figure 1.11 Deformation of Metallic Dampers (adapted from Li et al., 2014) 10

Figure 1.12 Looped and U-shaped steel dampers (adapted from Atasever et al., 2017) 10

Figure 1.13 Friction damper (adapted from Mualla, 2000) 11

Figure 1.14 Activation of the friction damper (adapted from Mualla & Jakupsson, 2010) 11

Figure 1.15 Fluid Viscous Damper (adapted from Alotta et al., 2016) 12

Figure 1.16 Viscoelastic Damper (adapted from Christopoulos & Montgomery, 2013) 13

Figure 1.17 Buckling Restrained Brace (adapted from Xie, 2005) 14

Figure 1.18 A comparison study in Japan (adapted from Xie, 2005)............................. 14

Figure 2.1 Structural model of Kahramanmaraş State Hospital 18

Figure 2.2 Architectural plan of Kahramanmaraş State Hospital.................................. 18

Figure 2.3 Elevation view of Kahramanmaraş State Hospital....................................... 19

Figure 2.4 Center of rigidity and center of mass of the structure (B1)........................... 20

Figure 2.5 Selected points of the structure (B1)..20
Figure 2.6 Damper configurations of each case 22
Figure 2.7 Location of the structure (B1)..23
Figure 2.8 Target spectrum and mean SRSS of all GMs for B1 24
Figure 2.9 Results of SDOF analysis for B1 26
Figure 2.10 Force – displacement capacity curves of isolators (DBE UB) 27
Figure 2.11 Force – displacement capacity curves of isolators (MCE LB) 28
Figure 2.12 Example Link Properties – Friction Isolator...28
Figure 2.13 Force – displacement capacity curves of metallic dampers (DBE UB).......29
Figure 2.14 Force – displacement capacity curves of metallic dampers (MCE LB) 30
Figure 2.15 Example Link Properties – Metallic Damper 31
Figure 2.16 Selected damper and isolator 32
Figure 2.17 Structural model of Adıyaman Residential Building..................................33
Figure 2.18 Architectural plan of the structure of Adıyaman Residential Building 33
Figure 2.19 Elevation view of the Adıyaman Residential Building 34
Figure 2.20 Center of rigidity and center of mass of the structure (B2) 35
Figure 2.21 Selected points of the structure (B2)...35
Figure 2.22 Damper configurations of each analysis..36
Figure 2.23 Location of the structure (B2)..37
Figure 2.24 Target spectrum and mean SRSS of all GMs for B2 38
Figure 2.25 Results of SDOF analysis for B2 39
Figure 2.26 Force – displacement capacity curves of isolators (DBE UB – MCE LB)..40
Figure 2.27 Force – displacement capacity curves of metallic dampers (DBE UB).......41
Figure 2.28 Force – displacement capacity curves of metallic dampers (MCE LB) 41
Figure 2.29 Selected damper and isolator 42
Figure 2.30 Structural model of Bolu PMR Hospital...43

Figure 2.31 Architectural plan of Bolu PMR Hospital 43
Figure 2.32 Center of rigidity and center of mass (B3) 44
Figure 2.33 Selected points of the structure (B3) 45
Figure 2.34 Damper configuration for each analysis 46
Figure 2.35 Location of the structure (B3) 47
Figure 2.36 Target spectrum and mean SRSS of all GMs for B3 48
Figure 2.37 Results of SDOF analysis for B3 49
Figure 2.38 Hysteretic behavior of isolators (DBE UB) 49
Figure 2.39 Hysteretic behavior of isolators (MCE LB) 50
Figure 2.40 Force-Velocity relation of viscous damper 50
Figure 2.41 Example link properties of viscous dampers 51
Figure 2.42 Viscous damper and isolators 51
Figure 3.1 Orbital displacements and capacity of isolators 57
Figure 3.2 Resultant story accelerations of all cases 59
Figure 3.3 Resultant story accelerations of all cases (continued) 60
Figure 3.4 Resultant story accelerations of all cases (continued) 61
Figure 3.5 Interstorey drift ratios of all cases 61
Figure 3.6 Interstorey drift ratios of all cases (continued) 62
Figure 3.7 Interstorey drift ratios of all cases (continued) 63
Figure 3.8 Base shear ratios of all cases 64
Figure 3.9 Orbital displacements and capacity of isolators 68
Figure 3.10 Orbital displacements and capacity of isolators (continued) 69
Figure 3.11 Resultant story accelerations of all cases 69
Figure 3.12 Resultant story accelerations of all cases (continued) 70
Figure 3.13 Interstorey drift ratios of all cases 71
Figure 3.14 Interstorey drift ratios of all cases (continued) 72

Figure 3.15 Base shear ratios of all cases..72

Figure 3.16 Orbital displacements and capacity of isolators 74

Figure 3.17 Orbital displacements and capacity of isolators (continued).......................75

Figure 3.18 Resultant story accelerations of isolated structure......................................76

Figure 3.19 Resultant story accelerations of system with additional dampers 76

Figure 3.21 Interstorey drift ratios of all cases...77

Figure 3.22 Base shear ratios of all cases..78

Figure 3.23 Comparison of resultant accelerations for U Damper – Kahramanmaraş (B1) 79

Figure 3.24 Comparison of resultant story accelerations for U Damper-Stiffer – Kahramanmaraş (B1) 80

Figure 3.25 Comparison of interstorey drifts for U Damper – Kahramanmaraş (B1)....81

Figure 3.26 Comparison of interstorey drift ratios for U Damper-Stiffer – Kahramanmaraş (B1)..82

Figure 3.27 Comparison of maximum displacement demands – Kahramanmaraş (B1) 84

Figure 3.28 Comparison of base shear ratios – Kahramanmaraş (B1)............................85

Figure 3.29 Comparison of accelerations and drifts for FPS and UD4 – Kahramanmaraş(B1) 86

Figure 3.30 Comparison of maximum displacements for FPS and UD4 – Kahramanmaraş(B1) 87

Figure 3.31 Comparison of base shear ratios for FPS and UD4 – Kahramanmaraş(B1) 87

Figure 3.32 Comparison of Force-Displacement Behaviors for One Link – DBE UB ..88

Figure 3.33 Comparison of Force-Displacement Behaviors for One Link – MCE LB ..88

Figure 3.34 Comparison of story accelerations – Adıyaman UD 90

Figure 3.35 Comparison of story accelerations – Adıyaman UDs.................................90

Figure 3.36 Comparison of interstorey drifts - Adıyaman 91

Figure 3.37 Comparison of maximum displacements – Adıyaman................................92

Figure 3.38 Comparison of base shear ratios – Adıyaman 93

Figure 3.39 Comparison of accelerations and drifts of FPS and UD1 - Adıyaman 93

Figure 3.40 Comparison of maximum displacements of FPS and UD1 – Adıyaman 93

Figure 3.41 Comparison of base shear ratios of FPS and UD1 - Adıyaman 94

Figure 3.42 Comparison of Force-Displacement Behaviors for One Link – DBE UB .. 94

Figure 3.43 Comparison of Force-Displacement Behaviors for One Link – MCE LB .. 95

Figure 3.44 Comparison of story accelerations – Bolu 96

Figure 3.45 Comparison of interstorey drifts – Bolu 97

Figure 3.46 Comparison of maximum displacements – Bolu 98

Figure 3.47 Comparison of base shear ratios – Bolu 98

Figure 3.48 Comparison of accelerations and drifts for FPS and VD4 - Bolu 99

Figure 3.49 Comparison of maximum displacements for FPS and VD4 – Bolu............ 99

Figure 3.50 Comparison of base shear ratios for FPS and VD4 - Bolu.......................... 99

Figure 3.51 Comparison of Force-Displacement Behaviors for One Link – DBE UB 100

Figure 3.52 Comparison of Force-Displacement Behaviors for One Link – MCE LB 100

ABBREVIATONS

CoR	Center of Rigidity
CoM	Center of Mass
CSS	Curved Surface Sliders
DBE	Design Basis Earthquake
FNA	Fast Nonlinear Analysis
FPS	Friction Pendulum System
GM	Ground Motion
HDRB	High Damping Rubber Bearing
LB	Lower Bound
LRB	Lead Rubber Bearing
MCE	Maximum Credible Earthquake
Nom	Nominal
NRB	Natural Rubber Bearing
UB	Upper Bound
UD	U-shaped Damper
UDs	Stiffer U-shaped Damper
PEER	Pacific Earthquake Engineering Research Center
PSA	Peak Story Acceleration
RSN	Record Sequence Number from PEER database
SI	Seismic Isolation
TBDY2019	Turkish Building Seismic Code 2019
VD	Viscous Damper

1. INTRODUCTION

In the conventional approach, buildings are designed to be damaged in an earthquake most of the time. Essentially, the goal is to prevent loss of life and protect the people inside. An economical design is not possible otherwise. Therefore, any possible damage is limited and kept under control. Since it is impossible to build structures without accepting that they may sustain damage to some extent based on their ductility, all national and international earthquake rules are developed with this understanding. Under the projected design earthquake in that place, all structures will sustain a given amount of damage. The restrictions are not meant to do harm, but rather to protect lives by keeping the structures from collapsing. During an earthquake or any dynamic effect, structural elements get damage and absorb energy in inelastic regions to prevent collapse. Using additional devices is the most effective way to stop financial losses that will happen after a major earthquake, even if the number of fatalities can be reduced when buildings are built in compliance with the regulations.

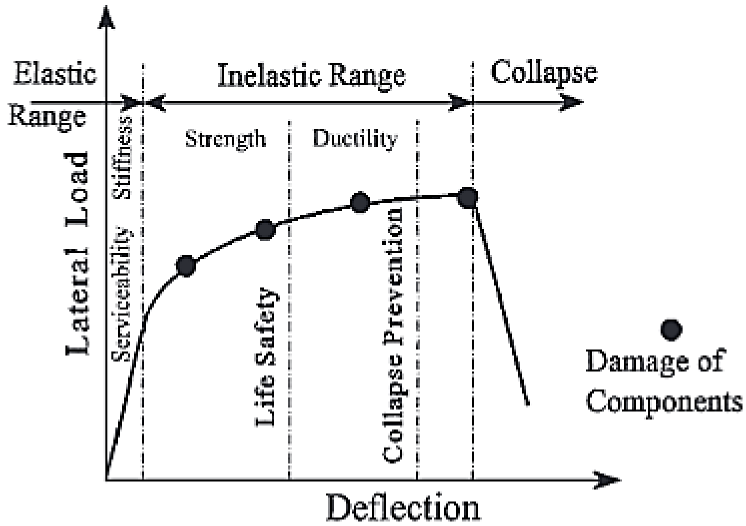

Figure 1.1 Typical performance curve for the structure (adapted from Ghobarah, 2001)

A high-technology application to protect structures from the destructive effects of earthquakes or any dynamic effects is to install specially designed devices having some energy absorption capacity. These devices are called as energy dissipation devices.

The development of energy dissipation systems for seismic applications has been ongoing for some time, and the number of implementations is growing quickly. Reducing the inelastic energy dissipation demand on a structure's frame system is the main purpose of an energy dissipation system. The primary goal is to decrease drifts and accelerations as the period increases. Based on building performance levels, interstorey drifts are limited and possible damage is prevented. These performance levels of buildings are mentioned in Figure 1.2.

Energy dissipation devices are primarily used in structures to prevent structural or non-structural components from deforming harmfully. The intrinsic qualities of the fundamental structure, the attributes of the device and its connecting components, the features of the ground motion, and the limit state under investigation all affect how well a particular device may achieve this aim.

Building Performance Levels

	Collapse Prevention Level	**Life Safety Level**	**Immediate Occupancy Level**	**Operational Level**
Overall Damage	Severe	Moderate	light	Very light
General	Little residual stiffness and strength, but load bearing Columns and walls function. Large permanent drifts. Some exits blocked. Infills and unbraced Parapets failed or at incipient failure. Building is near collapse	Some residual Strength and stiffness left in all stories. Gravity-load-bearing elements function. No Out-of-plane failure of walls or tipping of parapets. Some permanent drift. Damage to partitions. Building may be beyond economical repair.	No permanent drift. Structure substantially retains original Strength and stiffness. Minor cracking of facades, partitions, and ceilings as well as structural elements. Elevators can be restarted. Fire protection operable.	No permanent drift; structure substantially Retains original strength and stiffness. Minor cracking of facades, partitions, and ceilings as well as structural elements. All Systems important to normal operation are functional.
Non-structural Components	Extensive damage.	Falling hazards mitigated but many architectural, mechanical, and electrical systems	Equipment and contents are generally secure, but may not operate due to mechanical	Negligible damage occurs. Power and other utilities are available, possibly from

Figure 1.2 Building Performance Levels

Several energy dissipation devices are either commercially available or under development. With the development of technology, many methods have been widely used to increase the performance of structures during earthquakes in recent years. These systems can be grouped into three main headings: base isolation; passive energy dissipation; and active control. (Soong and Spencer, 2002). Of the three, base isolation can now be considered a more mature technology with wider applications as compared with the other two, and earthquake isolation and energy damping are grouped under the heading of passive control.

In order to improve stiffness, strength, and damping, a variety of materials and devices are used in passive energy dissipation systems. These systems can be applied to both the rehabilitation of old or inadequate structures as well as the mitigation of seismic hazards. These systems can improve energy dissipation in the structural systems in which they are installed, which is how they are generally identified. These devices generally operate on principles such as frictional sliding, yielding of metals, phase transformation in metals, deformation of viscoelastic solids or fluids, and fluid orifice. Devices that have most commonly been used for seismic protection of structures include elastomeric bearings, friction pendulums, fluid viscous dampers, viscoelastic solid dampers, friction dampers, metallic dampers, BRB, etc. There are many other devices such as tuned mass dampers, and tuned liquid dampers but they can be grouped differently.

1.1 Seismic Isolation

Unlike the classical approach, earthquake isolation has become quite common with the development of technology in recent years. Performance-based earthquake engineering, which works on the performance levels of structures, has come to the fore.

The technique known as seismic isolation creates a barrier between the building and the ground using specific devices positioned between the building and its base, shielding the structure and every internal component from the damaging impacts of an earthquake. The superstructure is isolated from the ground and foundation by placing multiple earthquake isolators beneath the shear walls and one under each column in buildings. Earthquake isolation guarantees that the building will withstand any earthquake with no damage and will continue to function normally by shielding the superstructure's structural and non-structural components.

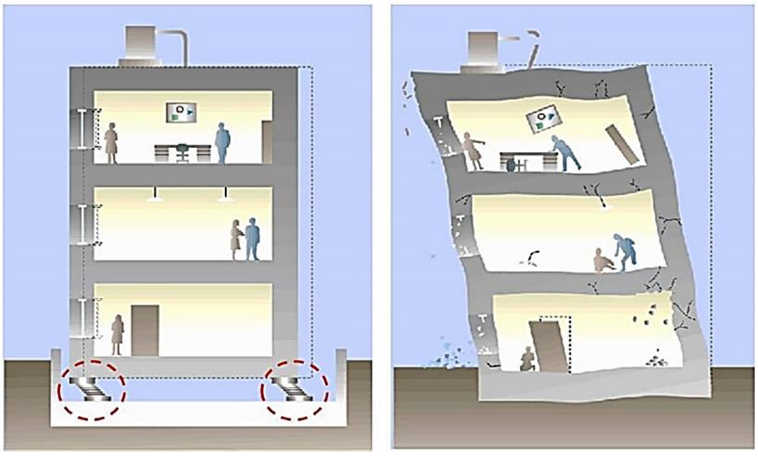

Figure 1.3 Base-isolated structure and conventional structure
(adapted from Nakamura & Okada, 2019)

Earthquake isolation devices have lateral flexibility and basically have advantages such as increasing the period of the structure, decreasing the acceleration, and increasing the energy absorption capacity (Patil & Reddy, 2012). By creating an interface between the structure and the ground, it prevents the building from feeling the destructive effects of the earthquake. Moreover, the damping, which is accepted as 5% in conventional structures, increases to more than 20% (Figure 1.4)

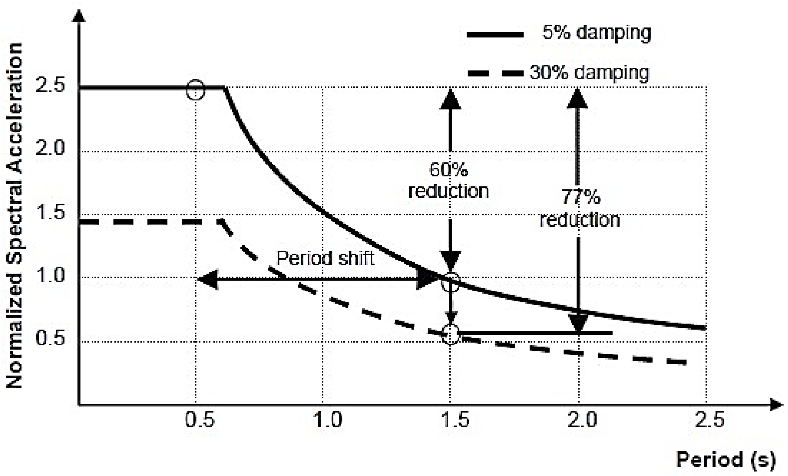

Figure 1.4 Effects of Base Isolation (adapted from Buckle et al., 2006)

The interest in these systems have been increasing due to their proven better performance during real earthquakes (Murota et al., 2021). The 2020 Elazığ earthquake is one of the closest examples. Elazığ City Hospital was able to remain operational right after the earthquake and stayed in its operational performance level as designed. Similarly, there was nine isolated hospitals in the Kahramanmaraş region and these hospitals was able to remain operational after 6th February earthquakes.

Seismic isolators can be grouped as Rubber Isolators and Friction Pendulum Isolators. Rubber Isolators also grouped as Natural Rubber Bearing (NRB), Lead Rubber Bearing (LRB) and High Damping Rubber Bearing (HDRB). Moreover, pendulum isolators are grouped as Single-Double-Triple Pendulum Isolator.

1.1.1 Rubber (Elastomeric) Isolators

Rubber type of isolators is the first isolator developed in a modern sense in the 1970s. They basically consist of thin rubber layers and steel plates. These materials vulcanized and glued together. Rubber isolators work with the displacement ability of rubber material and energy is absorbed. Steel plates help carry axial loads. Due to these steel plates, these bearings are very stiff in vertical direction, however very flexible in horizontal direction (Naeim & Kelly, 1999). Rubber type of isolators can be divided into three types: Natural Rubber Bearing (NRB), High Damping Rubber Bearing (HDRB) and Lead Rubber Bearing (LRB). NRB and HDRB are quite similar, both are including rubber and steel plates. The only difference between NRB and HDRB is the rubber material used during their production. HDRB includes specific type of rubber and damping coefficient of isolator is quite high compared to NRB. However, Lead Rubber Bearing, the isolator has some specific differences. In the core of rubber, there is a lead material layer to enhance the energy absorption capacity of the isolator (Figure 1.5).

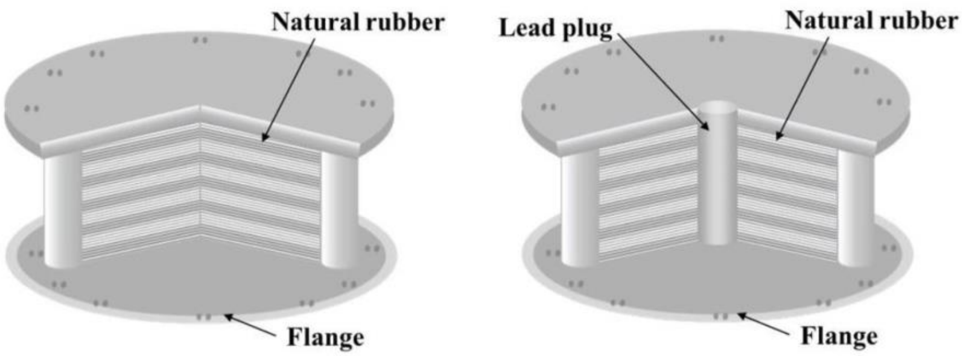

Figure 1.5 NRB and LRB (adapted from Cho et al., 2020)

1.1.2 Curved Surface Sliders

Curved surface sliders are pendulum type of sliders developed in the 1990s. Pendulum isolators work based on the principle of a pendulum (Akyuz et al, 2020). The system combines a sliding action and a restoring force thanks to its geometry. They have steel backing plates and a specific friction material that has a low friction coefficient under high pressure. The device is quite stiff in the vertical direction and very flexible in the horizontal direction. Steel backing plates have a radius surface and this shape provides energy absorption capacity and re-centering capacity. (Figure 1.6). These friction pendulum types of isolators are generally evaluated in three headings: Single Pendulum, Double Pendulum, and Triple Pendulum. The main principle is the same for all types of pendulums. The only difference is the sliding and rotational surfaces. Single pendulums have two different surfaces; one of them is for displacement, the other is for rotation. However, double pendulum-type isolators have two same backing plates and both surface works for displacement at the same time. As can be predicted, Triple Pendulums have more sliding surfaces and have different friction materials (Figure 1.7 and 1.8).

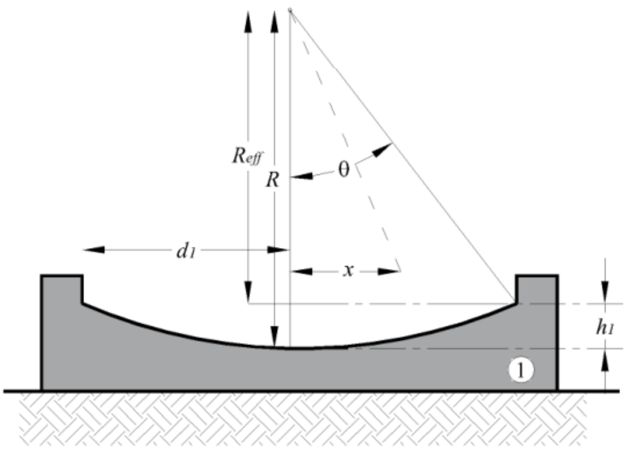

Figure 1.6 Geometry of pendulum isolators (adapted from Barrera-Vargas et al., 2020)

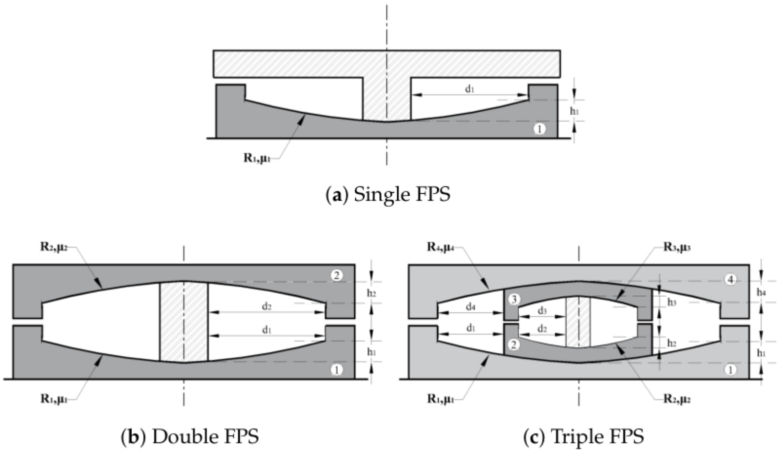

Figure 1.7 Pendulum type of isolators (adapted from Barrera-Vargas et al., 2020)

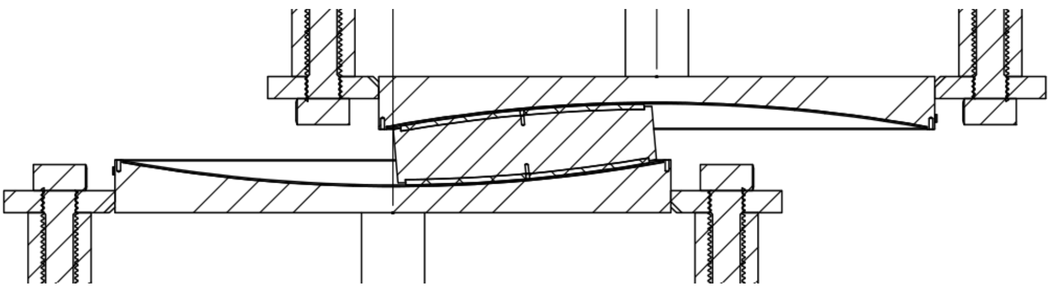

Figure 1.8 Double pendulum type of isolator at maximum displacement

1.2 Dampers

The basic logic of the dampers, which have different operating principles such as the yielding of steel, the friction caused by movement, the viscoelastic behavior of rubber-like materials and the movement of liquids, is the same (Constantinou and Symans, 1993). Hysteretic behaviors of dampers are shown in Figure 1.9. Besides, the advantages and disadvantages of all dampers will be presented in the study conducted by Symans et al., 2008. These devices are basically grouped as metallic, friction, viscoelastic, viscous dampers, and BRBs. Details on these types are given in the following subsections.

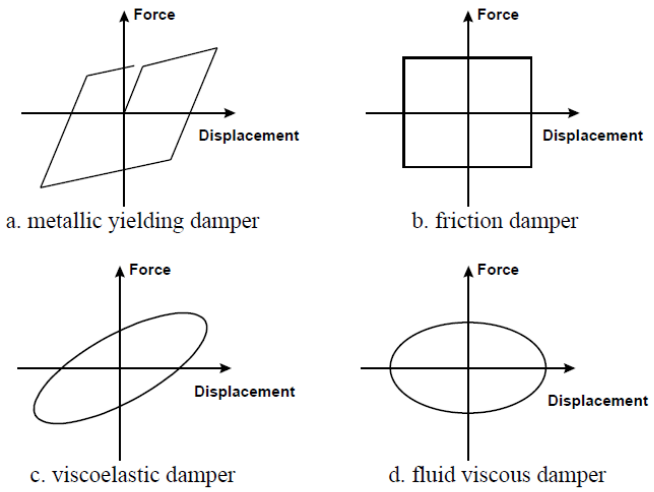

1.9 Hysteretic behaviors of dampers (adapted from Constantinou & Whittaker, 2005)

1.2.1 Metallic Dampers

Metallic Damper is a type of displacement activated device. This means that whenever any dynamic situation occurs, a displacement demand occurs in response. So, the working theory is that the metallic device yields and deforms plastically, dissipating the vibration energy of the device and reducing the effect of damage to the structural components. Deformation of metallic dampers is shown in Figure 1.11. The device contains some special metal or alloys. This material has elastic deformation, yielding mechanism and this mechanism is effective in dissipating energy due to ductility. The reasons why metal material is preferred are its high elastic hardness, good ductility and high energy dissipation potential in the post-yield region. There are many types of metallic dampers named as U-strip damper, torsional beam damper, flexural beam damper, single-axis damper, X-shaped, ADAS and TADAS (Javanmardi et al., 2019) and these different types are shown in Figure 1.10. Based on the seismic demand, these types can be increased and designed specially for structure. Moreover, there is special type of damper that can be used with seismic isolators (Figure 1.12).

Advantages of Metallic Dampers;

- It can be used for RC/Steel buildings.
- Stable hysteretic behavior of metals
- Longtime reliability
- Lack of sensitivity to outside temperature
- Materials and behavior familiar to practicing engineers

Disadvantages of Metallic Dampers;

- Device can be damaged after earthquake; may require replacement
- Nonlinear behavior, may require nonlinear analysis

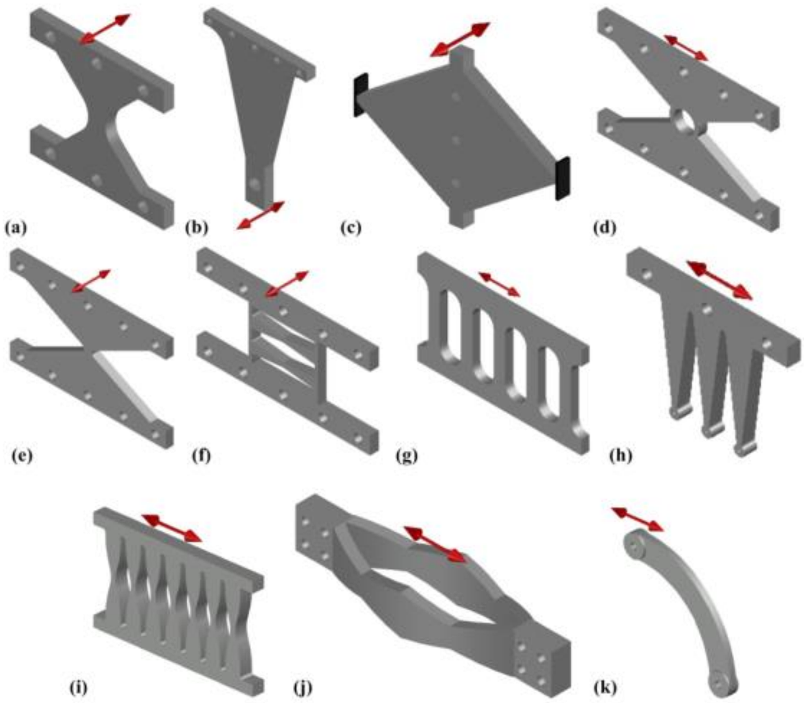

Figure 1.10 Metallic damper types (adapted from Javanmardi et al., 2019)

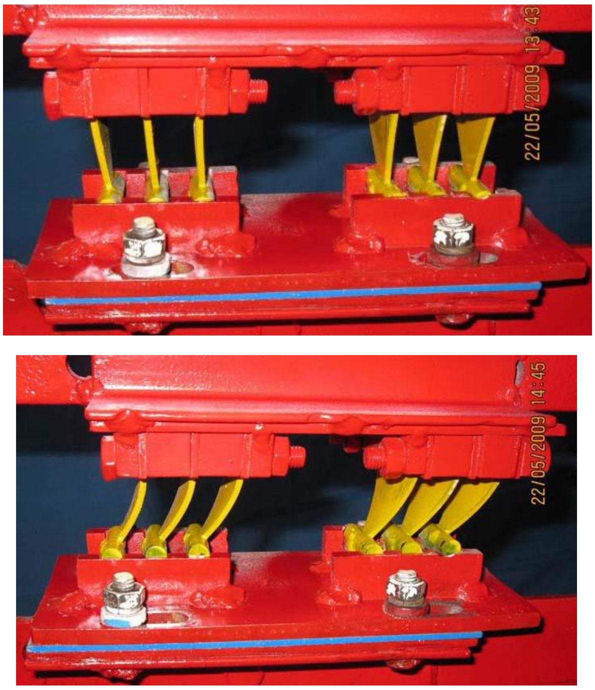

Figure 1.11 Deformation of Metallic Dampers (adapted from Li et al., 2014)

(a) Looped steel dampers (b) U-shaped steel damper

Figure 1.12 Looped and U-shaped steel dampers (adapted from Atasever et al., 2017)

1.2.2 Friction Dampers

Friction dampers utilize the mechanism of solid friction that develops between two solid bodies sliding relative to one another to provide the desired energy dissipation (Figure 1.13). Several types of friction dampers have been developed for the purpose of improving seismic response loops (Figure 1.14). They are types of displacement-activated device as metallic dampers. These devices generally used at tall buildings (i.e., skyscrapers) to limit interstorey drifts.

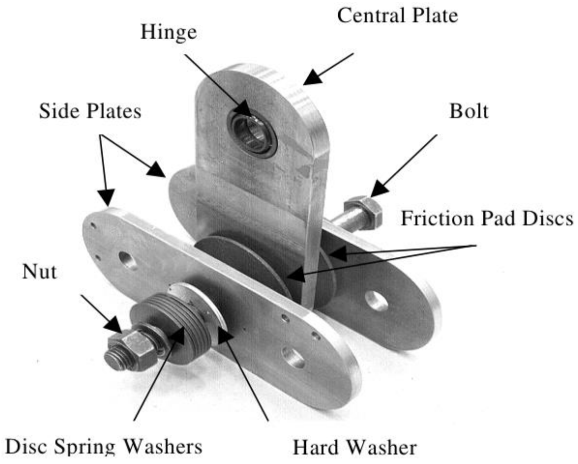

Figure 1.13 Friction damper (adapted from Mualla, 2000)

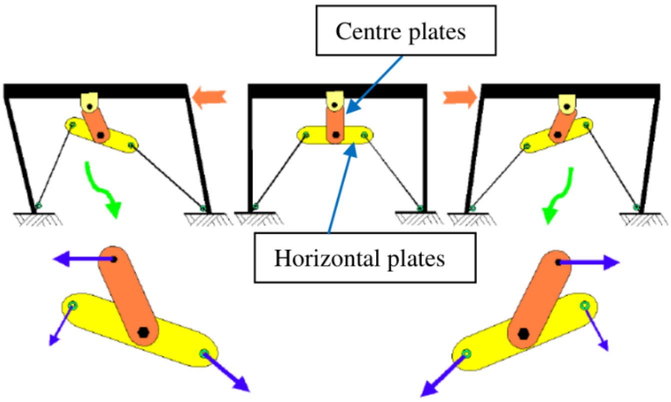

Figure 1.14 Activation of the friction damper (adapted from Mualla & Jakupsson, 2010)

Advantages of Friction Dampers;

- Large energy dissipation per cycle
- Lack of sensitivity to outside temperature
- Not need to be inspected regularly
- Maintenance requirements are very low (compared to viscous dampers)
- The dampers are not active during low velocity wind and service loads.

Disadvantages of Friction Dampers;

- Sliding interface conditions may change with time (reliability concern)
- Strongly nonlinear behavior; may excite higher modes and require nonlinear analysis
- Permanent displacements if no restoring force mechanism provided
- There is no re-centering

1.2.3 Fluid Viscous Dampers

Fluid Viscous Dampers work based on the principle of fluid flowing through orifices. The damper consists of a steel cylinder divided into two champers by the piston head, a compressible hydraulic fluid (silicon oil), a stainless steel piston and an accumulator for smooth fluid circulation (Figure 1.15). They are types of velocity activated devices and their maximum force depends on the velocity demand.

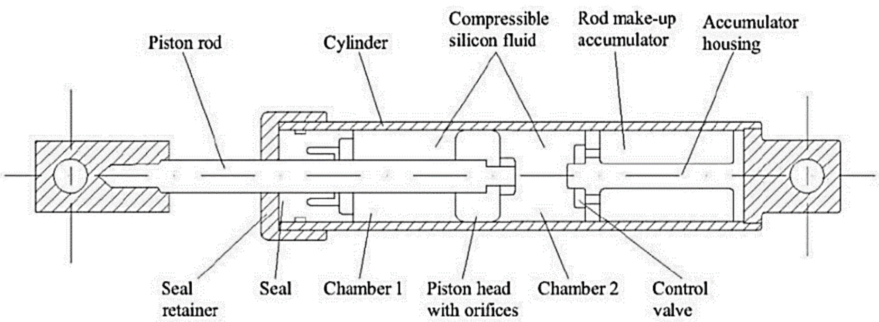

Figure 1.15 Fluid Viscous Damper (adapted from Alotta et al., 2016)

Advantages of Fluid Viscous Dampers;

- They can be activated at low displacements
- Minimal restoring force
- For linear damper, modelling of damper is simplified
- Generally, temperature independent

Disadvantage of Fluid Viscous Dampers;

- Possible fluid seal concern (reliability concern)

1.2.4 Viscoelastic Solid Damper

Viscoelastic dampers were developed in the 2010s and consist of multiple layers of viscoelastic materials, placed between layers of steel plate (Figure 1.16). These dampers dissipate energy through shear deformations of viscoelastic materials. Viscoelastic materials develop viscous force and elastic restoring force. They are a type of displacement-velocity activated dampers.

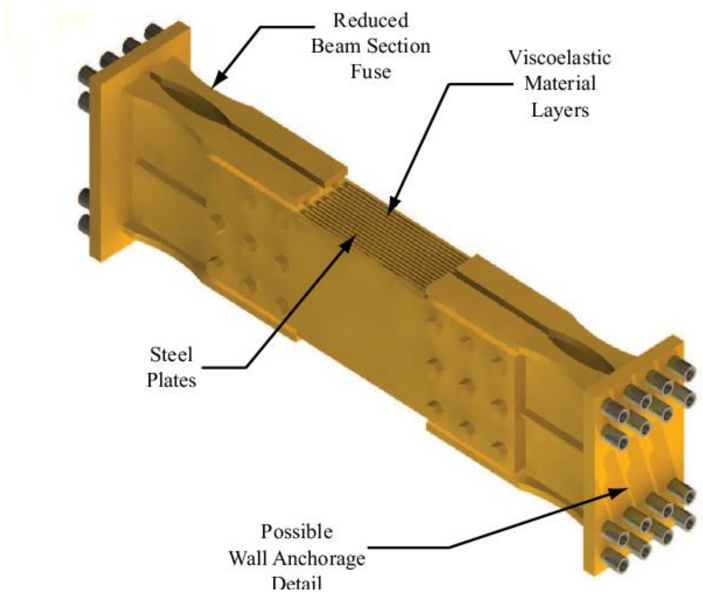

Figure 1.16 Viscoelastic Damper (adapted from Christopoulos & Montgomery, 2013)

Advantages of Viscoelastic Dampers;

- Activated at low displacements
- Provides restoring force
- Linear behavior, simplified modelling of damper

Disadvantages of Viscoelastic Dampers;

- Limited deformation capacity
- Temperature dependent
- Debonding and tearing problem of material due to maximum shear capacity
- Inspection and maintenance required

1.2.5 Buckling Restrained Braces (BRB)

BRBs are different types of metallic dampers. It consists of a steel core and a concrete covering cover (Figure 1.17). The device has an axial force-carrying unit, a stiffened transition segment (projection), and a buckling-restraining unit. BRBs mostly preferred in high-rise buildings and the seismic retrofit of existing buildings. It can be used for high-rise buildings, schools, and hospitals as dampers and lateral stiffeners. It can resist cyclical lateral loadings satisfactorily.

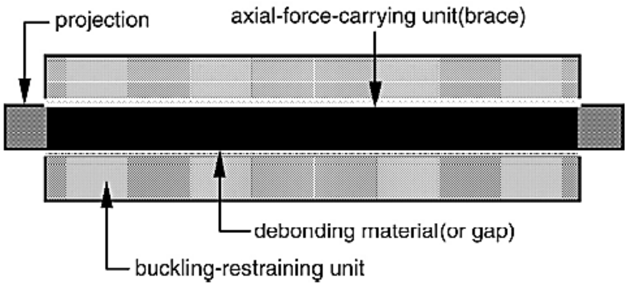

Figure 1.17 Buckling Restrained Brace (adapted from Xie, 2005)

A study conducted in Japan shows that BRBs and viscous dampers are mostly preferred in high-rise buildings constructed from 1995 to 1999 (Figure 1.18). Although steel brace is very effective in providing strength and stiffness, it can be buckled under high compression loading. That’s why most of the time BRBs are preferred rather than steel brace.

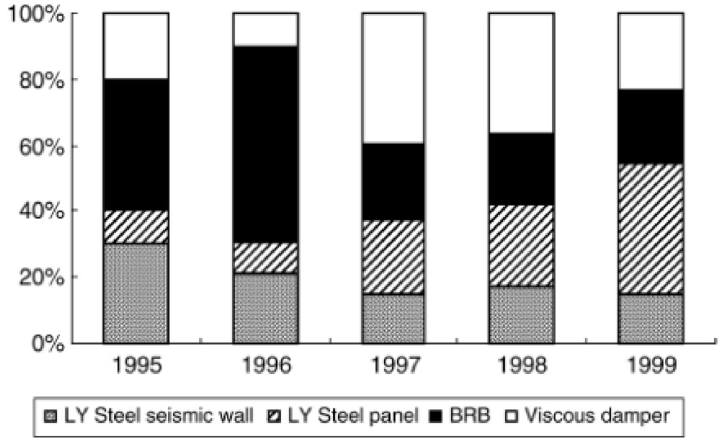

Figure 1.18 A comparison study in Japan (adapted from Xie, 2005)

1.3 Motivation for this Dissertation

In regions with high earthquake hazard, the displacement demands of seismic isolated structures can be very high due to displacement demands, which negatively affect the cost of earthquake isolation. In such design situations, extra dampers can be used as an alternative to reduce the displacement demands. Dampers reduce displacements, but at the expense of significant increases in interstorey drifts and story accelerations in the superstructure (Kelly, 1999).

Among the energy dissipation devices, metallic dampers, which can be one of the most advantageous in terms of capacity and usability, will be modeled with appropriate yield values and evaluated together with the isolation system in this study. Besides, fluid viscous dampers will be modeled for one structure due to the required higher damping ratio. Moreover, for the structures with significant eccentricity (i.e., center of mass and center of rigidity are not closely located to each other.), some of the structural elements including base isolators should resist more lateral load demands compared to others, resulting in significant changes in the isolator designs. For this purpose, the design of the seismic isolators according to current regulations has a procedure to consider torsion effects (i.e., maximum isolator demands are multiplied by an amplification coefficient).

When a damper system added to an isolated structure, there will be changes in the seismic behavior of the structure. Interstorey drifts could increase, story acceleration values could also change. In this study, these changes will be discussed by considering current performance levels. Two structures with a metallic damper system and one structure with a viscous damper system will be investigated.

In summary, the effectiveness of the additional damping system will be investigated for different types of structures and a comparison will be made based on displacement demand, drift ratios, and acceleration values. The reduction of possible isolator sizes and the reduction of displacement demands will also be evaluated in terms of total cost.

1.4 Scope of the Work

In this study, two different hospital type of structures which have different architectures will be investigated. In addition to that, one residential structure will be evaluated to see effects of damper to a building type of structure.

In Chapter 1, introduction and history of seismic isolation, isolator types and damper types are mentioned. Literature review about additional damping system is mentioned.

Chapter 2 includes building information, design of seismic isolation system and damper selection. Moreover, selected ground motions and seismicity are mentioned too.

Chapter 3 covers analysis results of all selected structures for different cases. Maximum isolator displacement demands for different links, interstorey drifts, peak story accelerations and base shear ratios will be mentioned. After presenting these results, they will be compared with current structure results. The most appropriate case among all the results will be selected.

Finally, Chapter 4 will summarize the entire study. Conclusions and recommendations will be discussed.

2. STRUCTURAL MODELLING AND ANALYSIS

In this chapter, structural modeling for different reinforced concrete structures and details of structural members are explained. To compare the seismic performance of isolated structures and isolated structures with extra dampers, a total of three different structures are analyzed with different cases. Two of them are hospital projects located in a highly active seismic regions and the last one is a residential building.

2.1 Building 1: Kahramanmaraş State Hospital (B1)

2.1.1 Building Model Information

The first project (B1) is a state hospital located in Kahramanmaraş. The hospital was designed in 2020 and its construction continues. Its structural system is composed of moment frames entirely (i.e., no shearwall exists). The plan geometry is 150 m in the X direction, 125 m in the Y direction, the total height is 458 m, and the structure has 11 stories.

The column dimensions are mostly 800×800 mm, beam dimensions are mostly 500×700 mm and 600×700 mm. All beams and columns have C35/45 type concrete above the isolation level. At under isolation level, column sizes will be different and these columns named as pedestals. Pedestal sizes are 1800×1800 mm due to isolator diameters and these pedestals have C40/50 type concrete.

A 3D structural model was created and analyzed in ETABS v19.1.0 and the 3D view and plan geometry are given in Figures 2.1 and 2.2.

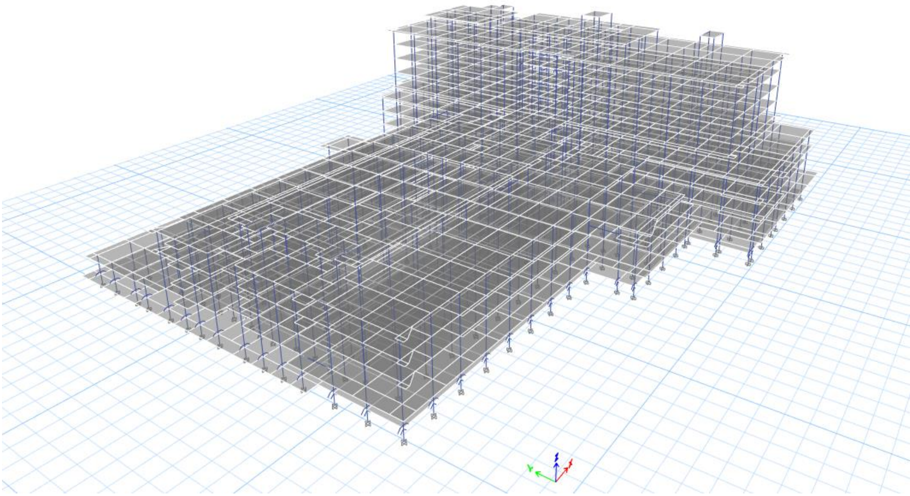

Figure 2.1 Structural model of Kahramanmaraş State Hospital

The project includes a total of 10 blocks but only the main hospital block (i.e., Block A) designed as isolated structure. Therefore, in the scope of this dissertation, only Block A is modelled.

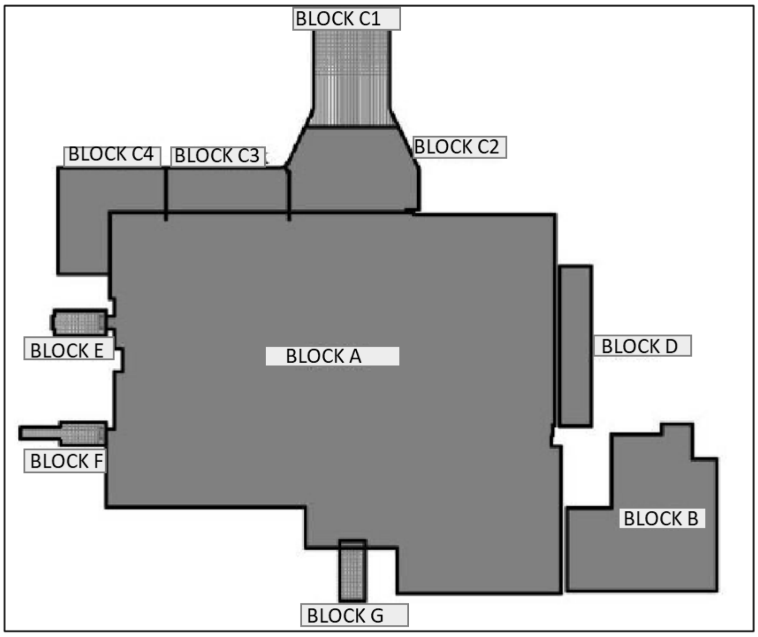

Figure 2.2 Architectural plan of Kahramanmaraş State Hospital

In addition to the self-weight of the structure, 2.2 kN/m^2 uniform load is assigned as dead load to simulate all the coverings and levelling concrete layers, and 3.5 kN/m^2 uniform load is assigned as live load in accordance with TS498. Snow load is also assigned as 0.5 kN/m^2 as per TS498.

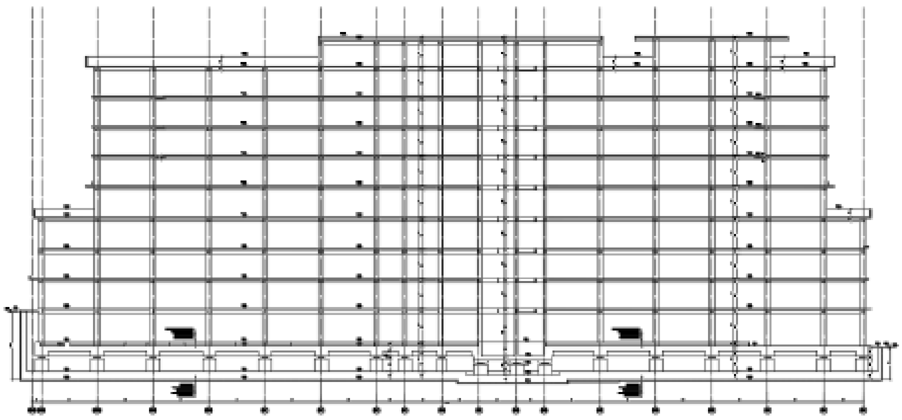

Figure 2.3 Elevation view of Kahramanmaraş State Hospital

The project includes 361 curved surface sliders which have a 1000 mm displacement capacity. To decrease displacement demand, metallic dampers will be used in this model and the behavior of the superstructure will be investigated; interstorey drifts, story accelerations, base shear of structure, and isolators' displacements will be compared with the original building design (i.e., isolated building without dampers).

To reduce the eccentricity of the building, dampers are added to the building to decrease the distance between the center of rigidity and center of mass shown in the Figure 2.4. These centers taken from analysis program. Three different points were selected to compare analyses results (i.e., displacements, accelerations, velocities, etc.). To this end, 2 points are selected from the far corners of the building plan (P1-P2), and one point is taken close to the centers (C). These points are illustrated in Figure 2.5.

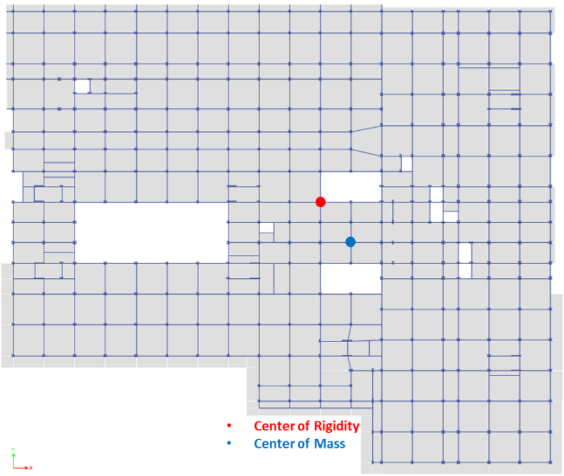

Figure 2.4 Center of rigidity and center of mass of the structure (B1)

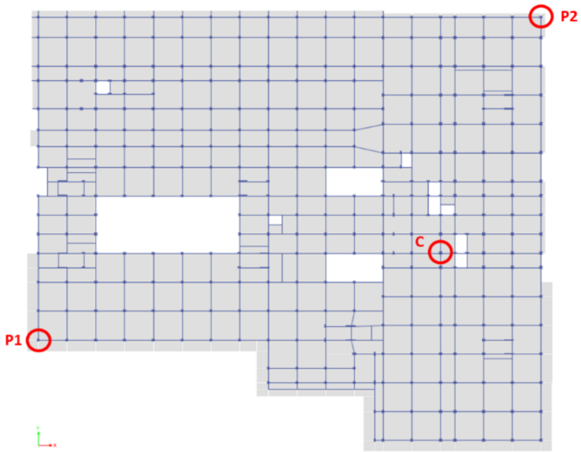

Figure 2.5 Selected points of the structure (B1)

In the first step, a total of 39 metallic dampers were added to decrease the eccentricity between the center of mass and the center of rigidity. Afterwards, the quantity of dampers increased to investigate the effect of number of dampers installed to the isolated building (B1). To this end, 39, 67, 83, and 109 dampers with and without stiffer metallic dampers were modelled, and the results of all analyses were examined. Performed analyses and their damper details are summarized in Table 2.1. The orientation of the dampers is also shown in Figure 2.6. These orientations selected based on a trial-error way.

Table 2.1 Conducted Numerical Analyses for B1 and their used abbreviations

No	**Analyses**	**Detail**
1	FPS	Friction Pendulum × 361
2	FPS-UD1	FPS + Metallic Damper × 39
3	FPS-UD1s	FPS + Stiffer Metallic Damper × 39
4	FPS-UD2	FPS + Metallic Damper × 67
5	FPS-UD2s	FPS + Stiffer Metallic Damper × 67
6	FPS-UD3	FPS + Metallic Damper × 83
7	FPS-UD3s	FPS + Stiffer Metallic Damper × 83
8	FPS-UD4	FPS + Metallic Damper × 109
9	FPS-UD4s	FPS + Stiffer Metallic Damper × 109
10	FPS-UD5	FPS + Metallic Damper × 361
11	FPS-UD5s	FPS + Stiffer Metallic Damper × 361

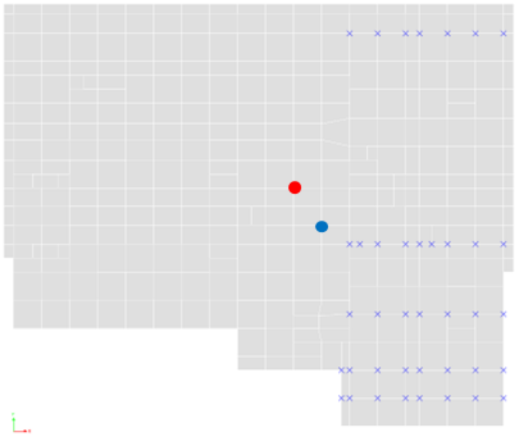

(a) FPS + Metallic Damper × 39

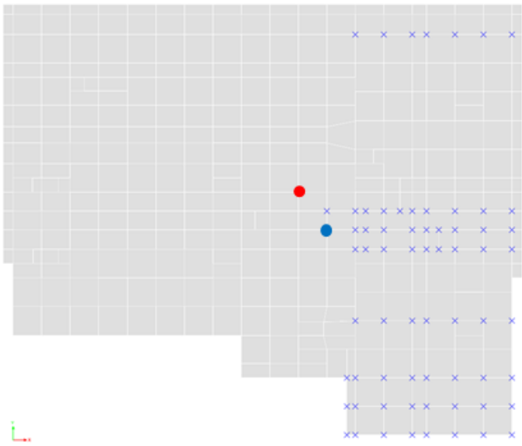

(b) FPS + Metallic Damper × 67

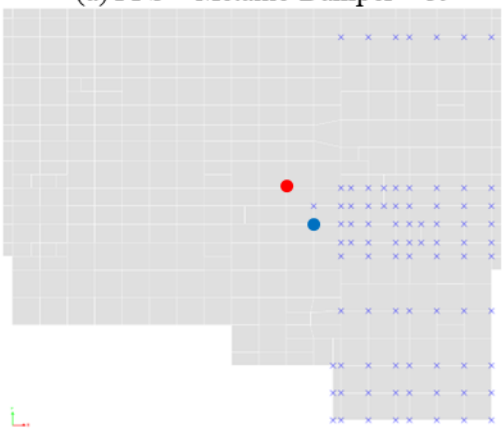

(c) FPS + Metallic Damper × 83

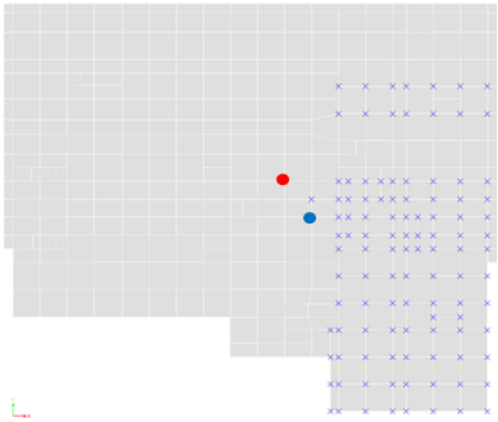

(d) FPS + Metallic Damper × 109

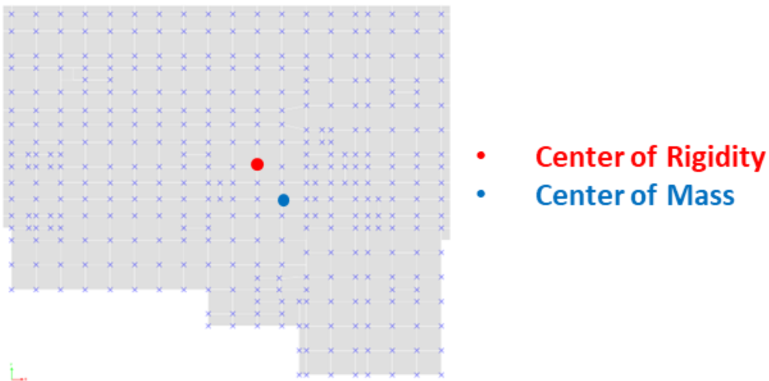

(e) FPS + Metallic Damper × 361

Figure 2.6 Damper configurations of each case

2.1.2 Seismicity and Selected Ground Motions

The hospital is located in a high seismic region in Turkey's South-East Anatolian Region (Figure 2.7). The soil class is ZC. Elastic spectra of Design Basis Earthquake (DBE) and Maximum Credible Earthquake (MCE) level earthquakes (Figure 2.8) were obtained from the Seismic Hazard Map of Disaster and Emergency Management Presidency (AFAD). These spectras were increased by a factor of 1.3 to consider the maximum direction of the earthquake as per TEC 2018.

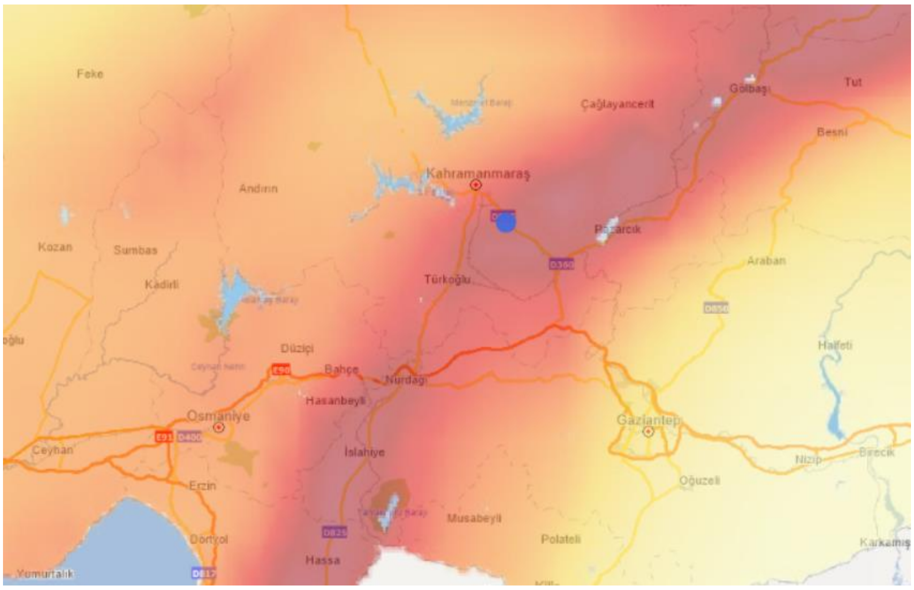

Figure 2.7 Location of the structure (B1)

To perform non-linear analysis, 11 strong ground motion records were selected from the PEER NGA-West2 Ground Motion Database and scaled based on the maximum target spectra of DBE and MCE hazard levels, separately. As shared in Figure 2.8, design period is determined as 3.6 sec and maximum period is determined as 5.2 sec. Design period is based on nominal friction parameters with design basis earthquake, maximum period is lower bound properties with maximum credible earthquake. As mentioned in TEC 2018, interval is determined as 0.5Td – 1.25Tm. Since the maximum allowed period is 6 sec, the upper limit of the range is limited to 6 seconds. Details of the selected ground motions are summarized in Table 2.2.

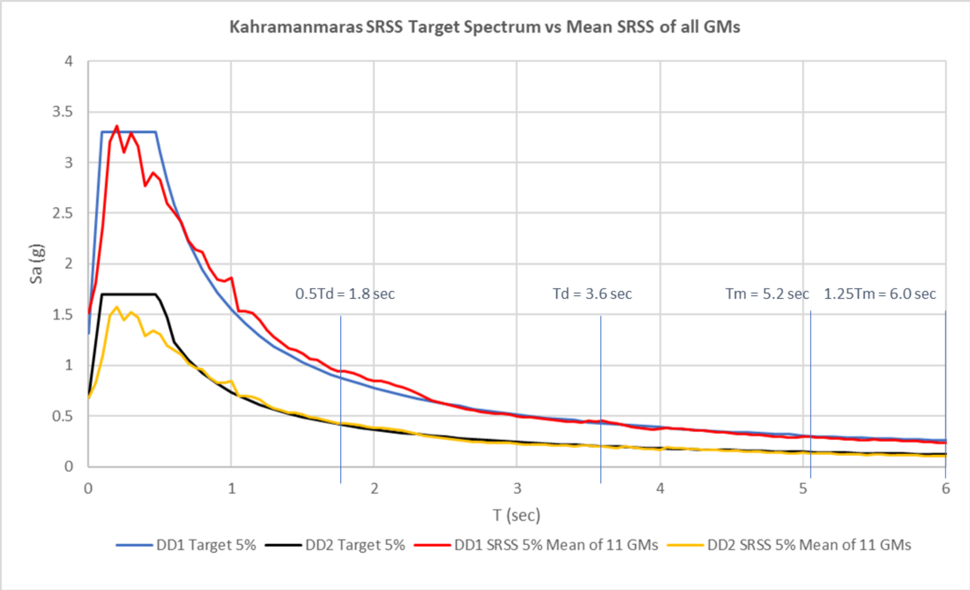

Figure 2.8 Target spectrum and mean SRSS of all GMs for B1

Table 2.2 Selected ground motions for B1

Record Name	Event Name	M_w *	R_{JB} * (km)	$V_{S,30}$ * (m/s)	FM	SF	
						DD1	DD2
126	Gazli, USSR	6.8	4	660	R	2.0	0.9
767	Loma Prieta	6.9	12	350	R	3.4	1.6
802	Loma Prieta	6.9	8	371	R	3.1	1.5
821	Erzincan, Turkey	6.7	0	275	S	2.5	0.8
1004	Northridge-01	6.7	0	380	R	2.0	1.0
1013	Northridge-01	6.7	0	629	R	0.9	0.9
1063	Northridge-01	6.7	0	282	R	4.5	0.4
1493	Chi-Chi, Taiwan	7.6	6	455	R	4.8	2.4
1515	Chi-Chi, Taiwan	7.6	5	473	R	4.0	1.9
1546	Chi-Chi, Taiwan	7.6	9	475	R	2.2	2.3
1605	Duzce, Turkey	7.1	0	276	S	2.4	1.1

* M_w: Richter magnitude, R_{JB}: Joyner and Boore (Ref) distance, $V_{s,30}$: Shear wave velocity in the top 30 m of the soil, FM: Fault mechanism, SF: Scale factor, DD1: Maximum credible earthquake and DD2: Design basis earthquake

2.1.3 Isolator and Damper Design

361 curved surface sliders were designed for this structure for its original design. Due to the variation of the axial loads, four different types of isolators were used to have an optimum solution. Based on service load, maximum static load and maximum seismic load isolators were grouped.

$$1.4G + 1.6Q \ (Maximum\ static\ axial\ load)$$

$$1.2G + Q \pm E \ (Maximum\ seismic\ axial\ load)$$

$$0.9G \pm E \ (Minimum\ seismic\ axial\ load)$$

$$G + 0.5Q \ (Maximum\ service\ axial\ load)$$

The design of isolator requires an iteration process. The design process starts with the assumption of the single-degree-of-freedom system's maximum displacement (d). First, the maximum horizontal force, effective horizontal stiffness, effective period, and effective damping of the single-degree-of-freedom system are calculated based on the equivalent friction coefficient, equivalent radius of curvature, total structure weight, and the assumed displacement.

$$F = N * \mu_{eq} + \frac{N * d}{R_{eq}}$$

$$K_{eff} = \frac{F}{d}$$

$$T_{eff} = 2 * \pi * \sqrt{\frac{W}{K_{eff}}}$$

$$\varepsilon_{eff} = \frac{2}{\pi} * \frac{\mu_{eq} * R_{eq}}{d + \mu_{eq} * R_{eq}}$$

From the design spectrum, S_{ae} is determined corresponding to T_{eff} and the displacement demand (d) is recalculated.

$$\eta_M = \sqrt{\frac{10}{5 + \varepsilon_{eff}}}$$

$$S_{ae,R} = S_{ae} * \eta_M$$

$$d_{new} = \frac{W * S_{ae,R}}{K_{eff}}$$

The iteration will continue until assumed displacement and the last displacement are equal or their difference falls below the tolerance value. The results of single degree system for B1 are given in Figure 2.9. Displacement demands, effective periods, effective rigidity, effective damping and base shear ratios are calculated based on equivalent radius of curvature and friction coefficient. Upper and lower bound properties are defined as 1.60 and 0.80, respectively. These values are determined by manufacturer. To define period range, period for “Lower Bound – DD1 Level” and period for “Nominal – DD2 Level” are used as stated in TEC 2018. For this project, these values are considered as 5.22 seconds and 3.60 seconds.

Total seismic weight, W	1.517.203 kN
Upper Bound Coefficient	1.6
Lower Bound Coefficient	0.80
Nominal - DD1 Level	
Equivalent friction coefficient of the system, μ	5.00%
Equivalent radius of curvature, R_{eq}	8700 mm
Effective period, T_{eff}	4.97 sn
Effective rigidity, K_{eff}	247549 kN/m
Effective damping, ξ	18.82 %
Maximum horizontal displacement	±1037mm
Maximum base shear	0.169W (R=1)
Nominal - DD2 Level	
Equivalent friction coefficient of the system, μ	5.00%
Equivalent radius of curvature, R_{eq}	8700 mm
Effective period, T_{eff}	3.60 sn
Effective rigidity, K_{eff}	472326 kN/m
Effective damping, ξ	40.16 % (%30 Limited)
Maximum horizontal displacement	±255mm
Maximum base shear	0.079W (R=1)
Lower Bound- DD1 Level	
Equivalent lower bound friction coefficient of the system, μ_{LB}	4.00%
Equivalent radius of curvature, R_{eq}	8700 mm
Effective period, T_{eff}	5.22 sn
Effective rigidity, K_{eff}	224412 kN/m
Effective damping, ξ	14.19 %
Maximum horizontal displacement	±1213mm
Maximum base shear	0.179W (R=1)
Upper Bound - DD2 Level	
Equivalent upper bound friction coefficient of the system, μ_{UB}	8.00%
Equivalent radius of curvature, R_{eq}	8700 mm
Effective period, T_{eff}	2.91 sn
Effective rigidity, K_{eff}	721444 kN/m
Effective damping, ξ	48.27 % (%30 Limited)
Maximum horizontal displacement	±222mm
Maximum base shear	0.105W (R=1)

Figure 2.9 Results of SDOF analysis for B1

Isolators are designed DBE upper bound parameters (DBE UB) and MCE lower bound parameters (MCE LB) separately. Upper bound represents friction coefficient is higher than designed value and lower bound represents friction coefficient lower than designed value. This designed value is named as nominal case. These parameters are determined by considering environmental conditions and production variability by the manufacturer. The superstructure's story acceleration and base shear are controlled based on DBE UB parameters and the displacement capacity of links is controlled based on MCE LB parameters as stated in TEC 2018. The force-displacement backbone curves of isolators are assumed to be bilinear and these bilinear force-displacement capacity curves as per DBE UB and MCE LB are shown in Figures 2.10 and 2.11. Isolators are modeled as link elements in the ETABS. Isolators are modeled as isolator links (friction pendulum). The inputs for the damper link elements are given in Figure 2.13. Moreover, as mentioned before, there is 361 isolators and these links are grouped based on the axial load variation. For this project, there will be 4 different isolators.

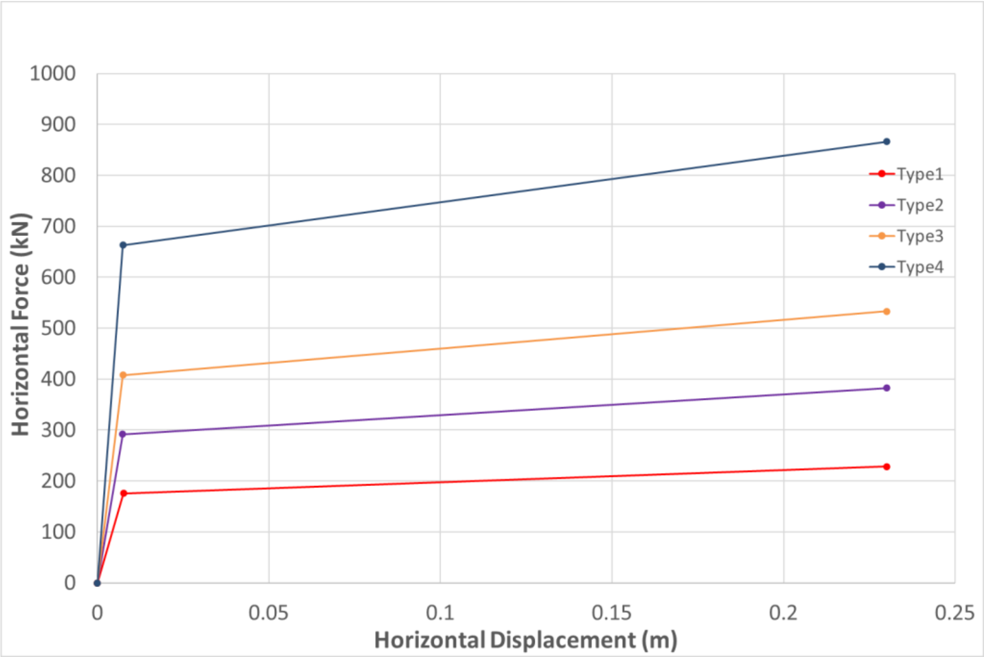

Figure 2.10 Force – displacement capacity curves of isolators (DBE UB)

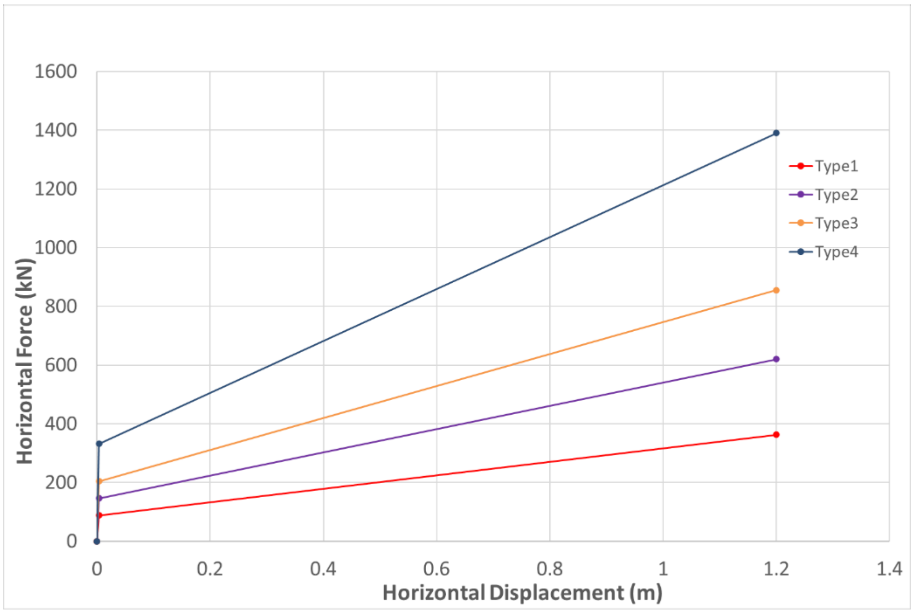

Figure 2.11 Force – displacement capacity curves of isolators (MCE LB)

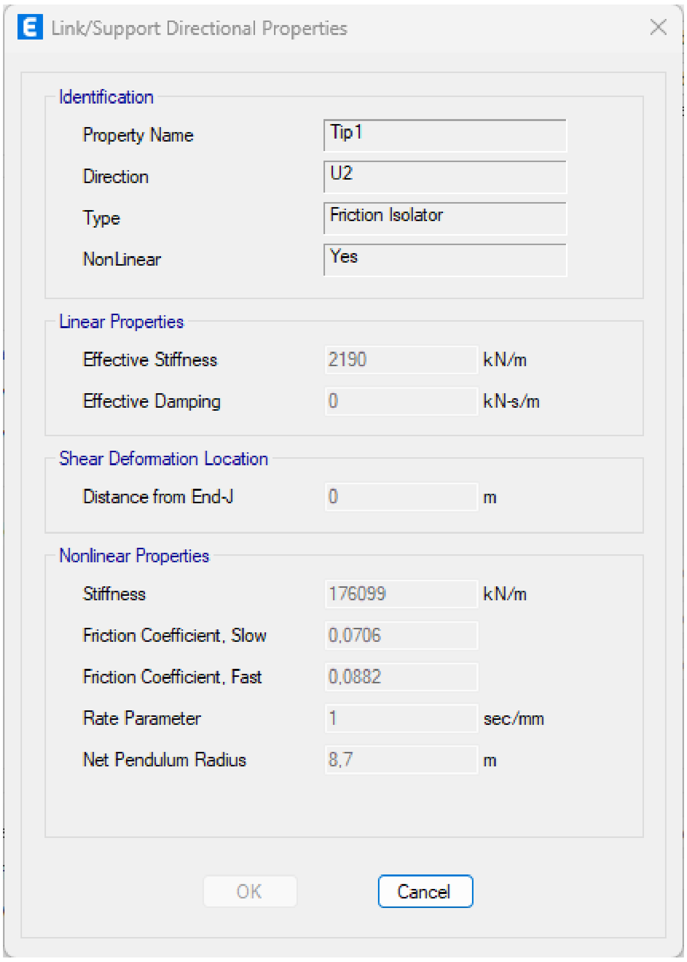

Figure 2.12 Example Link Properties – Friction Isolator

In the scope of this hospital project, metallic-yielding dampers are assumed to be used in the nonlinear analyses. Two different dampers are selected according to their rigidity and yielding parameters. One of the dampers has a low-yielding point, the other one is larger. The general philosophy to decide on the damper properties is the yielding sequence of dampers and isolators. In other words, the order of yielding for the two types of dampers are different. For U Damper (i.e., lower strength), it is aimed to have dampers yielding before isolators. Similarly, for U Damper - stiffer (i.e., higher strength), dampers are designed so that isolators yield before dampers. MCE LB and DBE UB force-displacement curves are shown in Figures 2.13 and 2.14. Yielding forces (characteristic strengths) of isolators and dampers are also shown in Table 2.3. These parameters are taken from manufacturer data sheet (Nippon Steel Metallic Damper Specification).

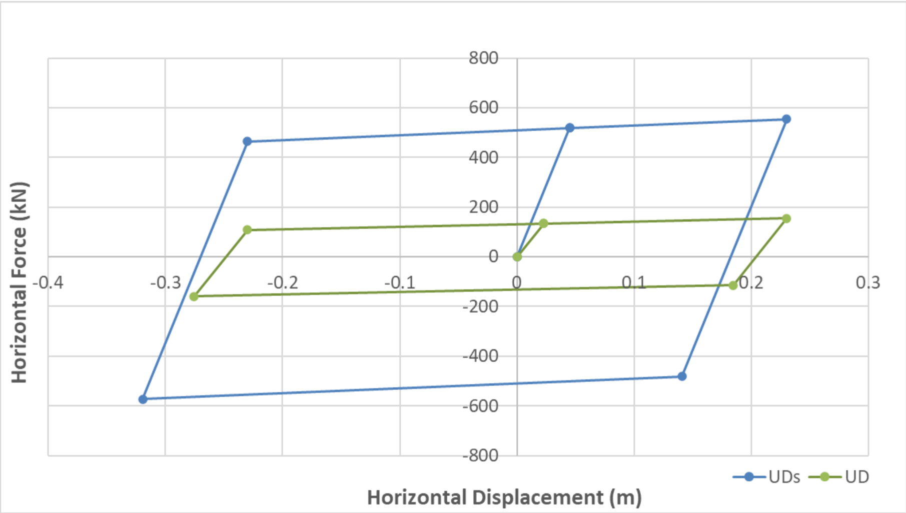

Figure 2.13 Force – displacement capacity curves of metallic dampers (DBE UB)

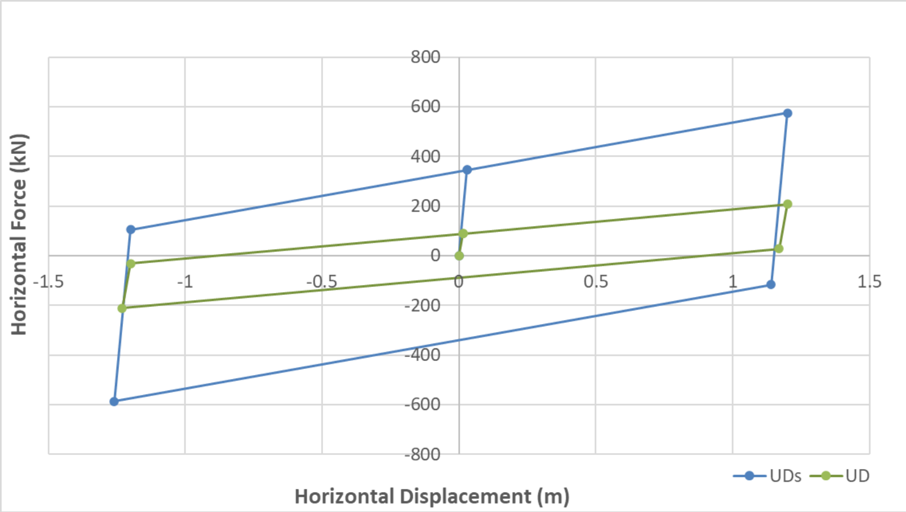

Figure 2.14 Force – displacement capacity curves of metallic dampers (MCE LB)

Table 2.3 Characteristic Strength of Devices (kN/m)

	DBE UB	MCE LB
Type1	178	89
Type2	291	145
Type3	408	204
Type4	663	331
U Damper	135	88
U Damper - stiffer	520	346

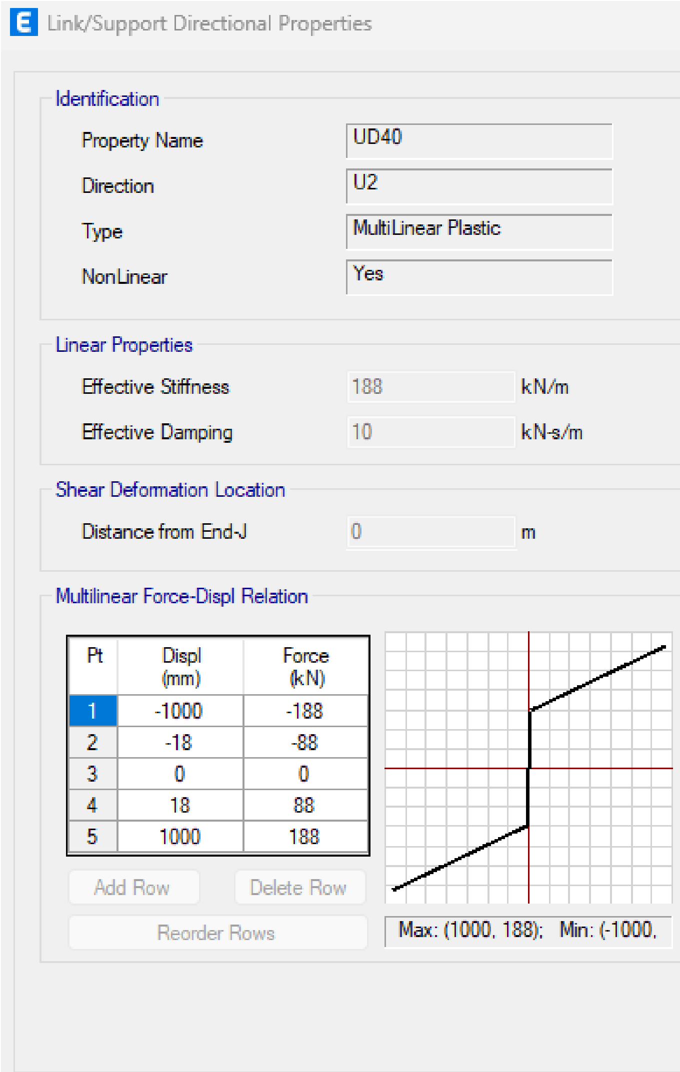

Figure 2.15 Example Link Properties – Metallic Damper

Metallic dampers are modeled as link elements in the 3D analysis program ETABS. To provide the same rigidity in all directions, four dampers are modeled for each isolator link (Multilinear Plastic). The orientation of the dampers is shown in Figure 2.16. The inputs for the damper link elements are given in Figure 2.15.

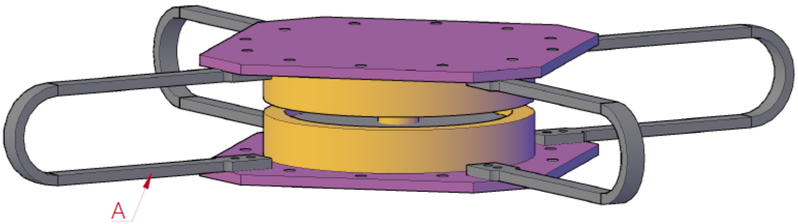

Figure 2.16 Selected damper and isolator

2.2 Adıyaman Residential Building

2.2.1 Building Information Modelling

The second project is a residential building located in Adıyaman, Kahta. The structure was designed in 2020 and construction has not started yet. The structural system consists of columns and beams, structure has a shear wall only under the isolation level at the basement level. The plan geometry is 30 m in the X direction, 16 m in the Y direction, the total height is 31 m and the structure has 11 stories.

The column dimensions are mostly 600x600 mm, beam dimensions are mostly 800x400 mm. At under isolation level, pedestal sizes are 1000x1000 mm due to isolator diameters and all reinforced concrete elements have C40/50 type concrete.

A 3D structural model was created and analyzed in ETABS v19.1.0 and the 3D view and plan geometry are given Figure 2.17 and Figure 2.18. Elevation view of the structure is shown in Figure 2.19.

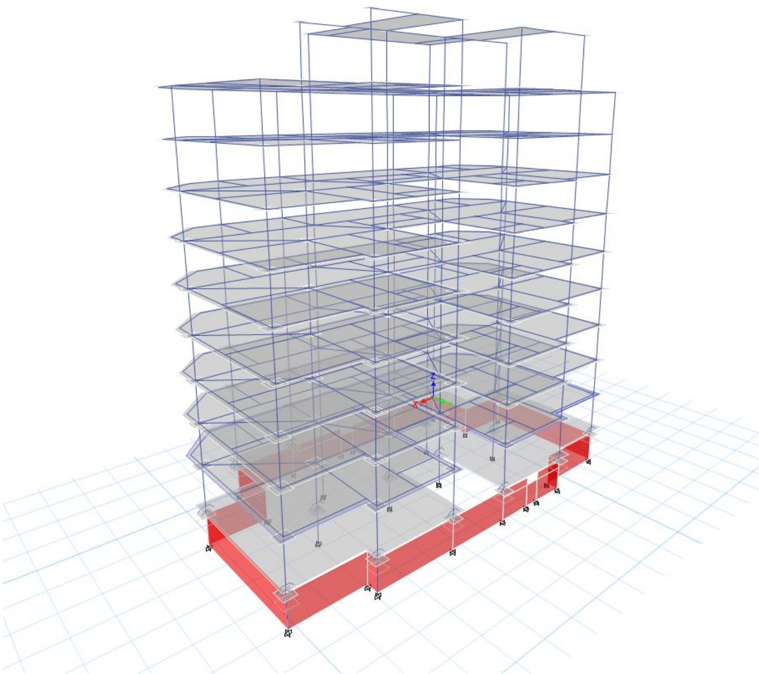

Figure 2.17 Structural model of Adıyaman Residential Building

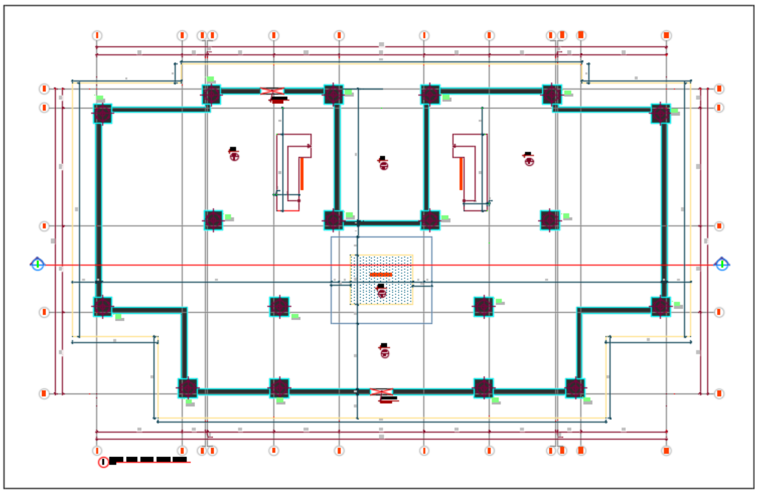

Figure 2.18 Architectural plan of the structure of Adıyaman Residential Building

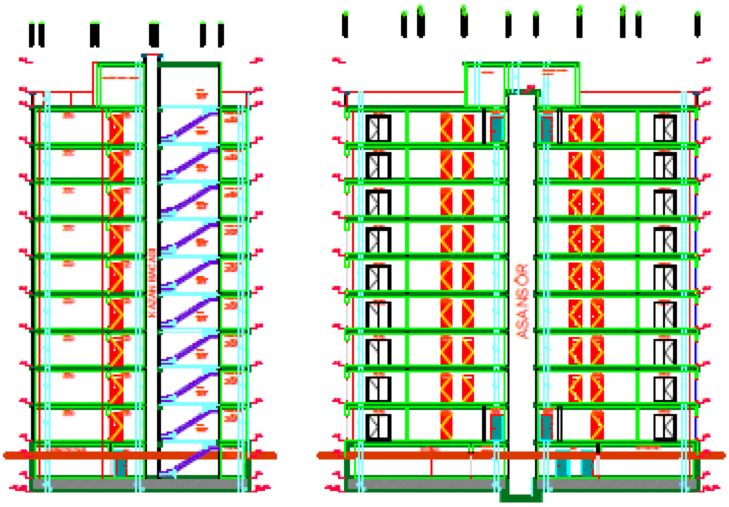

Figure 2.19 Elevation view of the Adıyaman Residential Building

In addition to the self-weight of the structure, 2.2 kN/m^2 uniform load is assigned as dead load, and 2 kN/m^2 uniform load is assigned as live load. Snow load is also assigned as 0.75 kN/m^2 on the roof.

The building includes 18 curved surface sliders which have a 250 mm displacement capacity. Even if displacement demands are not as higher as that of the previous structure, the aim is to observe the upper structure behavior of additional dampers here. To decrease displacement demand, metallic dampers will be used in this model, and the behavior of the superstructure will be investigated; interstorey drifts, story accelerations, base shear of structure, and isolators' displacements will be compared with the current model. To add dampers symmetrically, the center of rigidity and center of mass are calculated and shown in the Figure 2.20.

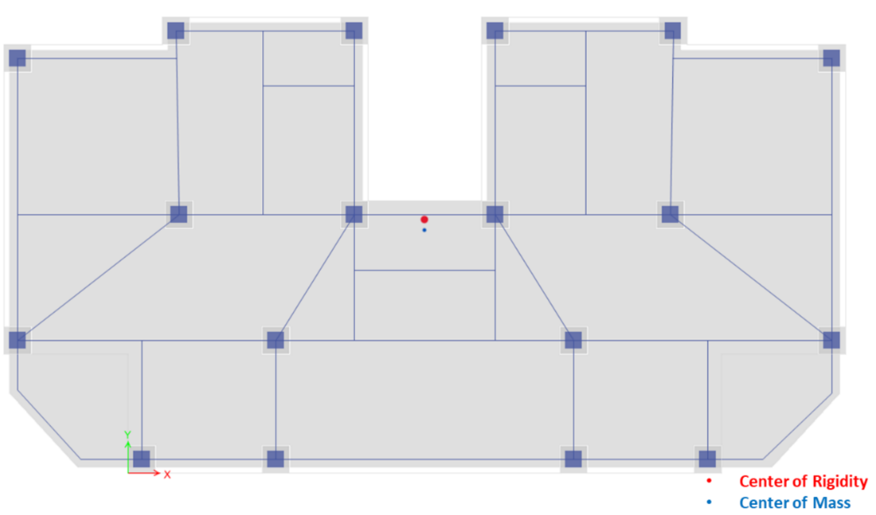

Figure 2.20 Center of rigidity and center of mass of the structure (B2)

The center of rigidity and center of mass are quite close to each other, that's why dampers will be assigned according to these points symmetrically. To investigate the different behavior of isolators, three different points were selected to compare displacements; 2 points from the far corners(P1-P2), and one point close to the centers(C).

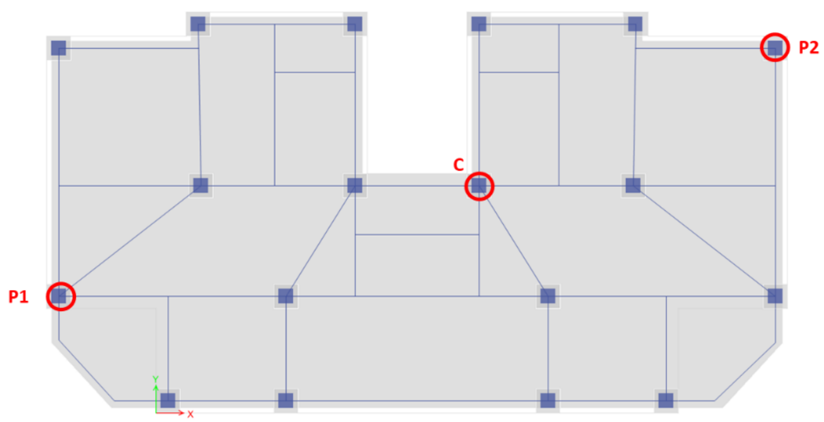

Figure 2.21 Selected points of the structure (B2)

In addition to 18 seismic isolators, 4, 8, and 18 metallic dampers are added. Two different types of metallic dampers are selected UD and UDs. The stiffness of the first one is lower than the second one, UDs means stiffer metallic damper. Selected points that have dampers are pointed in Figure 2.21. Analyses and abbreviations are also mentioned in Table 2.4.

Table 2.4 Conducted Numerical Analyses for B2 and their used abbreviations

Analyses	Detail
FPS	Friction Pendulum × 18
FPS-UD1	FPS + Metallic Damper × 4
FPS-UD1s	FPS + Stiffer Metallic Damper × 4
FPS-UD2	FPS + Metallic Damper × 8
FPS-UD2s	FPS + Stiffer Metallic Damper × 8
FPS-UD3	FPS + Metallic Damper × 18
FPS-UD3s	FPS + Stiffer Metallic Damper × 18

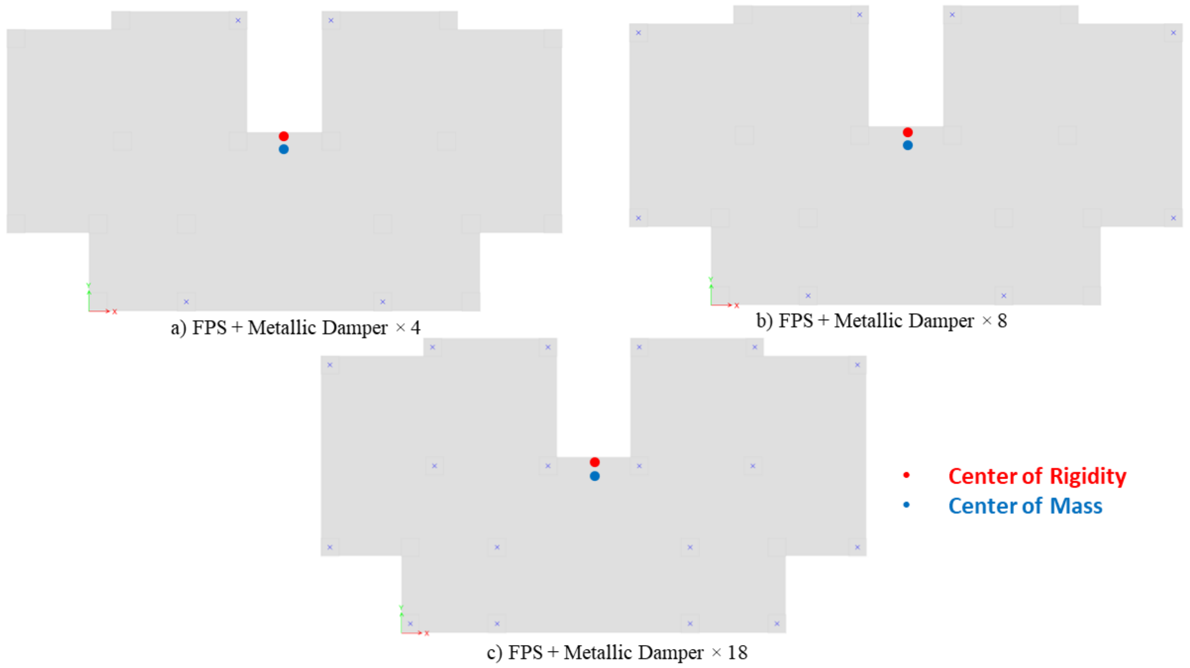

Figure 2.22 Damper configurations of each analysis

2.2.2 Seismicity and Selected Ground Motions

The building is in a high seismic region in Turkey's South-East Anatolian Region but the distance to the fault is more than 20 km and the soil class is ZC. That's why elastic spectras and accelerations are not too high. Elastic spectra of DBE and MCE level earthquakes were obtained from the Seismic Hazard Map of AFAD. These spectrums were increased by 1.3 times to consider the maximum direction of the earthquake.

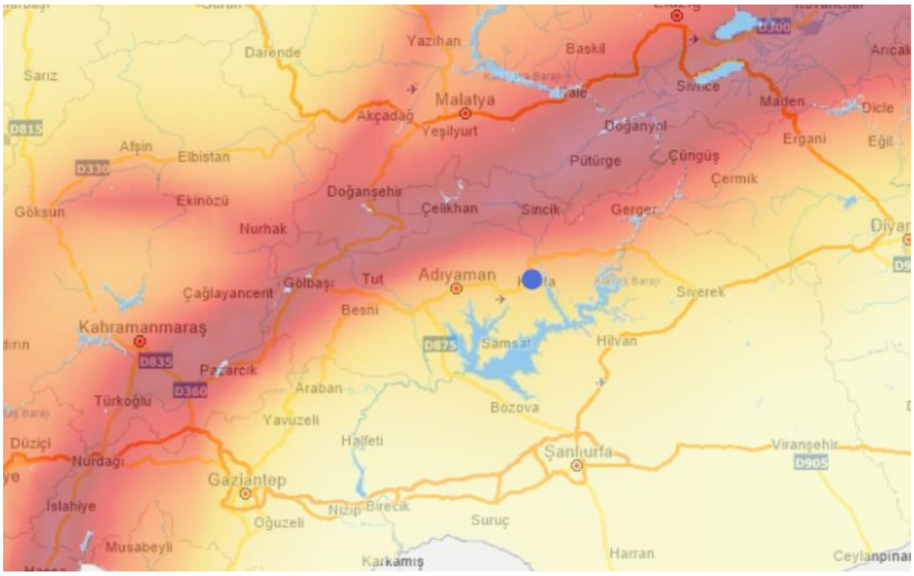

Figure 2.23 Location of the structure (B2)

To perform non-linear analysis, 11 ground motions are selected from the PEER NGA-West2 Ground Motion Database and scaled based on the maximum target spectrum DBE and MCE separately. As shared in Figure 2.24, design period is determined as 2.7 seconds and maximum period is determined as 3.4 sec. Design period is based on nominal friction parameters with design basis earthquake, maximum period is lower bound properties with maximum credible earthquake. As mentioned in TEC 2018, interval is determined as 0.5Td – 1.25Tm. So, range is considered as 1.4 – 4.3 seconds. Details of selected ground motions are given in Table 2.5.

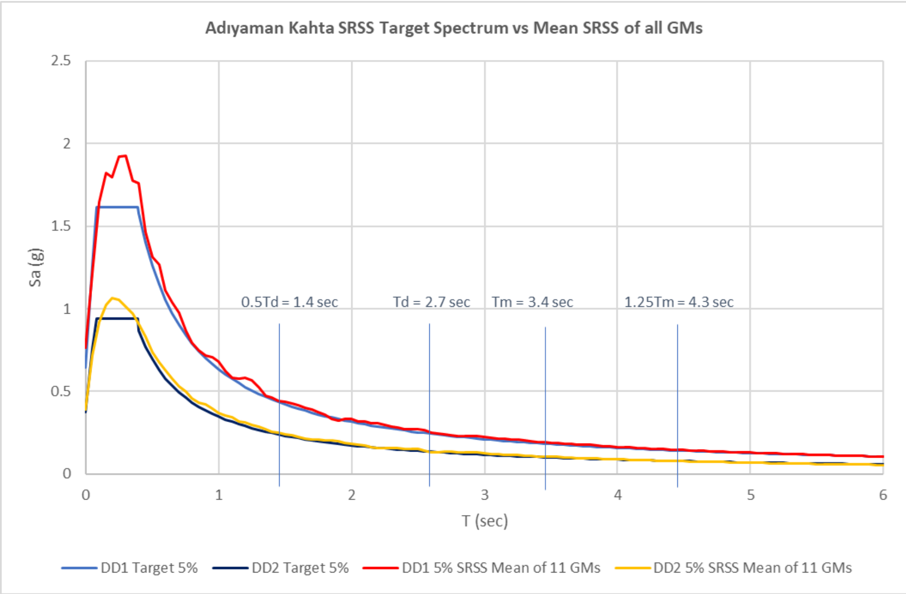

Figure 2.24 Target spectrum and mean SRSS of all GMs for B2

Table 2.5 Selected ground motions for B2

Record Name	Event Name	M_w *	R_{JB} * (km)	$V_{S,30}$ * (m/s)	FM	SF	
						DD1	DD2
1160	Kocaeli, Turkey	7.5	53	387	S	3.3	1.6
1205	Chi-Chi, Taiwan	7.6	19	492	R	1.8	1.0
1208	Chi-Chi, Taiwan	7.6	24	442	R	1.6	0.9
1794	Hector Mine	7.1	31	379	S	1.7	0.9
1813	Hector Mine	7.1	53	396	S	2.1	1.1
3752	Landers	7.3	45	436	S	3.2	1.9
3756	Landers	7.3	41	368	S	1.7	1.0
5776	Iwate, Japan	6.9	25	478	R	2.2	1.2
6915	Darfield, New Zealand	7.0	24	422	S	2.3	1.3
6928	Darfield, New Zealand	7.0	25	650	S	2.6	1.5
6948	Darfield, New Zealand	7.0	31	482	S	2.8	2.2

* M_w: Richter magnitude, R_{JB}: Joyner and Boore (Ref) distance, $V_{s,30}$: Shear wave velocity in the top 30 m of the soil, FM: Fault mechanism, SF: Scale factor, DD1: Maximum credible earthquake and DD2: Design basis earthquake

2.2.3 Isolator and Damper Design

18 curved surface sliders were designed for this structure. Due to the plan geometry of the structure being quite regular, one type of isolator was enough to have an optimum solution. Based on service load, maximum static load and maximum seismic load isolators were designed. The results of a single-degree-of-freedom system are shared in Figure 2.25.

Total seismic weight, W	44141 kN
Upper Bound Coefficient	1.6
Lower Bound Coefficient	0.80
Nominal - DD1 Level	
Equivalent friction coefficient of the system, μ	5.65%
Equivalent radius of curvature, R_{eq}	4900 mm
Effective period, T_{eff}	3.09 sn
Effective rigidity, K_{eff}	18633 kN/m
Effective damping, ξ	32.88 % (%30 Limited)
Maximum horizontal displacement	±259mm
Maximum base shear	0.109W (R=1)
Nominal - DD2 Level	
Equivalent friction coefficient of the system, μ	5.65%
Equivalent radius of curvature, R_{eq}	4900 mm
Effective period, T_{eff}	2.65 sn
Effective rigidity, K_{eff}	25389 kN/m
Effective damping, ξ	41.07 % (%30 Limited)
Maximum horizontal displacement	±152mm
Maximum base shear	0.088W (R=1)
Lower Bound- DD1 Level	
Equivalent lower bound friction coefficient of the system, μ_{LB}	4.52%
Equivalent radius of curvature, R_{eq}	4900 mm
Effective period, T_{eff}	3.35 sn
Effective rigidity, K_{eff}	15847 kN/m
Effective damping, ξ	27.47 %
Maximum horizontal displacement	±292mm
Maximum base shear	0.105W (R=1)
Upper Bound - DD2 Level	
Equivalent upper bound friction coefficient of the system, μ_{UB}	9.04%
Equivalent radius of curvature, R_{eq}	4900 mm
Effective period, T_{eff}	2.03 sn
Effective rigidity, K_{eff}	43192 kN/m
Effective damping, ξ	50.38 % (%30 Limited)
Maximum horizontal displacement	±117mm
Maximum base shear	0.114W (R=1)

Figure 2.25 Results of SDOF analysis for B2

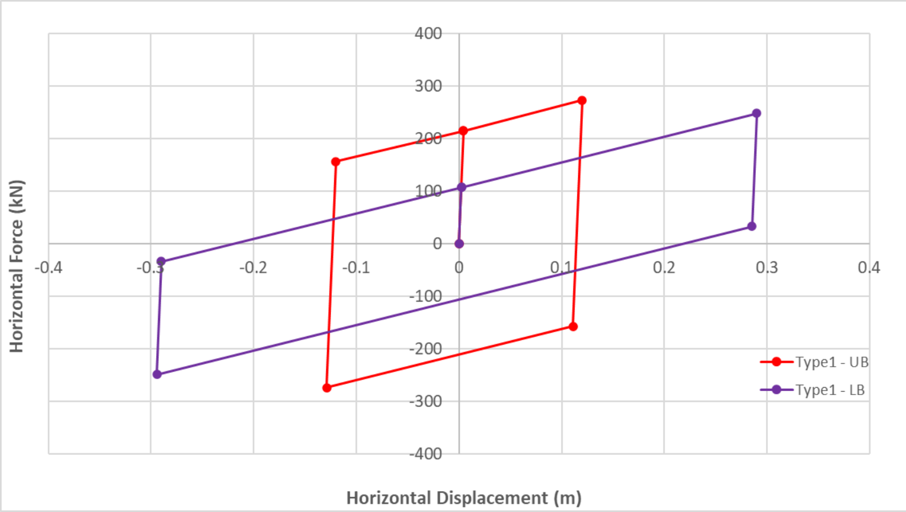

Figure 2.26 Force – displacement capacity curves of isolators (DBE UB – MCE LB)

The structure has total of 18 isolators and all isolators designed as same type based on axial load variation. Force-Displacement curves of isolators for DBE UB and MCE LB are shown in Figure 2.26. In the scope of this residential project, metallic-yielding dampers are assumed to be used in the nonlinear analyses. Two different dampers are selected according to their rigidity and yielding parameters. As in the B1, one of the dampers has a low-yielding point, the other one is larger. The general philosophy to decide on the damper properties is the yielding sequence of dampers and isolators. In other words, the order of yielding for the two types of dampers are different. For U Damper (i.e., low yielding), it is aimed to have dampers yielding before isolators. Similarly, for U Damper - stiffer (i.e., large yielding), dampers are designed so that isolators yield before dampers. Force-Displacement curves of these dampers are shown in Figures 2.27 and 2.28. Characteristic strengths of isolators and dampers are shown in Table 2.6.

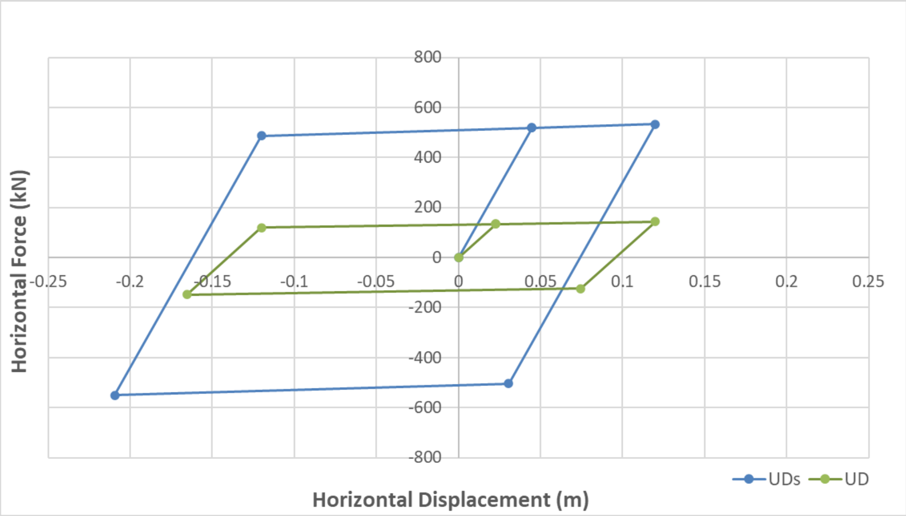

Figure 2.27 Force – displacement capacity curves of metallic dampers (DBE UB)

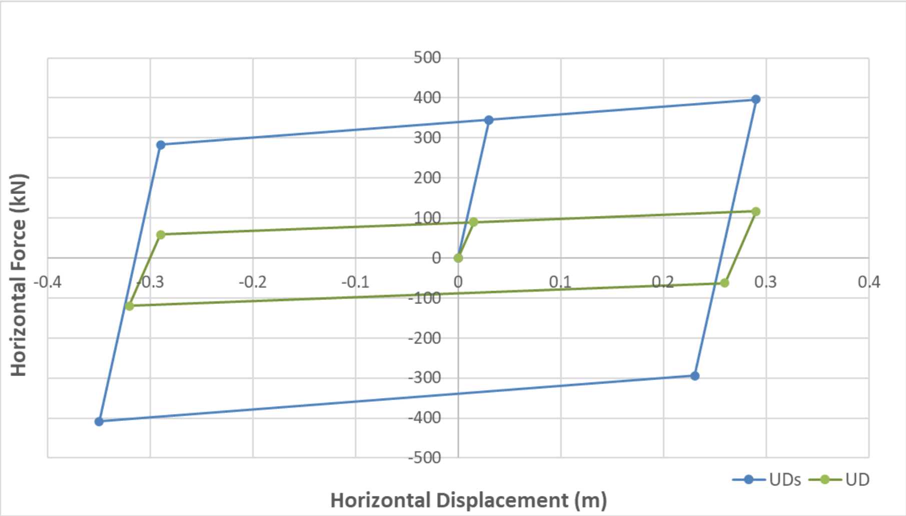

Figure 2.28 Force – displacement capacity curves of metallic dampers (MCE LB)

Table 2.6 Characteristic Strength of Devices (kN/m)

	DBE UB	**MCE LB**
Type1	215	108
U Damper	135	88
U Damper - stiffer	520	346

Metallic dampers are modeled as multilinear plastic elements in the 3D analysis program ETABS. To provide the same rigidity in all directions, four dampers are used for each isolator link. The orientation of the dampers is shown in Figure 2.29.

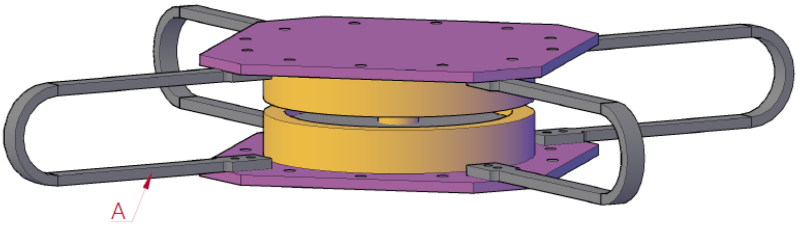

Figure 2.29 Selected damper and isolator

2.3 Bolu PMR Hospital

2.3.1 Building Model Information

The third project is a hospital project located in Bolu. The design of the structure continues in 2024. The structural system consists of columns and beams, structure has a shear wall only under the isolation level at the basement level. The plan geometry is 116 m in the X direction, 125 m in the Y direction, the total height is 39 m, and the structure has 8 stories.

The column dimensions are mostly 1000x1000 mm, beam dimensions are mostly 750x1000 mm. All beams and columns have C35/45 type concrete above the isolation level. At isolation level, pedestal sizes are 2500x2500 mm due to isolator diameters and pedestals have C45/55 type concrete. The structure has shear walls only at substructure.

A 3D structural model was created and analyzed in ETABS v19.1.0 and the 3D view and plan geometry are given below. (Figure 2.30 – Figure 2.31)

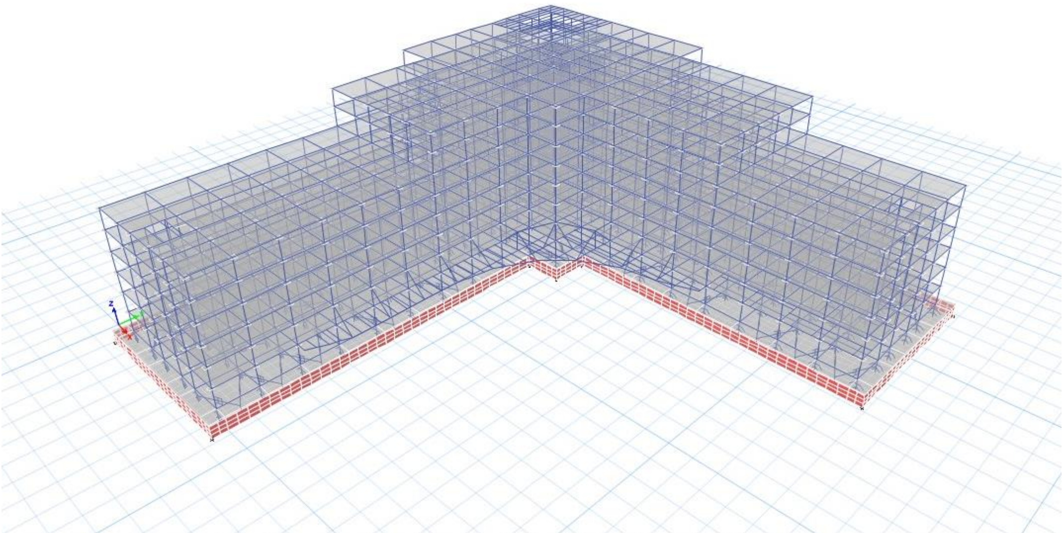

Figure 2.30 Structural model of Bolu PMR Hospital

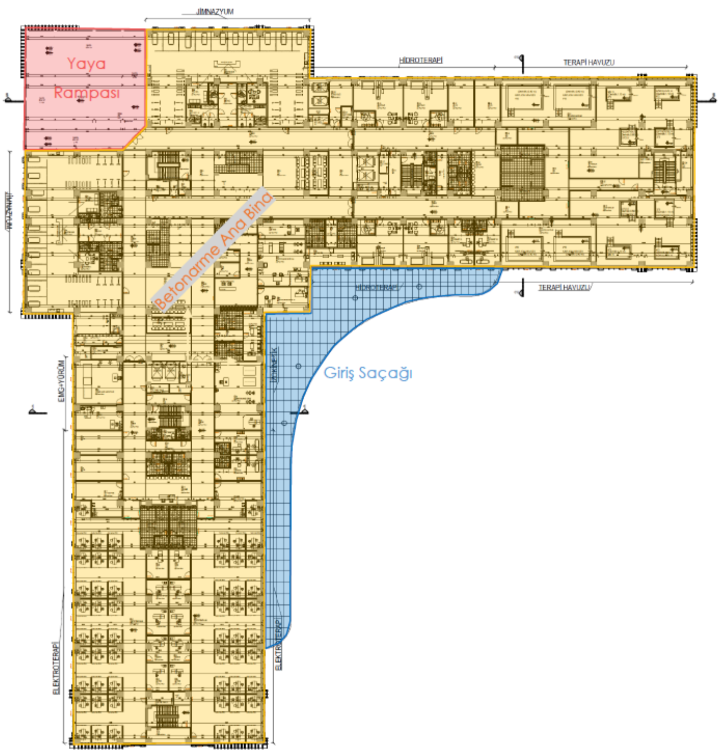

Figure 2.31 Architectural plan of Bolu PMR Hospital

In addition to the self-weight of the structure, 3 kN/m^2 uniform load is assigned as dead load, and 3.5 kN/m^2 uniform load is assigned as live load.

The building includes 184 curved surface sliders which have an 1800 mm displacement capacity. Since it is not possible to produce and test an isolator of this capacity, the use of dampers has become mandatory in the project. Apart from the first two structures, metallic dampers did not select for B3. To have higher damping ratio, fluid viscous dampers were chosen.

The aim is to decrease the displacement demand of isolators 1 meter around and observe the upper structure behavior of the additional damper. At each step, interstorey drifts, story accelerations, base shear of structure, and isolators' displacements will be compared with the current model without any extra energy dissipation devices.

To add dampers symmetrically, the center of rigidity and center of mass are calculated and shown in the figure. It is assumed that viscous dampers will not add any rigidity to the system because these dampers are velocity dependent device. So, there is no effective stiffness for this dampers and center of rigidity will not shift.

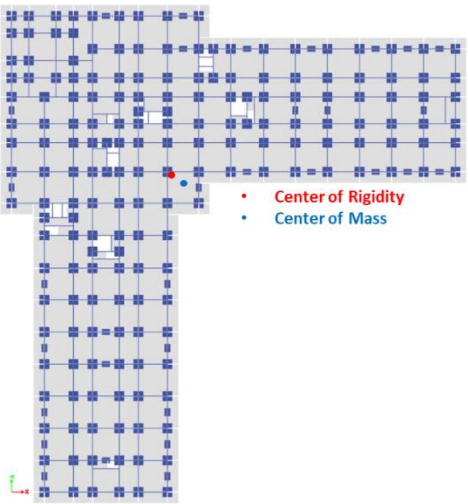

Figure 2.32 Center of rigidity and center of mass (B3)

The center of rigidity and center of mass are quite close to each other, that's why dampers will be assigned according to these points symmetrically. (Figure 2.32) To investigate the different behaviors of isolators, six different points were selected to compare displacements; five points from the far corners(P1-P2-P3-P4-P5), and one point close to the center(C). (Figure 2.33)

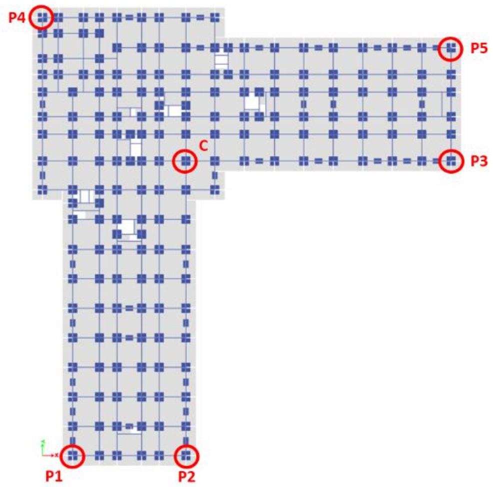

Figure 2.33 Selected points of the structure (B3)

To decrease displacement demand by around 1 meter, the quantity of viscous dampers is changed at each step. Including the original model, five different models are analyzed, and results are compared. The orientation and abbreviation of models are given in Figure 2.34 and Table 2.7.

Table 2.7 Conducted Numerical Analyses for B3 and their used abbreviations

No	Analyses	Detail
1	FPS	Friction Pendulum × 184
2	FPS-VD1	FPS + Viscous Damper × 32
3	FPS-VD2	FPS + Viscous Damper × 40
4	FPS-VD3	FPS + Viscous Damper × 52
5	FPS-VD4	FPS + Viscous Damper × 64

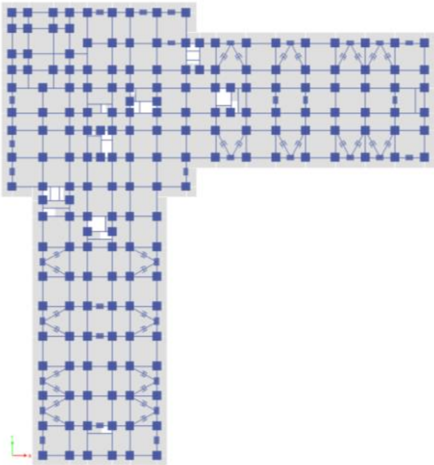

a) FPS + Viscous Damper × 32

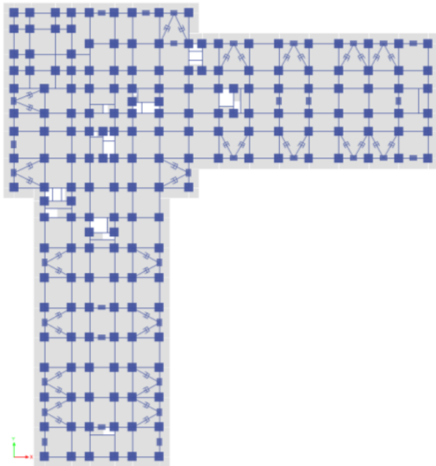

b) FPS + Viscous Damper × 40

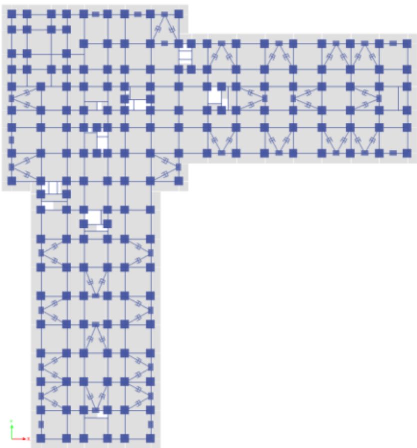

c) FPS + Viscous Damper × 52

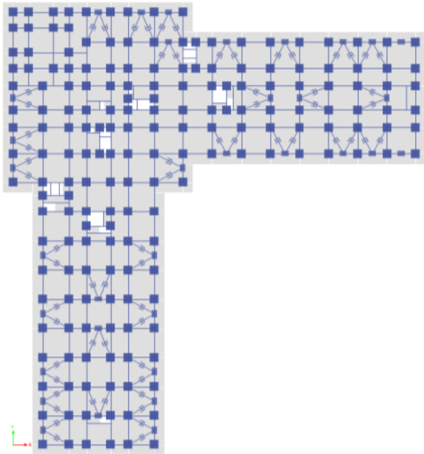

d) FPS + Viscous Damper × 64

Figure 2.34 Damper configuration for each analysis

2.3.2 Seismicity and Selected Ground Motions

The building is in a high seismic region in Turkey's North-West Anatolian Region and the distance to the fault is less than 1 km. The soil class is ZC. That’s why elastic spectrums and accelerations are too high. Elastic spectra of DBE and MCE level earthquakes were obtained from the Seismic Hazard Map of AFAD. These spectrums were increased by 1.3 times to consider the maximum direction of the earthquake.

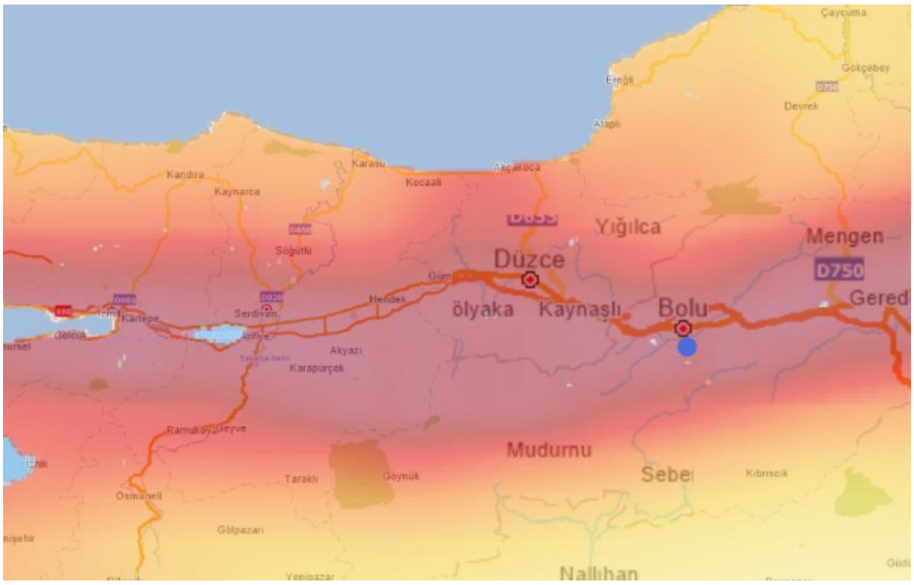

Figure 2.35 Location of the structure (B3)

To perform non-linear analysis, 11 ground motions are selected from the PEER NGA-West2 Ground Motion Database and scaled based on the maximum target spectrum DBE and MCE separately. As shared in Figure 2.37, design period is determined as 3.4 sec and maximum period is determined as 5.0 sec. Design period is based on nominal friction parameters with design basis earthquake, maximum period is lower bound properties with maximum credible earthquake. As mentioned in TEC 2018, interval is determined as 0.5Td – 1.25Tm. Since the maximum allowed period is 6 sec, the upper limit of the range is limited to 6 seconds. Details of selected ground motions are given in Table 2.8.

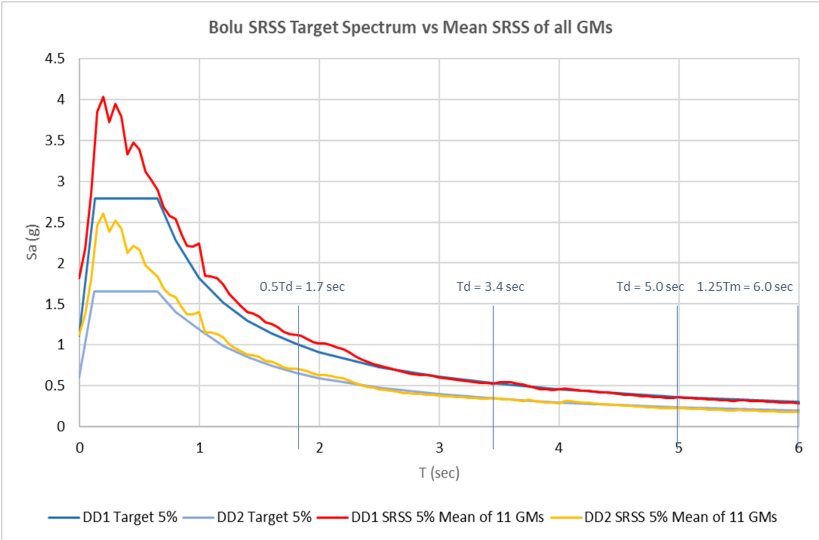

Figure 2.36 Target spectrum and mean SRSS of all GMs for B3

Table 2.8 Selected ground motions for B3

Record Name	**Event Name**	**M_w ***	**R_{JB} * (km)**	**$V_{S,30}$ * (m/s)**	**FM**	**SF**	
						DD1	**DD2**
173	Imperial Valley-06	6.5	8	203	S	2.9	1.6
181	Imperial Valley-06	6.5	0	203	S	1.2	0.7
1158	Kocaeli, Turkey	7.5	13	280	S	2.7	1.4
1176	Kocaeli, Turkey	7.5	1.4	300	S	1.7	0.9
1762	Hector Mine	7.1	41	383	S	4.9	2.5
5825	El Mayor-Cucapah, Mexico	7.2	8	242	S	2.9	1.2
5829	El Mayor-Cucapah, Mexico	7.2	13	242	S	3.1	2.1
5831	El Mayor-Cucapah, Mexico	7.2	14	242	S	3.7	1.6
6893	Darfield, New Zealand	7.0	12	344	S	4.2	1.3
6927	Darfield, New Zealand	7.0	5	263	S	1.6	1.0
6952	Darfield, New Zealand	7.0	19	263	S	2.0	1.0

* M_W: Richter magnitude, R_{JB}: Joyner and Boore (Ref) distance, $V_{s,30}$: Shear wave velocity in the top 30 m of the soil, FM: Fault mechanism, SF: Scale factor, DD1: Maximum credible earthquake and DD2: Design basis earthquake

2.3.3 Isolator and Damper Design

184 curved surface sliders were designed for this structure. Due to the variation of the axial loads, three different types of isolators were used to have an optimum solution. Based on service loads, maximum static loads and maximum seismic loads isolators were designed. Based on service axial loads, the Bi-Linear behaviors of isolators are shown below. (Figure 2.38 – 2.39) The results of a single-degree-of-freedom system are also

shared in Figure 2.37. For fluid viscous damper, parameters are taken from manufacturer specification (Taylor Devices).

Total seismic weight, W	1059417 kN
Upper Bound Coefficient	1.6
Lower Bound Coefficient	0.85
Nominal - DD1 Level	
Equivalent friction coefficient of the system, μ	5.20%
Equivalent radius of curvature, R_{eq}	7400 mm
Effective period, T_{eff}	4.94 sn
Effective rigidity, K_{eff}	174890 kN/m
Effective damping, ξ	11.55 %
Maximum horizontal displacement	±1736mm
Maximum base shear	0.287W (R=1)
Nominal - DD2 Level	
Equivalent friction coefficient of the system, μ	5.20%
Equivalent radius of curvature, R_{eq}	7400 mm
Effective period, T_{eff}	4.52 sn
Effective rigidity, K_{eff}	208380 kN/m
Effective damping, ξ	19.93 %
Maximum horizontal displacement	±845mm
Maximum base shear	0.166W (R=1)
Lower Bound- DD1 Level	
Equivalent lower bound friction coefficient of the system, μ_{LB}	4.42%
Equivalent radius of curvature, R_{eq}	7400 mm
Effective period, T_{eff}	5.04 sn
Effective rigidity, K_{eff}	167735 kN/m
Effective damping, ξ	9.33 %
Maximum horizontal displacement	±1906mm
Maximum base shear	0.302W (R=1)
Upper Bound - DD2 Level	
Equivalent upper bound friction coefficient of the system, μ_{UB}	8.32%
Equivalent radius of curvature, R_{eq}	7400 mm
Effective period, T_{eff}	3.84 sn
Effective rigidity, K_{eff}	288686 kN/m
Effective damping, ξ	32.09 % (%30 Limited)
Maximum horizontal displacement	±606mm
Maximum base shear	0.165W (R=1)

Figure 2.37 Results of SDOF analysis for B3

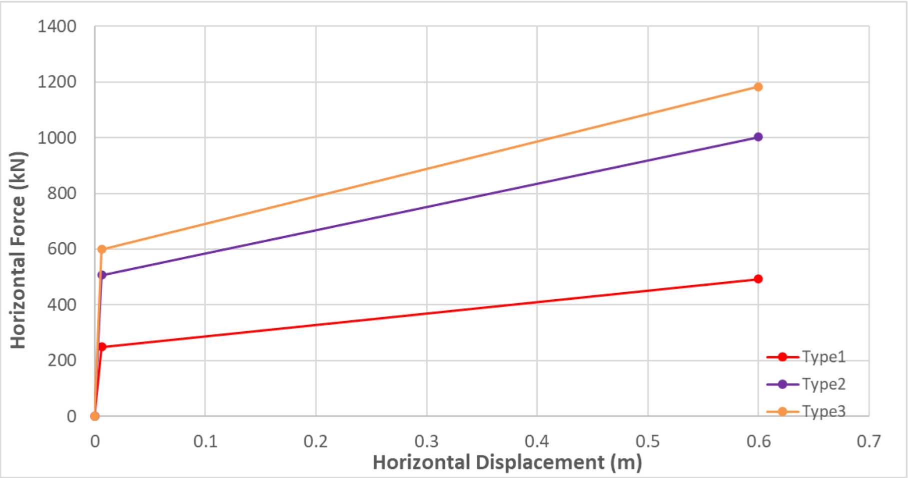

Figure 2.38 Hysteretic behavior of isolators (DBE UB)

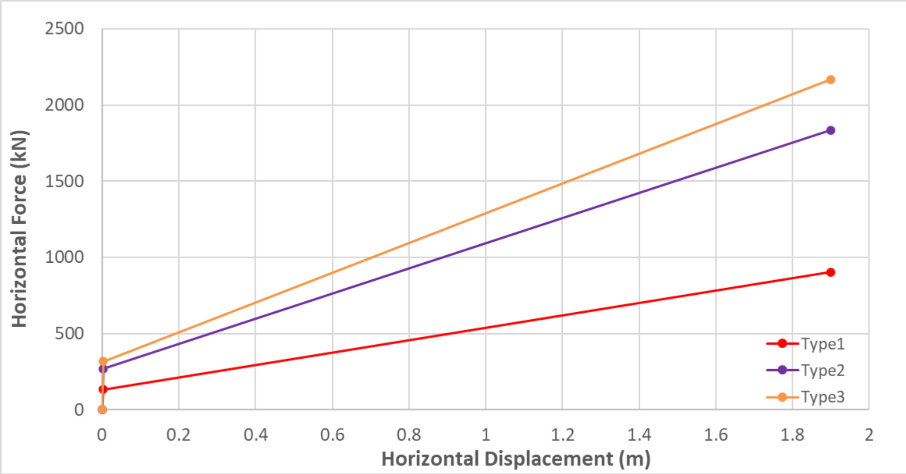

Figure 2.39 Hysteretic behavior of isolators (MCE LB)

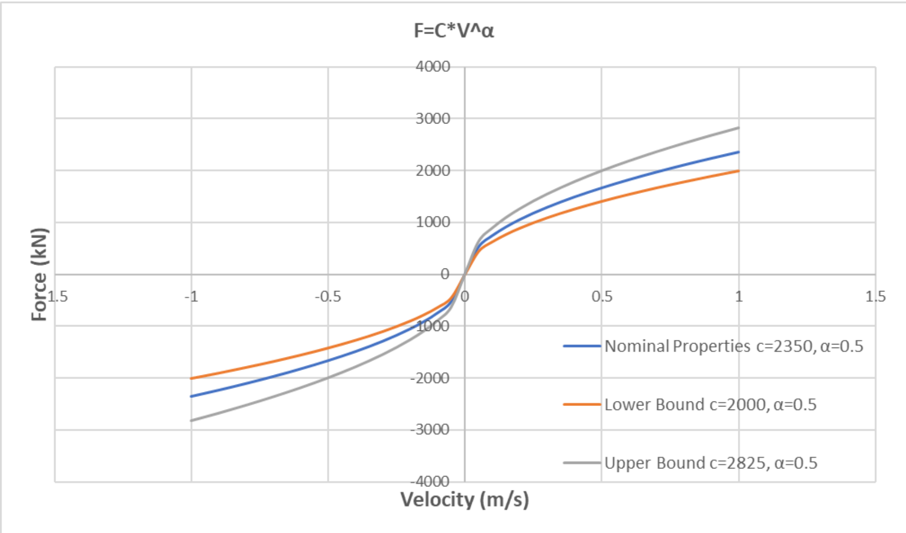

Figure 2.40 Force-Velocity relation of viscous damper

Viscous dampers modelled as exponential damper in ETABS and example link properties are shown in Figure 2.41. These parameters are taken from the manufacturer data sheet. Due to these devices are velocity dependent device, effective stiffness is assumed as zero and damping exponent taken as 0.5 from the manufacturer catalogues. The orientation of viscous dampers is shown in Figure 2.42. One edge was linked to pedestals on the basement level, the other edge was linked to the upper level of isolators. With this configuration, dampers will work on the horizontal axis and absorb the energy.

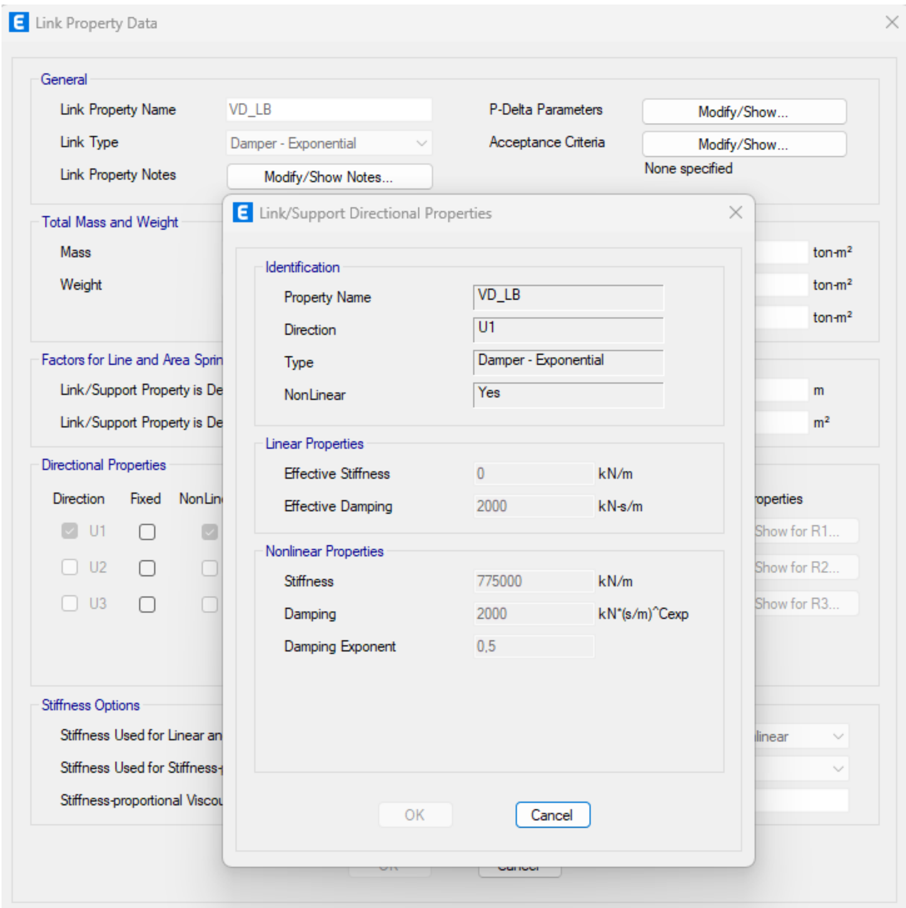

Figure 2.41 Example link properties of viscous dampers

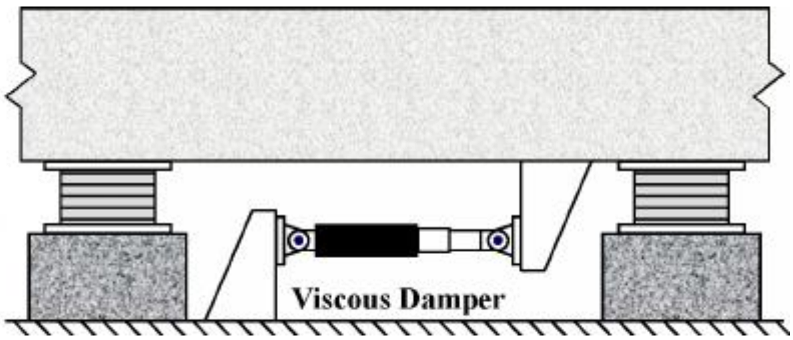

Figure 2.42 Viscous damper and isolators

3. ANALYSIS RESULTS

Time-history analysis is a step-by-step analysis to determine the dynamic response of a structure with proper ground motions. Ground motions were applied bi-directional and vertical component of ground motions does not included in analyses. Fast Non-linear Analysis (FNA) results will be presented in this chapter. Results of Kahramanmaraş State Hospital (B1), Adıyaman Residential Building (B2), and Bolu PMR Hospital project (B3) will be discussed. For DBE level earthquake with upper bound parameters, interstorey drifts, story accelerations, and base shear results will be shown; for MCE level earthquake with lower bound parameters maximum isolator displacements for different links will be presented. Based on these analysis results, a comparison of different cases will be investigated, and an optimum solution will be selected.

3.1 Kahramanmaraş State Hospital (B1)

3.1.1 Modal Analysis – Participating Mass Ratios

Modal analysis is performed in ETABS by using the Ritz method. DBE UB period for FPS is calculated as 3.34 s (Table 2.1) whereas MCE LB period for FPS is determined as 5.45 s (Table 2.2). It was noticed that periods decrease as dampers are added to the system. It should be noted that the maximum change in period is around 10%, which is because the added dampers are not very rigid compared to the entire system.

Besides, adding dampers did not change modal participating mass ratios significantly. For every case, mass ratios are greater than 95% in the first three modes. All periods and modal participating mass ratios are shown in Table 3.1 and 3.2.

Table 3.1 Modal analysis results for all cases – DBE UB

	Mode (#)	Period (sec)	X Direction Mass Participation Ratio	Y Direction Mass Participation Ratio	X Direction Mass Participation	Y Direction Mass Participation
DBE UB FPS	**1**	3.336	0.040	0.572	0.040	0.572
	2	2.987	0.901	0.064	0.941	0.635
	3	2.550	0.024	0.331	0.965	0.966
DBE UB UD1	**1**	3.307	0.038	0.577	0.038	0.577
	2	2.974	0.904	0.060	0.942	0.637
	3	2.546	0.023	0.329	0.964	0.966
DBE UB UD1s	**1**	3.253	0.033	0.588	0.033	0.588
	2	2.949	0.912	0.052	0.944	0.640
	3	2.539	0.019	0.325	0.964	0.965
DBE UB UD2	**1**	3.289	0.036	0.580	0.036	0.580
	2	2.965	0.907	0.057	0.943	0.636
	3	2.544	0.021	0.329	0.964	0.965
DBE UB UD2s	**1**	3.204	0.027	0.596	0.027	0.596
	2	2.923	0.920	0.043	0.947	0.639
	3	2.533	0.016	0.325	0.963	0.964
DBE UB UD3	**1**	3.280	0.036	0.579	0.036	0.579
	2	2.960	0.907	0.057	0.942	0.636
	3	2.544	0.022	0.329	0.964	0.965
DBE UB UD3s	**1**	3.180	0.027	0.594	0.027	0.594
	2	2.909	0.919	0.044	0.946	0.638
	3	2.532	0.017	0.326	0.963	0.964
DBE UB UD4	**1**	3.263	0.034	0.581	0.034	0.581
	2	2.951	0.909	0.055	0.943	0.635
	3	2.543	0.021	0.330	0.964	0.965
DBE UB UD4s	**1**	3.138	0.022	0.599	0.022	0.599
	2	2.886	0.926	0.036	0.948	0.635
	3	2.530	0.014	0.327	0.962	0.963
DBE UB UD5	**1**	3.214	0.039	0.570	0.039	0.570
	2	2.875	0.899	0.062	0.938	0.633
	3	2.450	0.024	0.331	0.962	0.963
DBE UB UD5s	**1**	3.019	0.037	0.569	0.037	0.569
	2	2.697	0.896	0.059	0.933	0.627
	3	2.289	0.022	0.330	0.955	0.958

Table 3.2 Modal analysis results for all cases – MCE LB

	Mode (#)	Period (sec)	X Direction Mass Participation Ratio	Y Direction Mass Participation Ratio	X Direction Mass Participation	Y Direction Mass Participation
MCE LB FPS	**1**	5.445	0.048	0.571	0.048	0.571
	2	4.908	0.901	0.077	0.950	0.648
	3	4.251	0.029	0.330	0.978	0.978
MCE LB UD1	**1**	5.285	0.040	0.592	0.040	0.592
	2	4.835	0.915	0.063	0.955	0.656
	3	4.230	0.023	0.322	0.978	0.978
MCE LB UD1s	**1**	5.018	0.022	0.643	0.022	0.643
	2	4.704	0.945	0.033	0.967	0.676
	3	4.189	0.011	0.302	0.978	0.978
MCE LB UD2	**1**	5.190	0.033	0.604	0.033	0.604
	2	4.786	0.926	0.052	0.959	0.656
	3	4.219	0.019	0.322	0.978	0.978
MCE LB UD2s	**1**	4.798	0.003	0.682	0.003	0.682
	2	4.575	0.972	0.005	0.976	0.687
	3	4.156	0.002	0.291	0.977	0.977
MCE LB UD3	**1**	5.143	0.034	0.601	0.034	0.601
	2	4.759	0.924	0.053	0.959	0.655
	3	4.218	0.019	0.323	0.978	0.978
MCE LB UD3s	**1**	4.693	0.003	0.682	0.003	0.682
	2	4.506	0.973	0.004	0.976	0.686
	3	4.151	0.001	0.291	0.977	0.977
MCE LB UD4	**1**	5.062	0.028	0.610	0.028	0.610
	2	4.715	0.935	0.043	0.962	0.653
	3	4.213	0.016	0.325	0.978	0.978
MCE LB UD4s	**1**	4.531	0.008	0.693	0.008	0.693
	2	4.402	0.965	0.012	0.973	0.705
	3	4.132	0.004	0.271	0.977	0.977
MCE LB UD5	**1**	4.834	0.048	0.571	0.048	0.571
	2	4.353	0.900	0.076	0.948	0.647
	3	3.763	0.029	0.330	0.977	0.977
MCE LB UD5s	**1**	4.097	0.046	0.571	0.046	0.571
	2	3.682	0.900	0.073	0.946	0.644
	3	3.170	0.027	0.331	0.974	0.974

3.1.2 Maximum Isolator Displacements

In the original base-isolated model (FPS), maximum isolator displacements for MCE-level earthquake with lower bound properties were calculated as 915 mm, 1020 mm, and 971 mm for P1, P2, and C points respectively (Figure 2.5). Maximum displacements for all analyses are shown in Figure 3.1 for these selected points.

Table 3.3 Maximum resultant displacements of selected link for each analysis -MCE LB

	P1 (mm)	**P2 (mm)**	**C (mm)**	**Max (mm)**	**Min (mm)**	**Max/Min**	**Reduction (%)**
FPS	915	1020	971	1020	915	1.11	-
UD1	874	967	922	967	874	1.11	5
UD1s	788	809	838	838	788	1.06	18
UD2	845	929	887	929	845	1.10	9
UD2s	725	716	730	730	716	1.02	28
UD3	832	904	867	904	832	1.09	11
UD3s	700	678	674	700	674	1.04	31
UD4	884	847	865	884	847	1.04	13
UD4s	747	583	642	747	583	1.28	27
UD5	611	670	641	670	611	1.10	34
UD5s	373	448	391	448	373	1.20	56

The orbital displacements are plotted for every analysis and shown in Figures 3.1 and 3.2. The average of 11 ground motions are calculated and to plot the capacity of isolators, average values are multiplied by 1.1 due to torsion effect as stated in TEC. It was noticed that as dampers are added to the system, peak values of ground motions are decreased and approached to the capacity circle.

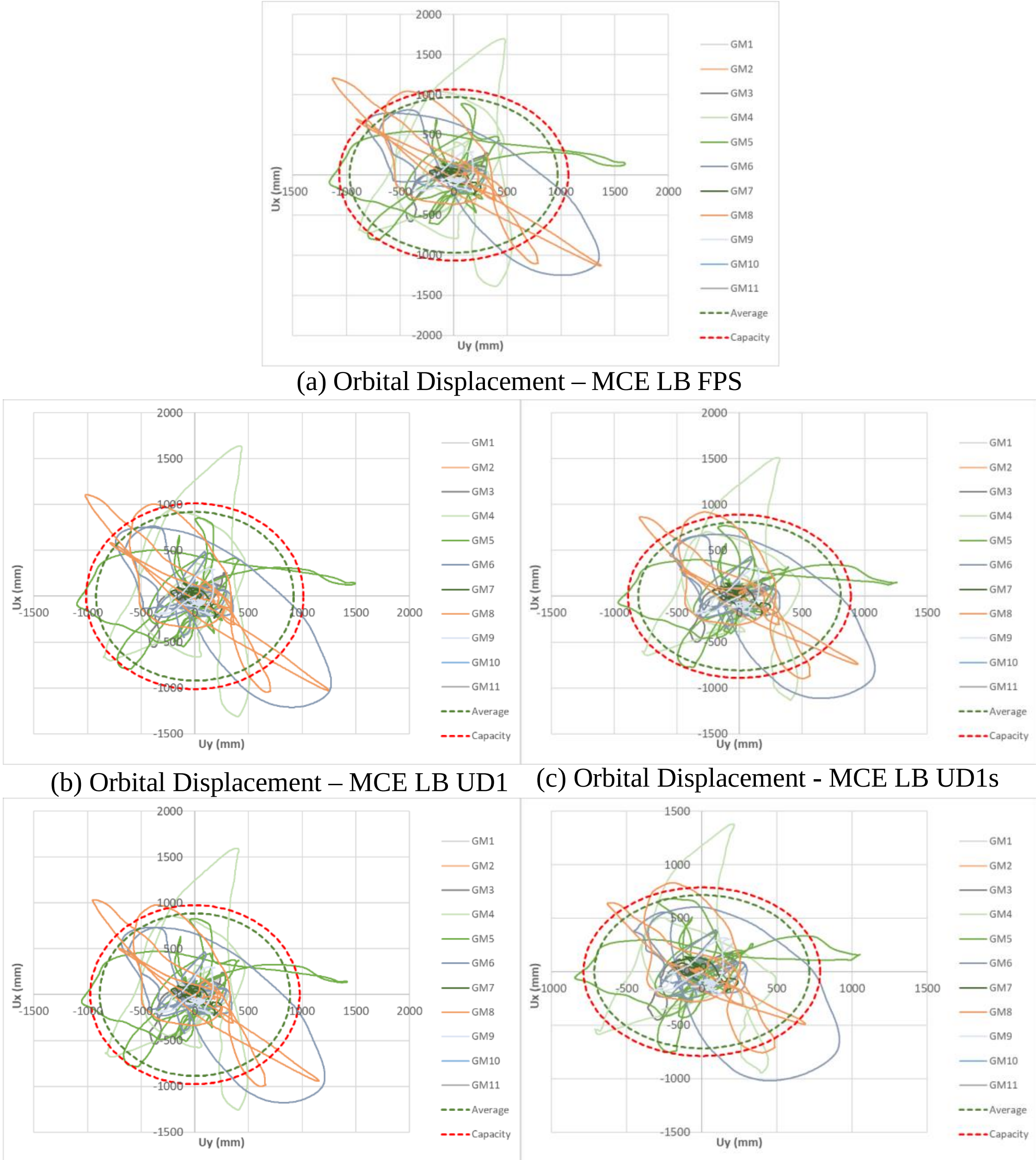

(a) Orbital Displacement – MCE LB FPS

(b) Orbital Displacement – MCE LB UD1

(c) Orbital Displacement - MCE LB UD1s

(d) Orbital Displacement – MCE LB UD2

(e) Orbital Displacement – MCE LB UD2s

Figure 3.1 Orbital displacements and capacity of isolators

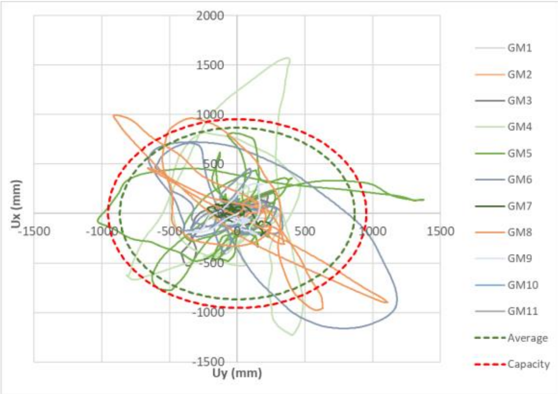

(f) Orbital Displacement – MCE LB UD3

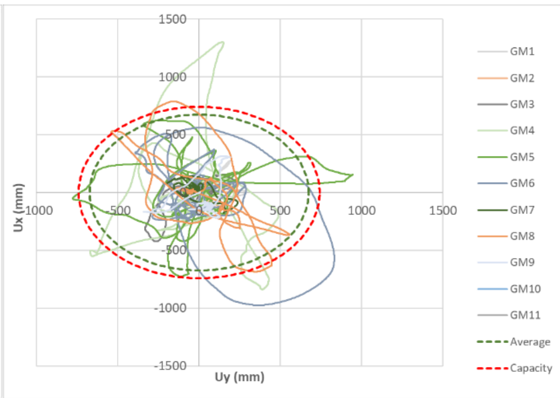

(g) Orbital Displacement – MCE LB UD3s

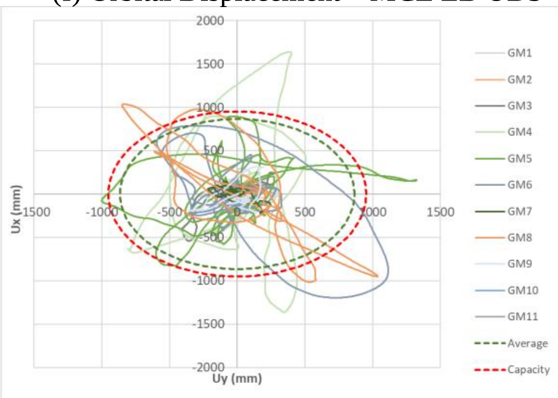

(h) Orbital Displacement – MCE LB UD4

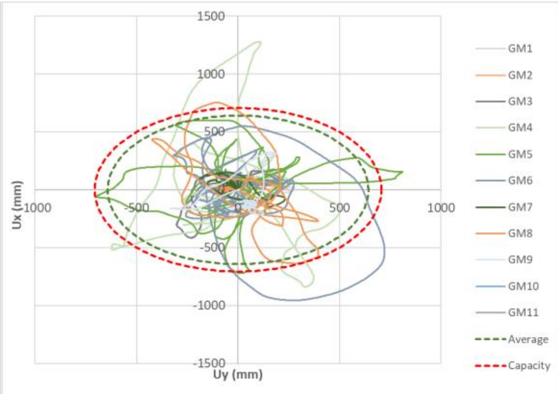

(i) Orbital Displacement – MCE LB UD4s

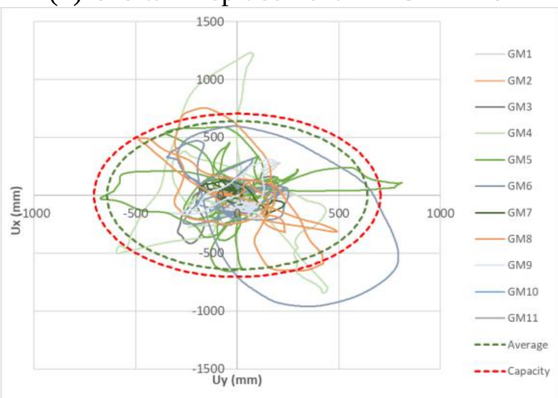

(j) Orbital Displacement – MCE LB UD5

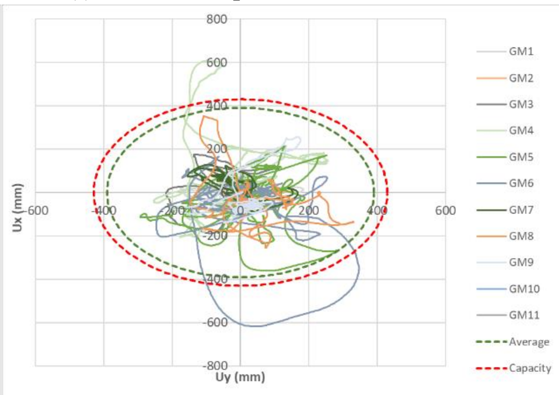

(k) Orbital Displacement – MCE LB UD5s

Figure 3.1 Orbital displacements and capacity of isolators (continued)

3.1.3 Story Accelerations

Peak story accelerations are shown in this chapter for ten stories. Moreover, ground-level acceleration is added to the graphs, this value is taken from the response spectrum. This value for this project equals 0.65g for DD2 level earthquake. The limit value is taken as 0.3g for every story based on the Ministry of the Health Specifications.

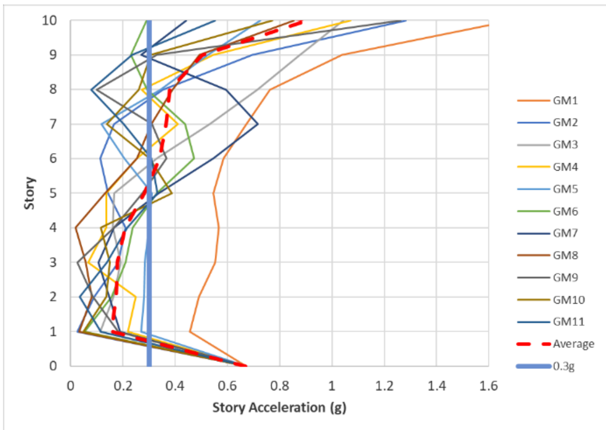

(a) Peak Story Accelerations – DBE UB FPS

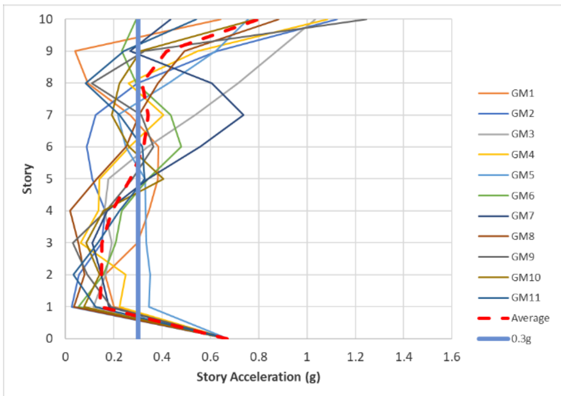

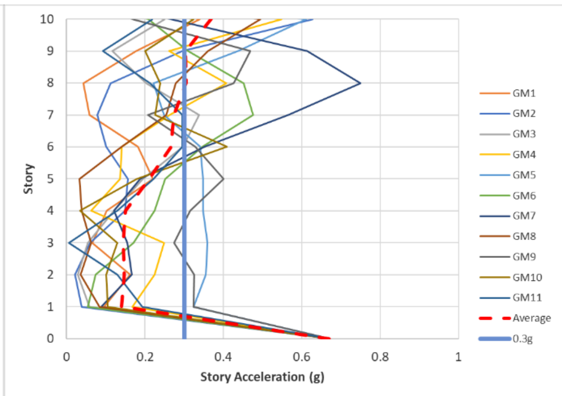

(b) Story Accelerations – DBE UB FPS-UD1 (c) Story Accelerations – DBE UB FPS-UD1s

Figure 3.2 Resultant story accelerations of all cases

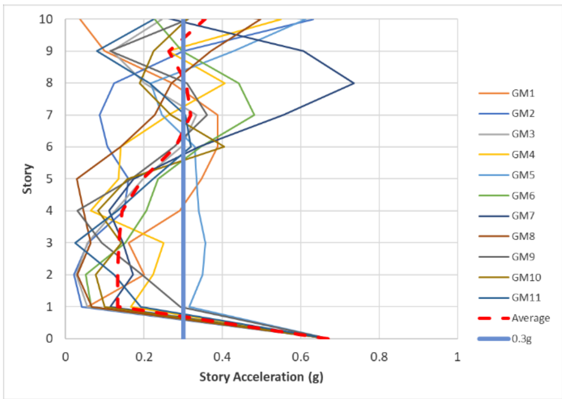

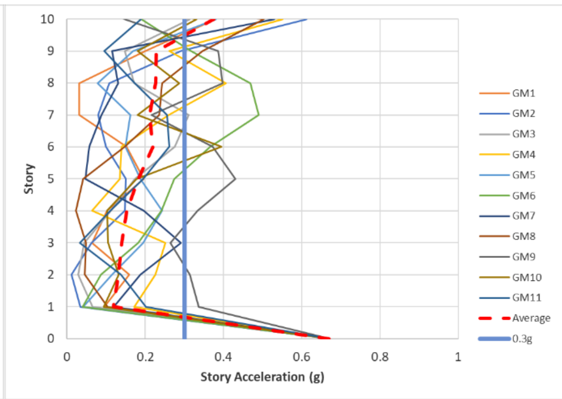

(d) Story Accelerations – DBE UB FPS-UD2 (e) Story Accelerations – DBE UB FPS-UD2s

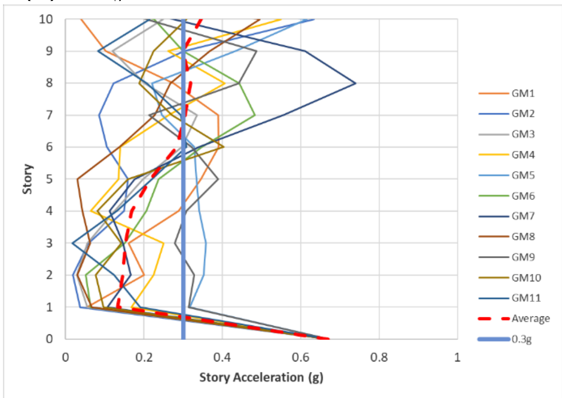

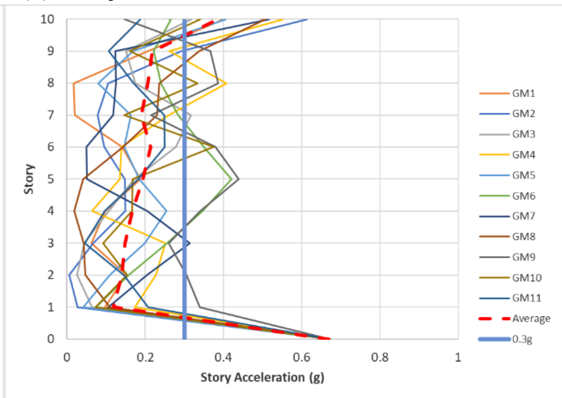

(f) Story Accelerations – DBE UB FPS-UD3 (g) Story Accelerations – DBE UB FPS-UD3s

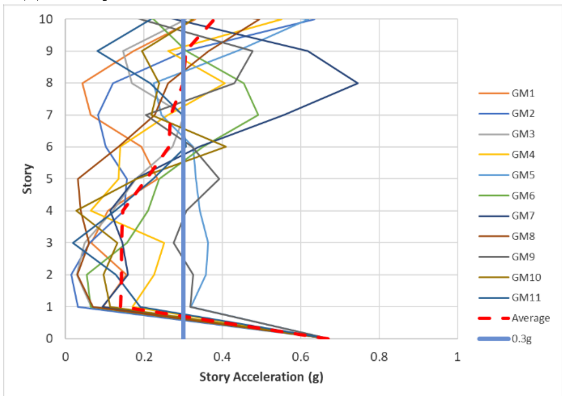

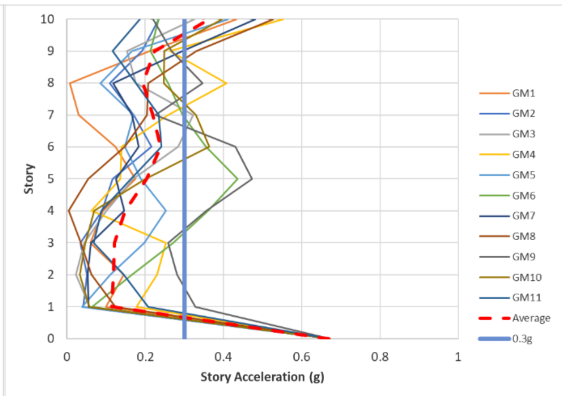

(h) Story Accelerations – DBE UB FPS-UD4 (i) Story Accelerations – DBE UB FPS-UD4s

Figure 3.3 Resultant story accelerations of all cases (continued)

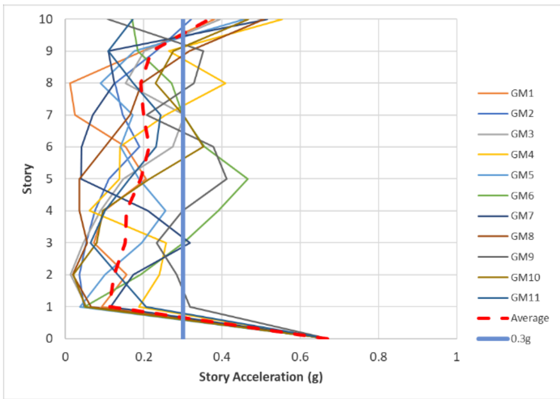

(j) Story Accelerations – DBE UB FPS-UD5

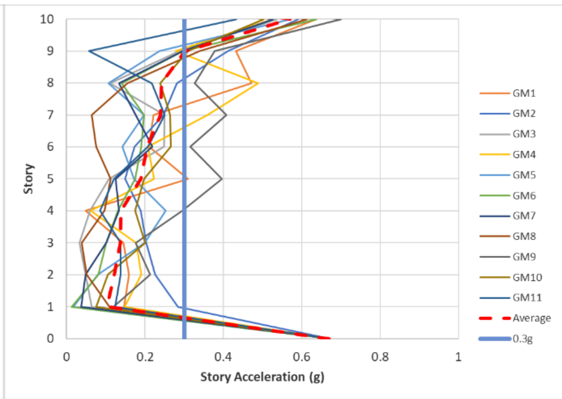

(k) Story Accelerations – DBE UB FPS-UD5s

Figure 3.4 Resultant story accelerations of all cases (continued)

3.1.4 Interstorey Drift Ratios

Interstorey drift ratios are shown in this part. The limit is taken as 0.005% for Intermediate Occupancy according to the Building Earthquake Code of Turkey (TEC 2018). This drift limit ensures operational performance level and aims for no or limited damage to both structural and non-structural elements.

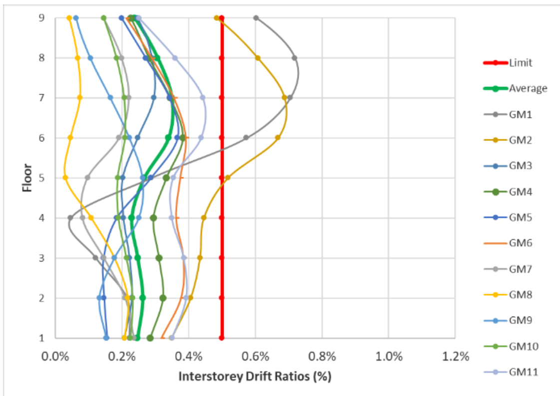

(a) Interstorey Drift Ratios – DBE UB FPS

Figure 3.5 Interstorey drift ratios of all cases

(b) Interstorey Drift Ratios – DBE UB UD1

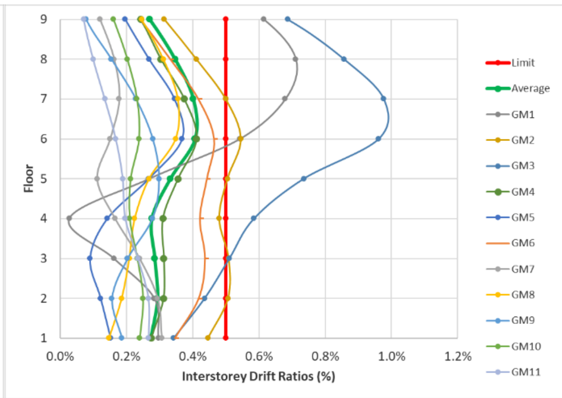

(c) Interstorey Drift Ratios – DBE UB UD1s

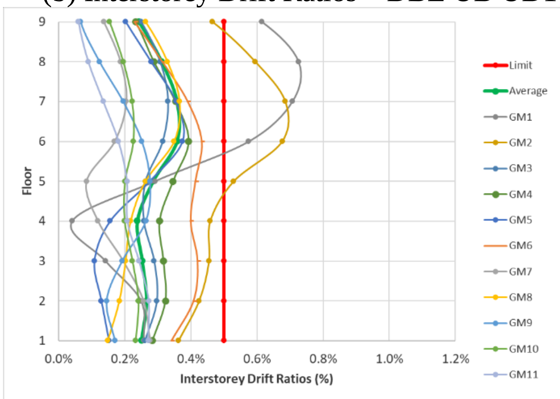

(d) Interstorey Drift Ratios – DBE UB UD2

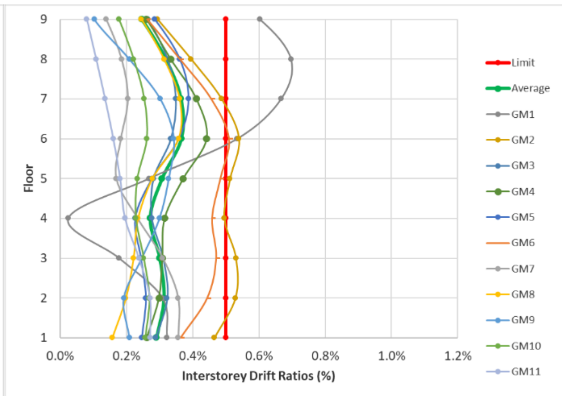

(e) Interstorey Drift Ratios – DBE UB UD2s

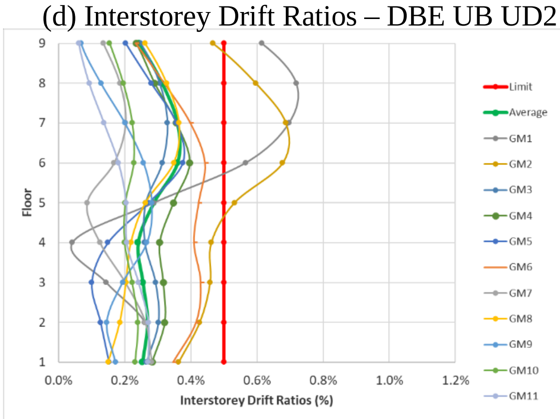

(f) Interstorey Drift Ratios – DBE UB UD3

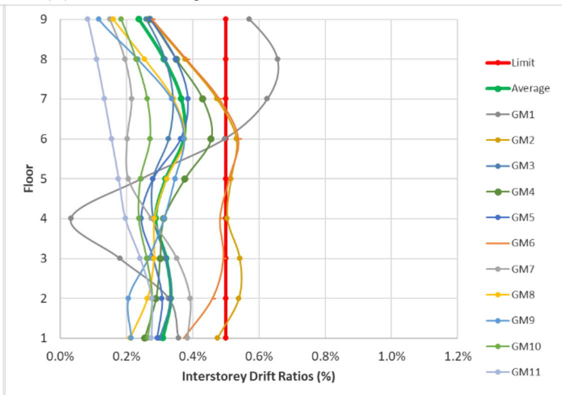

(g) Interstorey Drift Ratios – DBE UB UD3s

Figure 3.6 Interstorey drift ratios of all cases (continued)

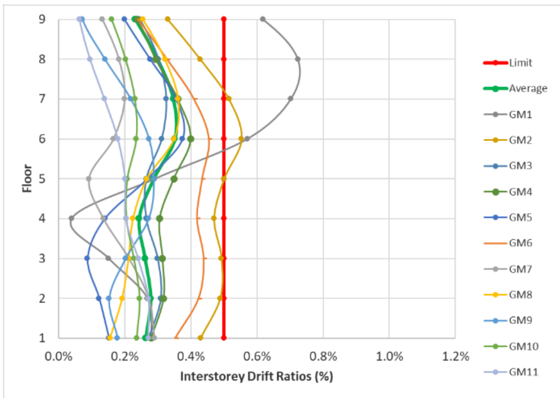

(h) Interstorey Drift Ratios – DBE UB UD4

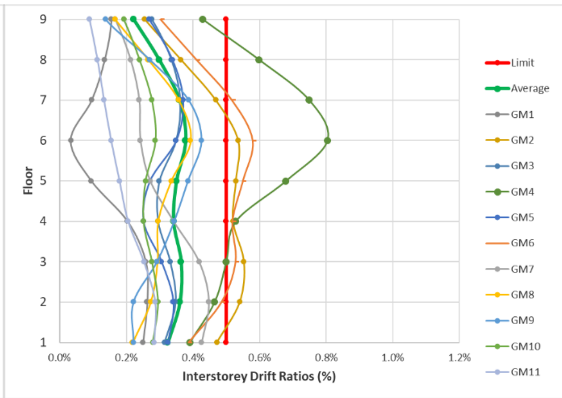

(i) Interstorey Drift Ratios – DBE UB UD4s

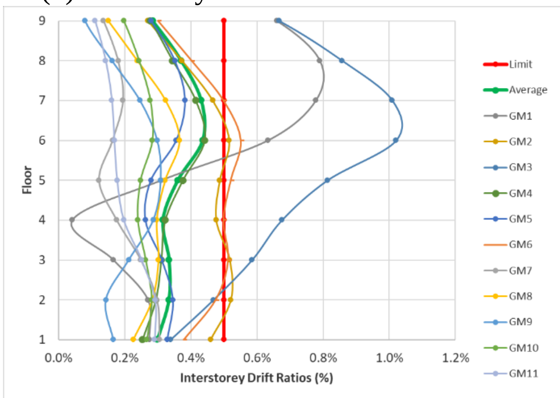

(j) Interstorey Drift Ratios – DBE UB UD5

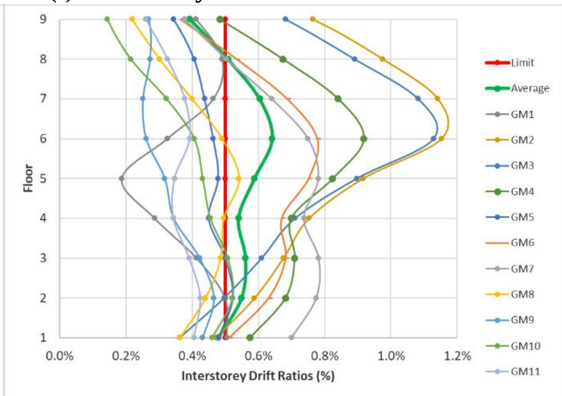

(k) Interstorey Drift Ratios – DBE UB UD5s

Figure 3.7 Interstorey drift ratios of all cases (continued)

3.1.5 Base Shear Ratio

The current structure is designed based on 15.5% base shear and this part is focused on whether adding dampers will increase the shear force (Figure 3.5). In some cases where displacement demand decreases, increases in total base shear are limited as in UD3 and UD4. It is clear that UD4 is the most ideal mode because base shear did not increase significantly although there are 109 metallic dampers. A comparison of these analyses will be presented in detail in Chapter 3.4.

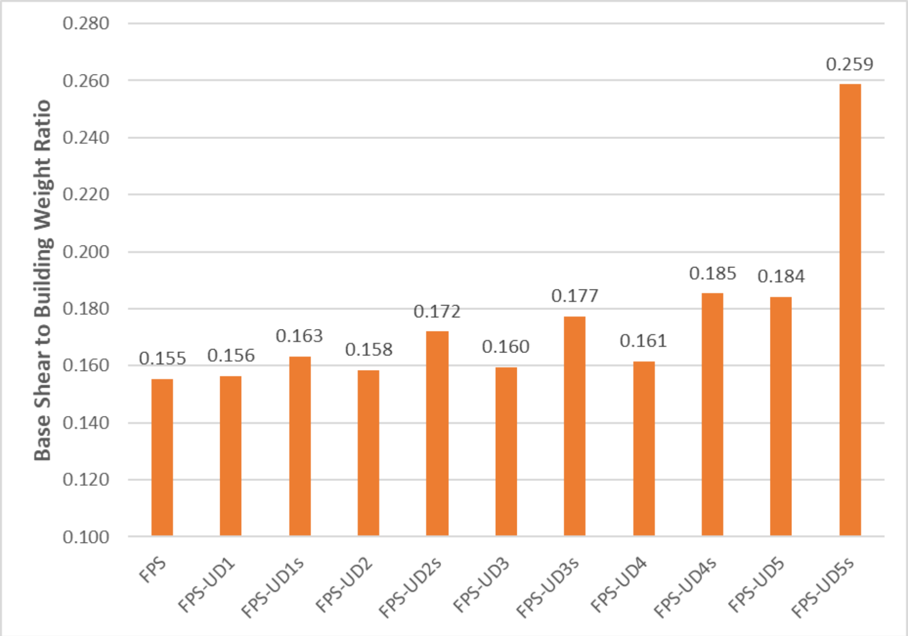

Figure 3.8 Base shear ratios of all cases

Table 3.4 Base shear ratios of all cases and change compared to FPS

Case	Base Shear to Building Weight Ratio	Change (%)
FPS	0.155	-
FPS-UD1	0.156	0.68
FPS-UD1s	0.163	5.02
FPS-UD2	0.158	2.00
FPS-UD2s	0.172	10.71
FPS-UD3	0.160	2.73
FPS-UD3s	0.177	14.08
FPS-UD4	0.161	3.98
FPS-UD4s	0.185	19.31
FPS-UD5	0.184	18.47
FPS-UD5s	0.259	66.51

3.2 Adıyaman Kahta Residential Project (B2)

3.2.1 Modal Analysis – Participating Mass Ratios

Modal analysis is performed in ETABS, and the results of analysis results are shown in Table 3.2 and 3.3 below. DBE UB period is calculated as 2.5 seconds and MCE LB period is calculated as 4.1 seconds. It has been noticed that periods decrease as dampers are added to the system.

Besides, adding dampers did not change modal participating mass ratios much. For every case, mass ratios are greater than 95% at the first five modes.

Table 3.5 Modal analysis results of all cases – DBE UB

	Mode (#)	Period (sec)	X Direction Mass Participation Ratio	Y Direction Mass Participation Ratio	X Direction Mass Participation	Y Direction Mass Participation
DBE UB FPS	1	2.477	0.000	0.936	0.000	0.936
	2	2.429	0.879	0.000	0.879	0.936
	3	2.273	0.063	0.000	0.942	0.936
	4	0.717	0.000	0.032	0.942	0.968
	5	0.688	0.020	0.000	0.962	0.968
DBE UB UD1	1	2.452	0.000	0.934	0.000	0.934
	2	2.403	0.870	0.000	0.870	0.934
	3	2.258	0.071	0.000	0.941	0.934
	4	0.714	0.000	0.033	0.941	0.967
	5	0.685	0.020	0.000	0.961	0.967
DBE UB UD1s	1	2.395	0.000	0.930	0.000	0.930
	2	2.345	0.843	0.000	0.843	0.930
	3	2.222	0.094	0.000	0.937	0.930
	4	0.706	0.000	0.037	0.937	0.967
	5	0.678	0.022	0.000	0.959	0.967
DBE UB UD2	1	2.428	0.000	0.933	0.000	0.933
	2	2.378	0.878	0.000	0.878	0.933
	3	2.215	0.061	0.000	0.939	0.933
	4	0.711	0.000	0.035	0.939	0.967
	5	0.681	0.022	0.000	0.961	0.967
DBE UB UD2s	1	2.328	0.000	0.924	0.000	0.924
	2	2.274	0.871	0.000	0.871	0.924
	3	2.106	0.061	0.000	0.932	0.924
	4	0.696	0.000	0.041	0.932	0.965
	5	0.667	0.029	0.000	0.960	0.965

DBE UB UD3	**1**	2.374	0.000	0.928	0.000	0.928
	2	2.322	0.864	0.000	0.864	0.928
	3	2.182	0.072	0.000	0.935	0.928
	4	0.703	0.000	0.038	0.935	0.966
	5	0.675	0.024	0.000	0.960	0.966
DBE UB UD3s	**1**	2.205	0.000	0.911	0.000	0.911
	2	2.146	0.825	0.000	0.825	0.911
	3	2.031	0.095	0.000	0.919	0.911
	4	0.674	0.000	0.051	0.919	0.962
	5	0.648	0.035	0.000	0.954	0.962

Table 3.6 Modal analysis results of all cases – MCE LB

	Mode (#)	**Period (sec)**	**X Direction Mass Participation Ratio**	**Y Direction Mass Participation Ratio**	**X Direction Mass Participation**	**Y Direction Mass Participation**
MCE LB FPS	**1**	4.061	0.000	0.967	0.000	0.967
	2	4.041	0.936	0.000	0.936	0.967
	3	3.693	0.032	0.000	0.968	0.967
	4	0.799	0.000	0.004	0.968	0.971
	5	0.763	0.002	0.000	0.970	0.971
MCE LB UD1	**1**	3.845	0.000	0.966	0.000	0.966
	2	3.824	0.919	0.000	0.919	0.966
	3	3.561	0.048	0.000	0.967	0.966
	4	0.794	0.000	0.005	0.967	0.971
	5	0.759	0.002	0.000	0.970	0.971
MCE LB UD1s	**1**	3.453	0.000	0.963	0.000	0.963
	2	3.431	0.829	0.000	0.829	0.963
	3	3.293	0.136	0.000	0.965	0.963
	4	0.781	0.000	0.008	0.965	0.971
	5	0.749	0.003	0.000	0.968	0.971
MCE LB UD2	**1**	3.667	0.000	0.965	0.000	0.965
	2	3.644	0.936	0.000	0.936	0.965
	3	3.243	0.030	0.000	0.966	0.965
	4	0.789	0.000	0.006	0.966	0.971
	5	0.752	0.003	0.000	0.969	0.971
MCE LB UD2s	**1**	3.099	0.000	0.958	0.000	0.958
	2	3.067	0.929	0.000	0.929	0.958
	3	2.676	0.031	0.000	0.960	0.958
	4	0.764	0.000	0.013	0.960	0.971
	5	0.729	0.008	0.000	0.968	0.971
MCE LB UD3	**1**	3.334	0.000	0.961	0.000	0.961
	2	3.303	0.925	0.000	0.925	0.961
	3	3.040	0.039	0.000	0.964	0.961

	4	0.776	0.000	0.010	0.964	0.971
	5	0.742	0.005	0.000	0.968	0.971
MCE LB UD3s	**1**	2.632	0.000	0.943	0.000	0.943
	2	2.586	0.891	0.000	0.891	0.943
	3	2.414	0.057	0.000	0.948	0.943
	4	0.729	0.000	0.025	0.948	0.968
	5	0.699	0.015	0.000	0.963	0.968

3.2.2 Maximum Isolator Displacements

In the original base-isolated model, maximum isolator displacements for MCE-level earthquake with lower bound properties were calculated as 203 mm, 203 mm, and 202 mm for P1, P2, and C points, respectively. Maximum displacements for all analyses are shown in Figure 3.6 for the selected three points; P1, P2, and Center. It is also shown that the maximum displacement can be reduced up to 96 mm if all links have dampers.

Table 3.7 Maximum resultant displacements of selected links for each case – MCE LB

	P1 (mm)	**P2 (mm)**	**C (mm)**	**Max (mm)**	**Min (mm)**	**Max/Min**	**Reduction (%)**
FPS	203	203	202	203	202	1.01	-
FPS-UD1	181	180	180	181	180	1.01	11
FPS-UD1s	159	158	158	159	158	1.01	22
FPS-UD2	164	163	162	164	162	1.01	19
FPS-UD2s	138	140	138	140	138	1.01	31
FPS-UD3	145	145	144	145	144	1.01	29
FPS-UD3s	96	96	93	96	93	1.03	53

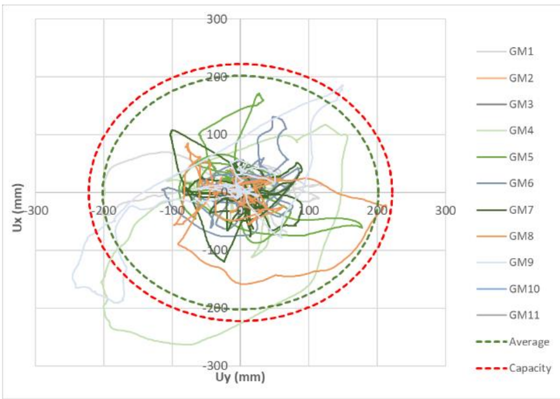

(a) Orbital Displacement – MCE LB FPS

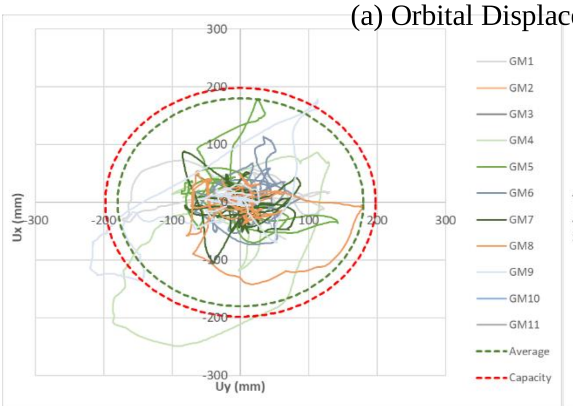

(b) Orbital Displacement – MCE LB UD1

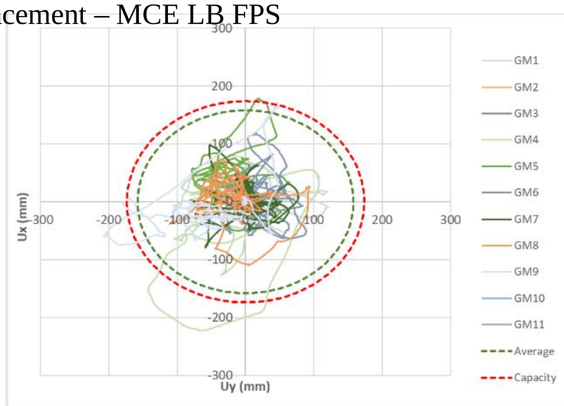

(c) Orbital Displacement – MCE LB UD1s

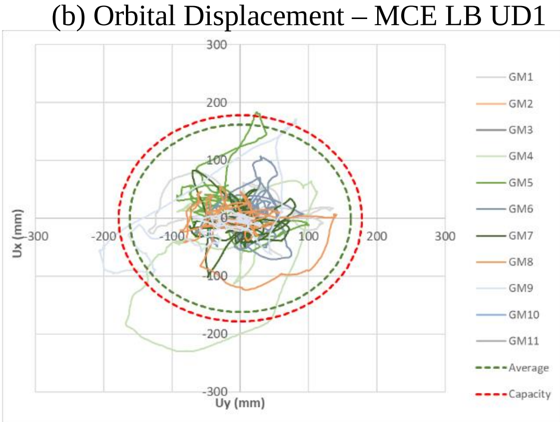

(d) Orbital Displacement – MCE LB UD2

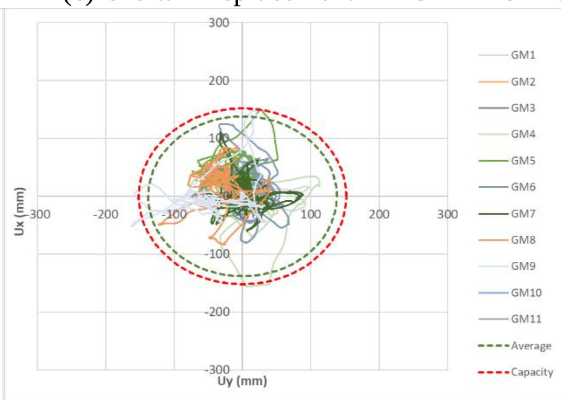

(e) Orbital Displacement – MCE LB UD2s

Figure 3.9 Orbital displacements and capacity of isolators

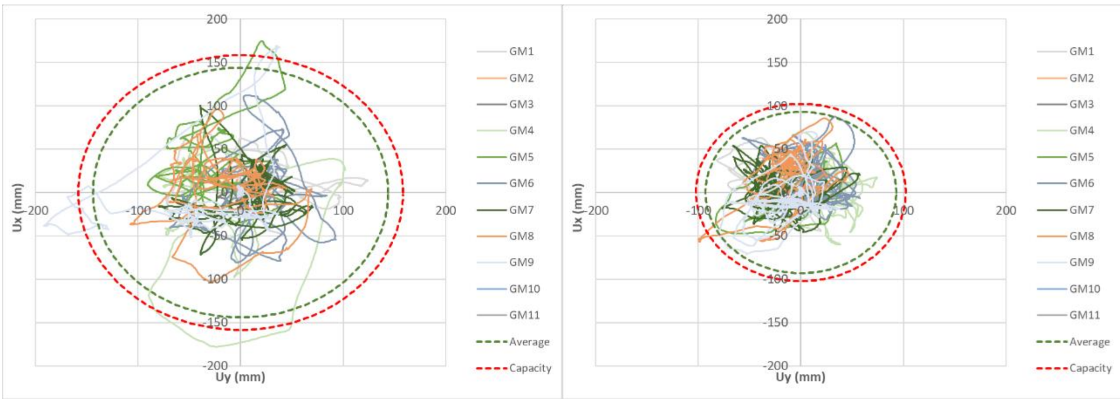

(f) Orbital Displacement – MCE LB UD3 (g) Orbital Displacement – MCE LB UD3s

Figure 3.10 Orbital displacements and capacity of isolators (continued)

3.2.3 Story Accelerations

A total of eleven acceleration values are shown in this chapter; 10 values belong to peak story accelerations of structure and ground acceleration. Ground acceleration is taken from the response spectrum. This value for this project equals to 0.25g for DBE level earthquake. The limit value is taken as 0.3g for every story.

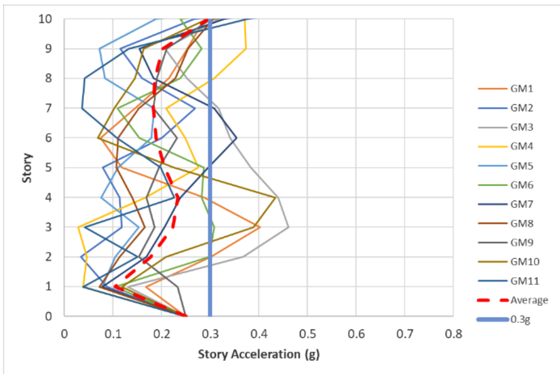

(a) Story Acceleration – DBE UB FPS

Figure 3.11 Resultant story accelerations of all cases

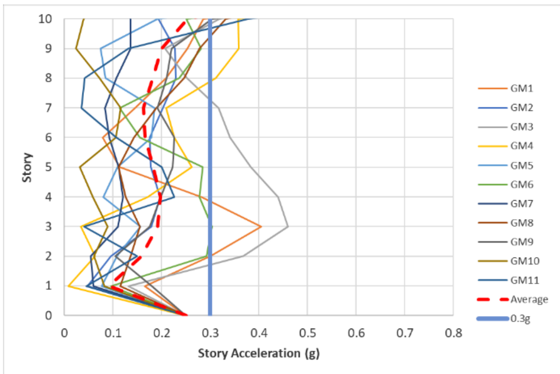

(b) Story Acceleration – DBE UB FPS-UD1

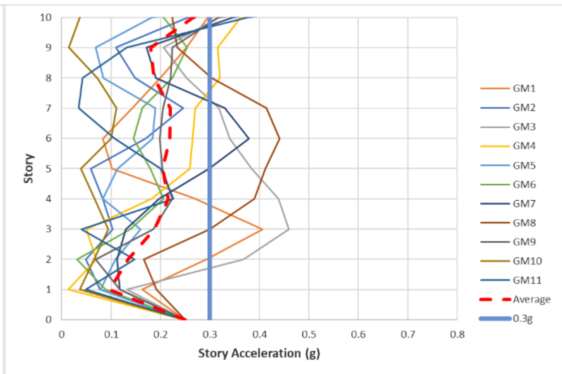

(c) Story Acceleration – DBE UB FPS-UD1s

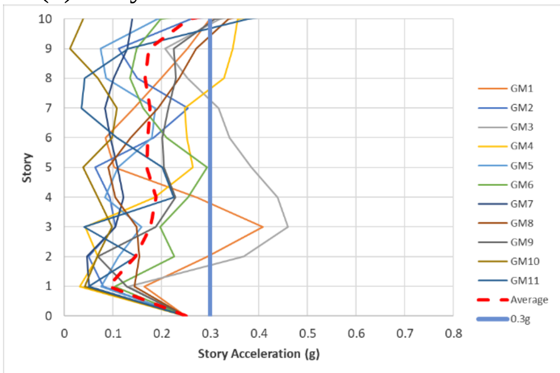

(d) Story Acceleration – DBE UB FPS-UD2

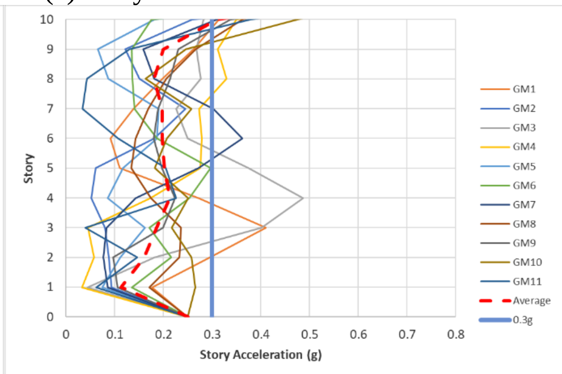

(e) Story Acceleration – DBE UB FPS-UD2s

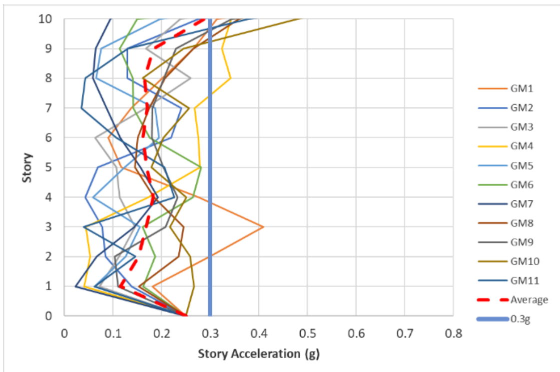

(f) Story Acceleration – DBE UB FPS-UD3

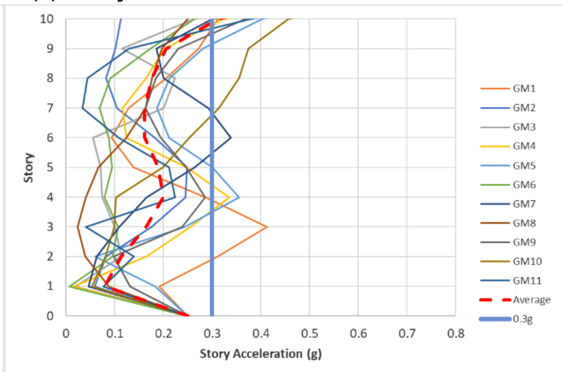

(g) Story Acceleration – DBE UB FPS-UD3s

Figure 3.12 Resultant story accelerations of all cases (continued)

3.2.4 Interstorey Drift Ratios

Interstorey drift ratios are shown in this chapter. As in the previous structure, the limit is assumed as 0.5% according to the Building Earthquake Code of Turkey. This limit states operational performance level and aims for no damage to both structural and non-structural elements.

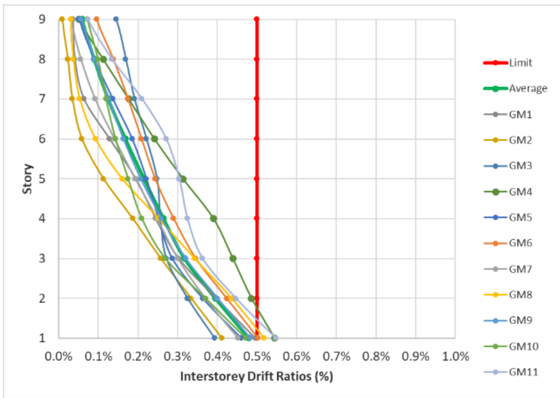

(a) Interstorey Drift Ratio – DBE UB FPS

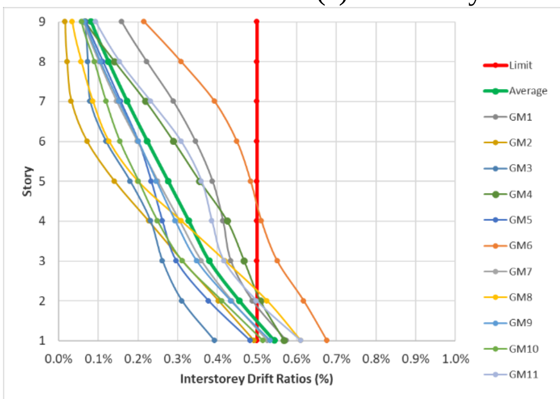

(b) Interstorey Drift Ratio – DBE UB UD1

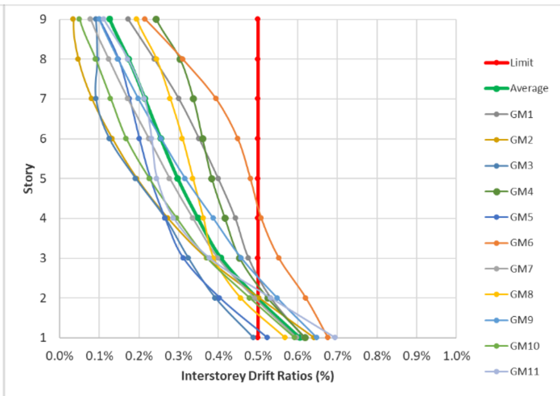

(c) Interstorey Drift Ratio – DBE UB UD1s

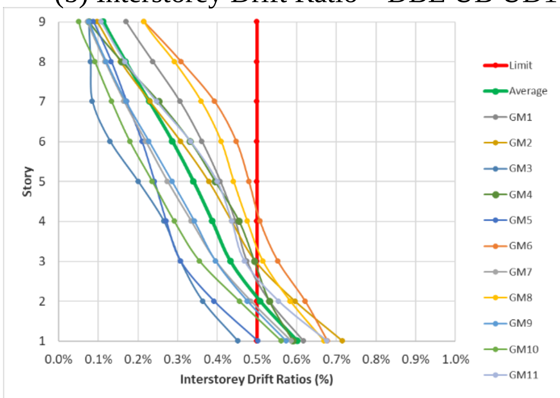

(d) Interstorey Drift Ratio – DBE UB UD2

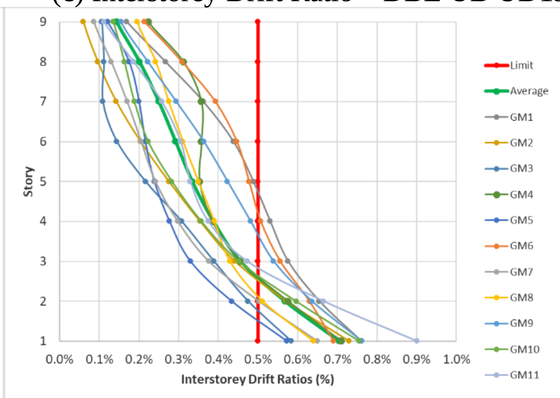

(e) Interstorey Drift Ratio – DBE UB UD2s

Figure 3.13 Interstorey drift ratios of all cases

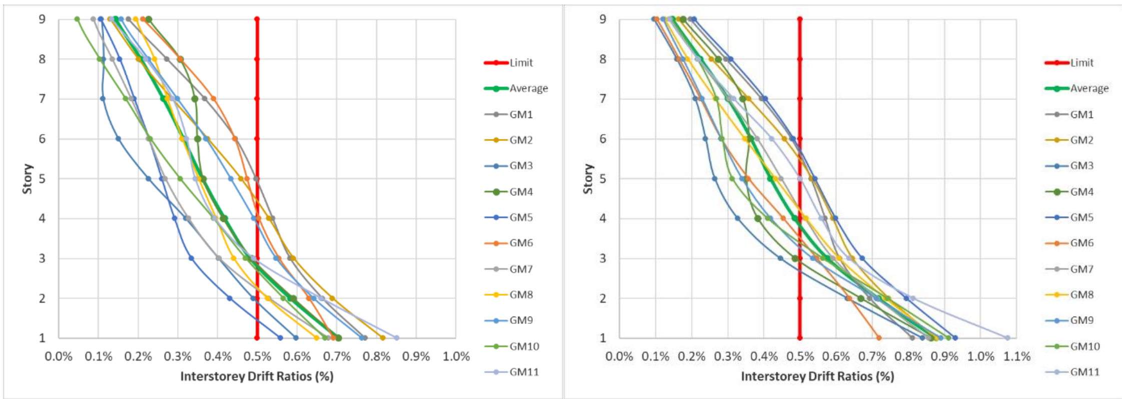

(f) Interstorey Drift Ratio – DBE UB UD3 (e) Interstorey Drift Ratio – DBE UB UD3s

Figure 3.14 Interstorey drift ratios of all cases (continued)

3.2.5 Base Shear Ratio

The current structure is designed based on 12.8% base shear and this chapter is focused on whether adding dampers will increase the shear force. In some cases where displacement demand decreases, increases in total base shear are limited. It seems clear that UD1-UD2 are the most ideal modes. A comparison of these analyses will be examined in detail in Chapter 3.4.

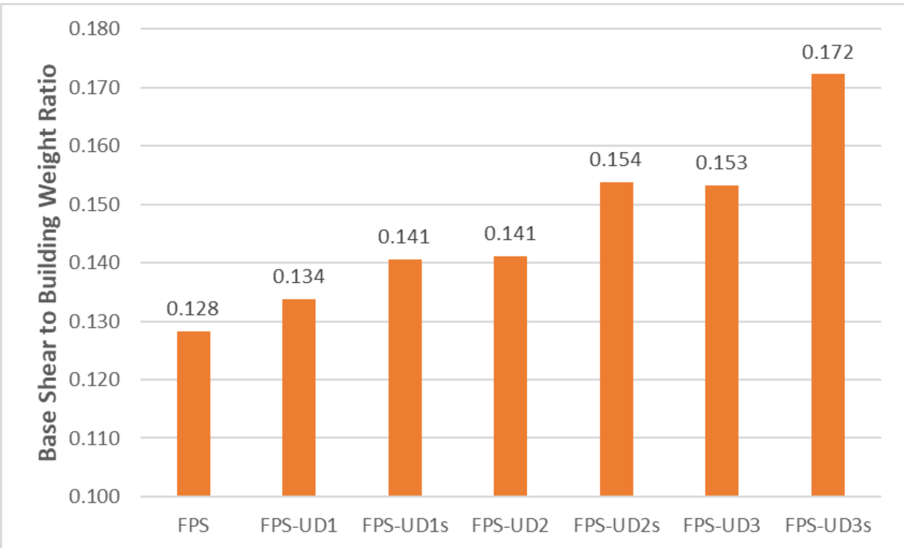

Figure 3.15 Base shear ratios of all cases

Table 3.8 Base shear ratios of all cases and change compared to FPS

Case	Base Shear to Building Weight Ratio	Change (%)
FPS	0.128	-
FPS-UD1	0.134	4.25
FPS-UD1s	0.141	9.63
FPS-UD2	0.141	10.05
FPS-UD2s	0.154	19.90
FPS-UD3	0.153	19.52
FPS-UD3s	0.172	34.27

3.3 Bolu PMR Hospital (B3)

3.3.1 Modal Analysis – Participating Mass Ratios

Modal analysis is performed in ETABS, and the results are shown in Table 3.3. DBE UB period is calculated as 3.5 seconds and MCE LB period is calculated as 4.8 seconds. As the effective stiffness of viscous dampers was assumed as zero, modal analysis results did not change.

Table 3.9 Modal analysis results of all cases

- DBE UB FPS

Mode (#)	Period (sec)	X Direction Mass Participation Ratio	Y Direction Mass Participation Ratio	X Direction Mass Participation	Y Direction Mass Participation
1	3.461	0.189	0.760	0.189	0.760
2	3.448	0.789	0.194	0.978	0.954
3	3.159	0.006	0.029	0.984	0.984

- MCE LB FPS

Mode (#)	Period (sec)	X Direction Mass Participation Ratio	Y Direction Mass Participation Ratio	X Direction Mass Participation	Y Direction Mass Participation
1	4.815	0.208	0.703	0.208	0.703
2	4.787	0.761	0.224	0.969	0.926
3	4.489	0.016	0.058	0.984	0.985

3.3.2 Maximum Isolator Displacements

Maximum isolator displacements are calculated as 1800 mm in the FPS model. For this project, adding dampers is a compulsory thing to design the structure. For this displacement capacity, it is not possible to use an isolator. That's why viscous dampers are used in this model and the quantity of dampers is increased at each step. In addition to the FPS model, four different models are analyzed and at the fourth step, displacement demands can be reduced to 900 mm.

Table 3.10 Maximum displacement of different links for each case – MCE LB

	P1 (mm)	P2 (mm)	P3 (mm)	P4 (mm)	P5 (mm)	C (mm)	Max (mm)	Min (mm)	Max/Min	Reduction (%)
FPS	1832	1839	1840	1862	1832	1866	1862	1832	1.01	-
FPS-VD1	1311	1239	1270	1148	1300	1196	1311	1148	1.14	29.60
FPS-VD2	1224	1158	1175	1057	1188	1091	1224	1057	1.15	34.28
FPS-VD3	1065	1017	1030	945	1013	963	1065	945	1.12	42.80
FPS-VD4	894	870	915	891	876	912	915	870	1.05	50.85

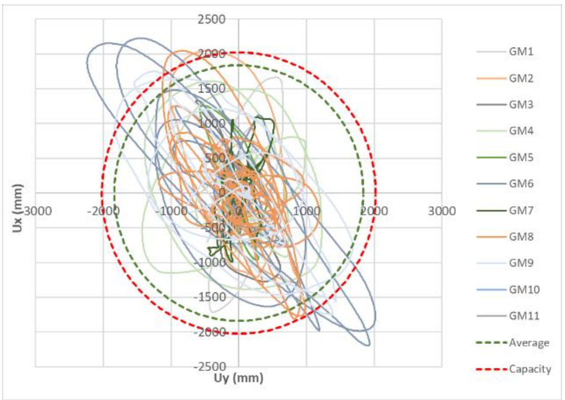

(a) Orbital Displacement – MCE LB FPS

Figure 3.16 Orbital displacements and capacity of isolators

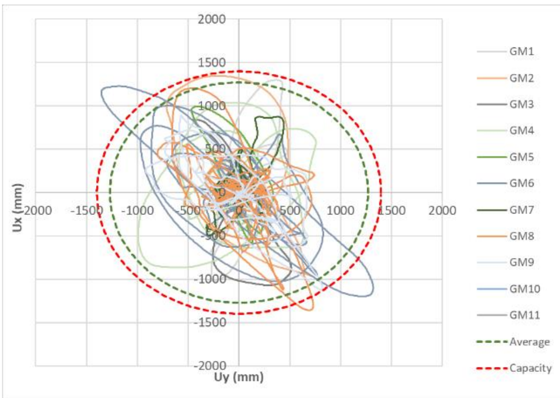

(b) Orbital Displacement – MCE LB FPS VD1

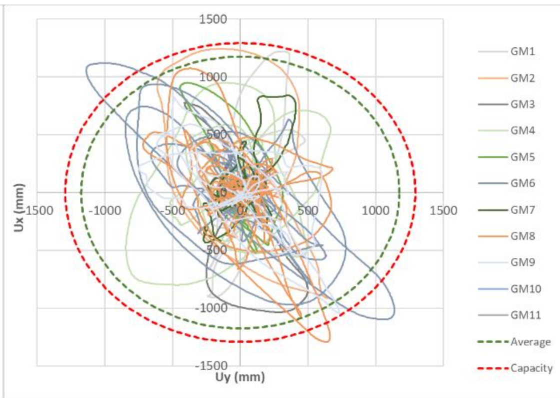

(c) Orbital Displacement – MCE LB FPS VD2

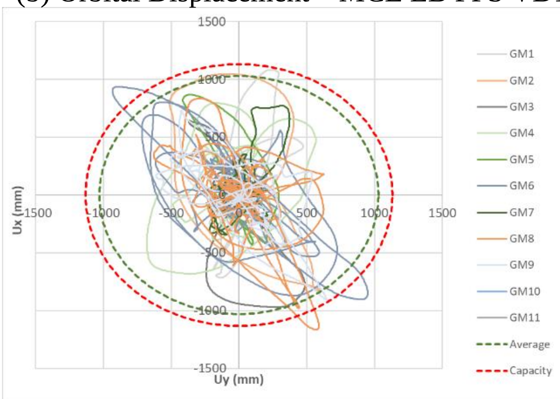

(d) Orbital Displacement – MCE LB FPS VD3

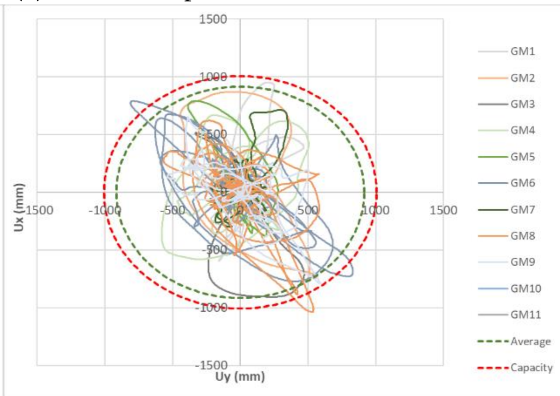

(e) Orbital Displacement – MCE LB FPS VD4

Figure 3.17 Orbital displacements and capacity of isolators (continued)

3.3.3 Story Acceleration

Due to high seismicity, even if the structure is designed as isolated, it is not possible to reduce story accelerations under 0.3g. That’s why there is no focus on limiting accelerations. A total of ten acceleration values are shown and compared in this chapter; nine values belong to peak story accelerations of structure and the last one belongs to ground acceleration. Ground acceleration is taken from the response spectrum. This value for this project equals 0.6g.

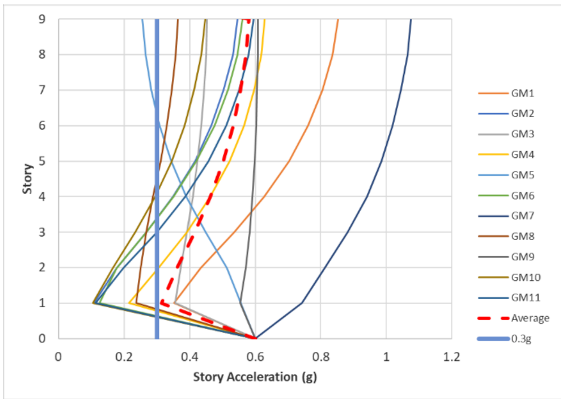

Figure 3.18 Resultant story accelerations of isolated structure

It has been observed that story accelerations decrease on the upper story of isolators but after two stories, acceleration values started to increase.

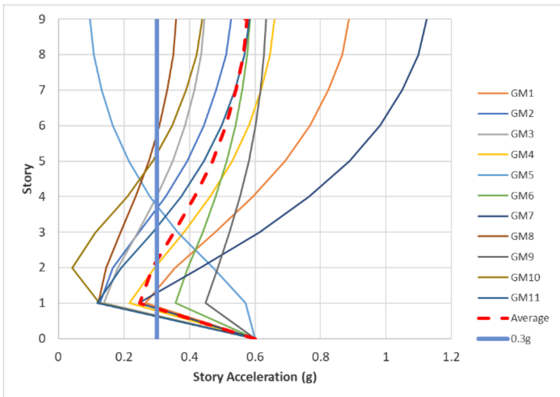

(a) Story Acceleration – DBE UB FPS-VD1

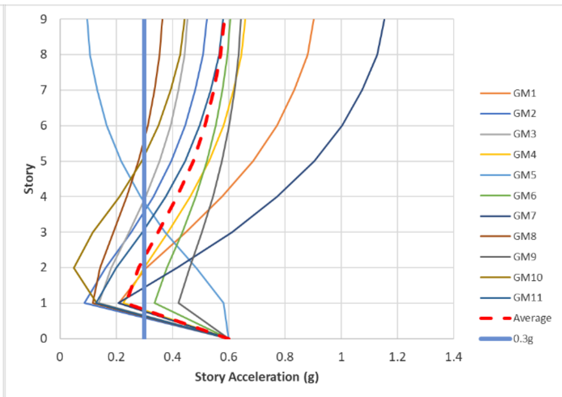

(b) Story Acceleration – DBE UB FPS-VD2

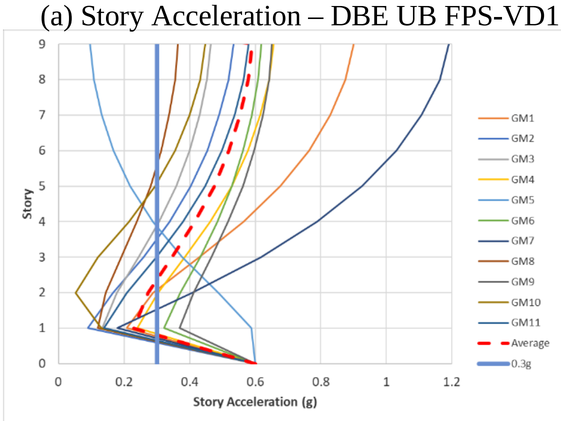

(c) Story Acceleration – DBE UB FPS-VD3

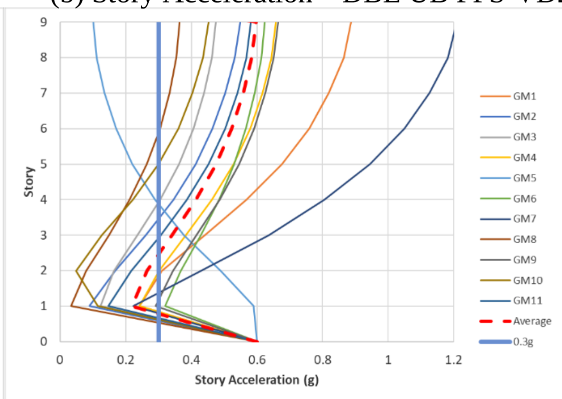

(d) Story Acceleration – DBE UB FPS-VD4

Figure 3.19 Resultant story accelerations of system with additional dampers

3.3.4 Interstorey Drift Ratios

Interstorey drift ratios of Bolu PMR Hospital are shown in this part. As in the previous structures, the limit is assumed as 0.005% according to the Building Earthquake Code of Turkey. This limit states operational performance level and aims for no damage to both structural and non-structural elements. Even if accelerations are too high, drift values are quite reasonable.

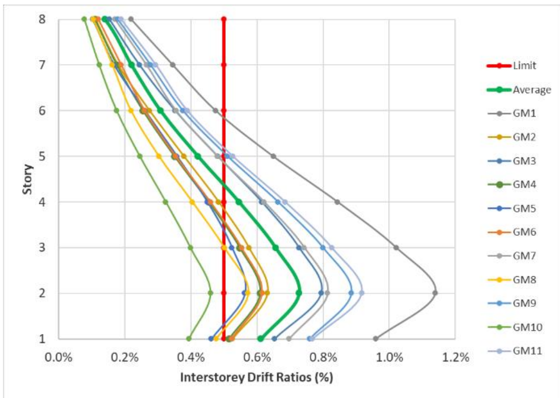

(a) Interstorey Drift Ratio – DBE UB FPS

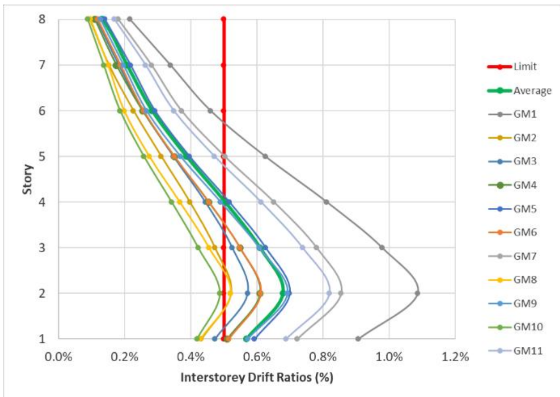

(b) Interstorey Drift Ratio – DBE UB FPS-VD1

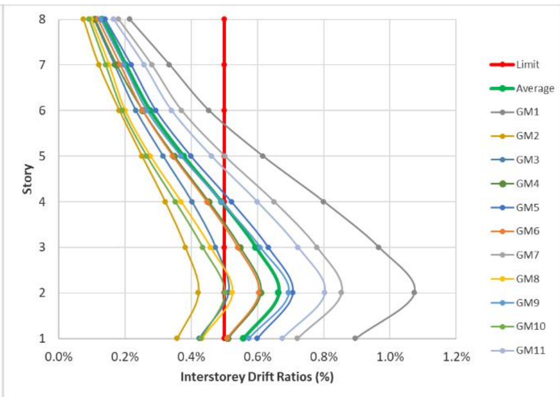

(c) Interstorey Drift Ratio – DBE UB FPS-VD2

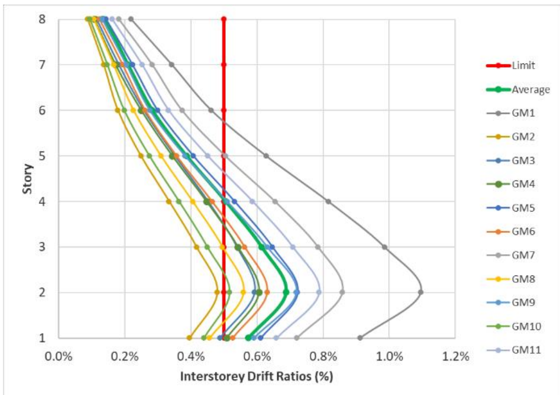

(d) Interstorey Drift Ratio – DBE UB FPS-VD3

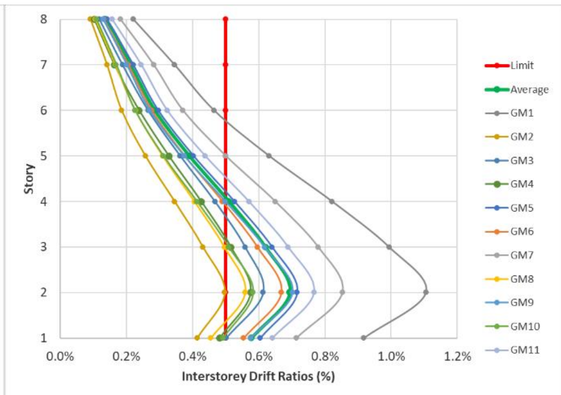

(e) Interstorey Drift Ratio – DBE UB FPS-VD4

Figure 3.20 Interstorey drift ratios of all cases

3.3.5 Base Shear Ratio

The structure with only an FPS system is designed based on 11.6% base shear and this chapter is focused on whether adding dampers will increase the shear force or not. Based on the reduction rate of displacements, base shear did not increase much. In all cases, the base shear value is calculated maximum of 12%. A comparison of these analyses will be examined in detail in Chapter 3.4.

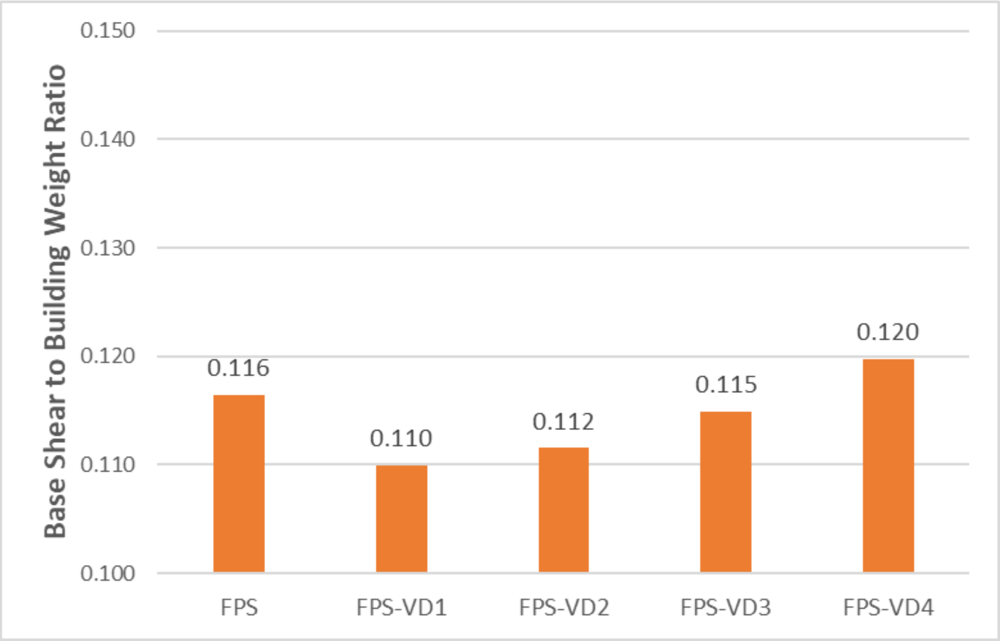

Figure 3.21 Base shear ratios of all cases

Table 3.11 Base shear ratios of all cases and change compared to FPS

Case	Base Shear to Building Weight Ratio	Change (%)
FPS	0.116	-
FPS-VD1	0.110	-5.58
FPS-VD2	0.112	-4.19
FPS-VD3	0.115	-1.30
FPS-VD4	0.120	2.86

3.4 Comparison of Results

In this chapter, all analysis results will be evaluated and compared for three different structures based on maximum displacement demands, story accelerations, interstorey drifts, and base shear ratios. Among all the cases, the most reasonable one will be selected and compared to the model with only isolators (i.e., FPS model).

As mentioned before, for Kahramanmaraş State Hospital (B1) and Adıyaman Residential Building (B2), two different dampers were modeled and named as UD and UDs. For this reason, these two damper results will be compared separately. For Bolu PMR Hospital (B3), the results of the viscous damper model will be compared with the FPS model.

3.4.1 Kahramanmaraş State Hospital Results (B1)

In the Kahramanmaraş State Hospital, it was observed that accelerations decreased significantly when a damper was added to the model. In the FPS model, limit values that cannot be achieved from the 6th story onwards are limited with the first alternative damper solution. Acceleration values of 0.9g were reduced to 0.3g with the inclusion of dampers.

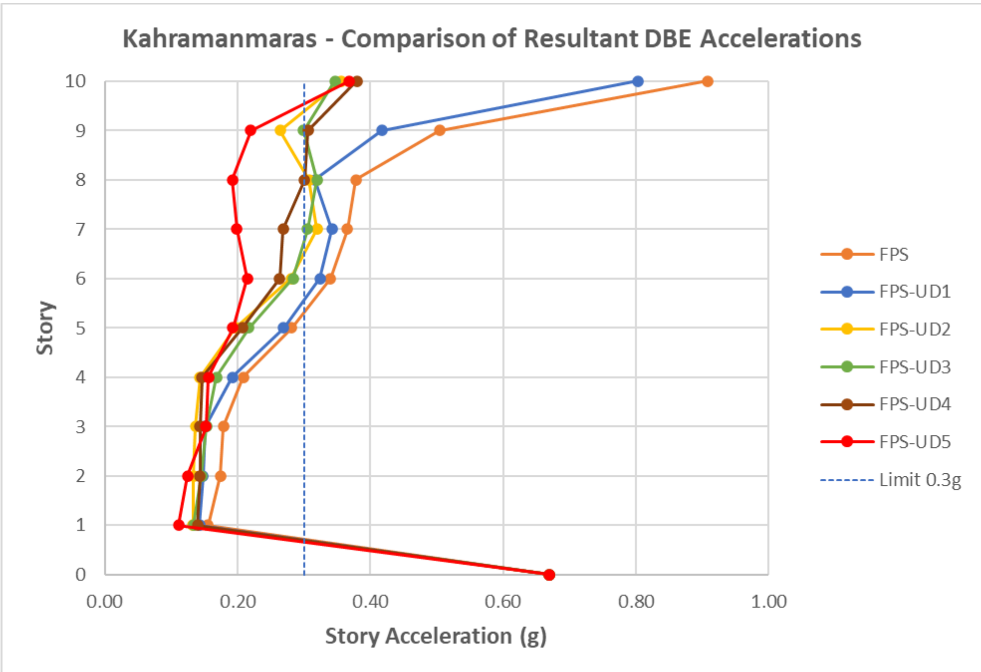

Figure 3.22 Comparison of resultant accelerations for U Damper – Kahramanmaraş (B1)

Table 3.12 Comparison of resultant accelerations for each story for U Damper – Kahramanmaraş (B1) (g)

Case/Story	0	1	2	3	4	5	6	7	8	9	10
FPS	0.67	0.15	0.17	0.18	0.21	0.28	0.34	0.37	0.38	0.50	0.91
FPS-UD1	0.67	0.14	0.15	0.15	0.19	0.27	0.32	0.34	0.32	0.42	0.80
FPS-UD2	0.67	0.13	0.13	0.14	0.14	0.20	0.28	0.32	0.31	0.26	0.36
FPS-UD3	0.67	0.13	0.15	0.15	0.17	0.22	0.28	0.31	0.32	0.30	0.35
FPS-UD4	0.67	0.14	0.14	0.14	0.15	0.21	0.26	0.27	0.30	0.31	0.38
FPS-UD5	0.67	0.11	0.12	0.15	0.16	0.19	0.21	0.20	0.19	0.22	0.37

Similar situations were observed for the second damper alternative. Since the dampers are stiffer than the first alternative, the rate of decrease in acceleration is larger. However, it was observed that as the number of dampers increases, the accelerations on the upper stories increase.

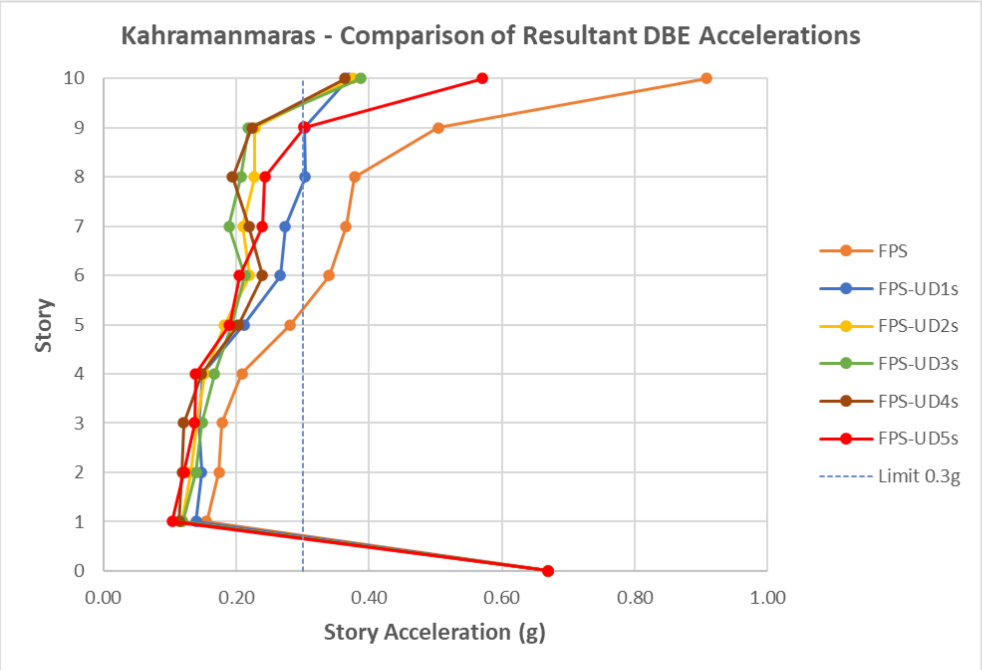

Figure 3.23 Comparison of resultant story accelerations for U Damper-Stiffer – Kahramanmaraş (B1)

Table 3.13 Comparison of resultant accelerations for each story for U Damper-Stiffer – Kahramanmaraş (B1) (g)

Case/Story	0	1	2	3	4	5	6	7	8	9	10
FPS	0.67	0.15	0.17	0.18	0.21	0.28	0.34	0.37	0.38	0.50	0.91
FPS-UD1s	0.67	0.14	0.15	0.14	0.15	0.21	0.27	0.27	0.30	0.30	0.37
FPS-UD2s	0.67	0.12	0.13	0.14	0.15	0.18	0.22	0.21	0.23	0.23	0.38
FPS-UD3s	0.67	0.12	0.14	0.15	0.17	0.19	0.21	0.19	0.21	0.22	0.39
FPS-UD4s	0.67	0.11	0.12	0.12	0.15	0.20	0.24	0.22	0.19	0.22	0.36
FPS-UD5s	0.67	0.10	0.12	0.14	0.14	0.19	0.20	0.24	0.24	0.30	0.57

Adding a damper to a base isolated structure generally tends to increase interstorey drifts. The number of dampers is important to keep the drifts at a certain rate and maintain the performance level of the structure. In cases where low-rigidity dampers are added, the increase in drifts is negligible. On the contrary, when a more rigid damper is added to all links, the behavior and performance level of the structure change significantly.

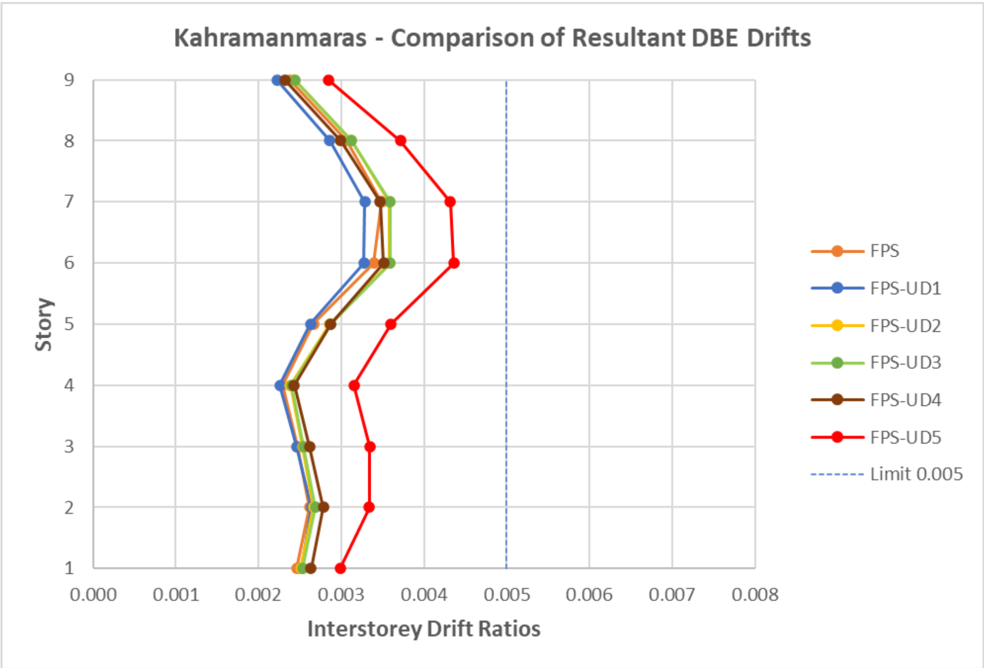

Figure 3.24 Comparison of interstorey drifts for U Damper – Kahramanmaraş (B1)

Table 3.14 Comparison of interstorey drifts for each story for U Damper – Kahramanmaraş (B1) (%)

Case/Story	1	2	3	4	5	6	7	8	9
FPS	0.002	0.003	0.002	0.002	0.003	0.003	0.003	0.003	0.002
FPS-UD1	0.003	0.003	0.002	0.002	0.003	0.003	0.003	0.003	0.002
FPS-UD2	0.003	0.003	0.003	0.002	0.003	0.004	0.004	0.003	0.002
FPS-UD3	0.003	0.003	0.003	0.002	0.003	0.004	0.004	0.003	0.002
FPS-UD4	0.003	0.003	0.003	0.002	0.003	0.004	0.003	0.003	0.002
FPS-UD5	0.003	0.003	0.003	0.003	0.004	0.004	0.004	0.004	0.003

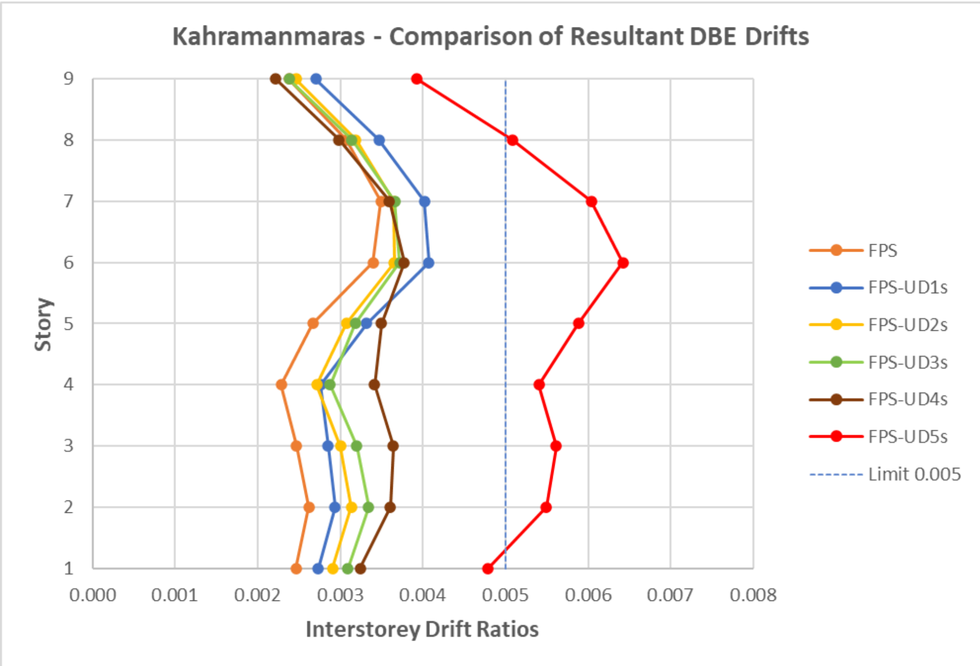

Figure 3.25 Comparison of interstorey drift ratios for U Damper-Stiffer – Kahramanmaraş (B1)

The behavior of the structure where the second alternative dampers (i.e., UDs) are used has changed significantly.

Table 3.15 Comparison of interstorey drift ratios for U Damper-Stiffer – Kahramanmaraş (B1) (%)

Case/Story	**1**	**2**	**3**	**4**	**5**	**6**	**7**	**8**	**9**
FPS	0.002	0.003	0.002	0.002	0.003	0.003	0.003	0.003	0.002
FPS-UD1s	0.003	0.003	0.003	0.003	0.003	0.004	0.004	0.003	0.003
FPS-UD2s	0.003	0.003	0.003	0.003	0.003	0.004	0.004	0.003	0.002
FPS-UD3s	0.003	0.003	0.003	0.003	0.003	0.004	0.004	0.003	0.002
FPS-UD4s	0.003	0.004	0.004	0.003	0.004	0.004	0.004	0.003	0.002
FPS-UD5s	0.005	0.005	0.006	0.005	0.006	0.006	0.006	0.005	0.004

In Figure 3.27, maximum isolator displacements and reduction rates for every case are shown. In the FPS model, the displacement demand of the structure is around 1000 mm, and it decreases at each step. The reduction rate is the largest in the second damper alternative, and it could reduce the displacement demand to 400 mm.

In addition, the ratio of maximum displacement demand in all links to minimum displacement demand in all links (i.e., max/min value) is determined for each analysis. The aim of considering this value is to examine structure behavior. As this value approaches 1, all links have the same displacement demand, corresponding to a rigid body motion without any eccentricities. In original structure, there was a difference between center of rigidity and center of mass. Due to this distance, links have not been same displacement at dynamic situation. Maximum and minimum demand ratio was 1.115. As dampers are added to the structure based on rigidity and mass center, this ratio is totally changed and approached to ideal situation - “1”. UD2s, UD3s and UD4 can be evaluated as the most appropriate case.

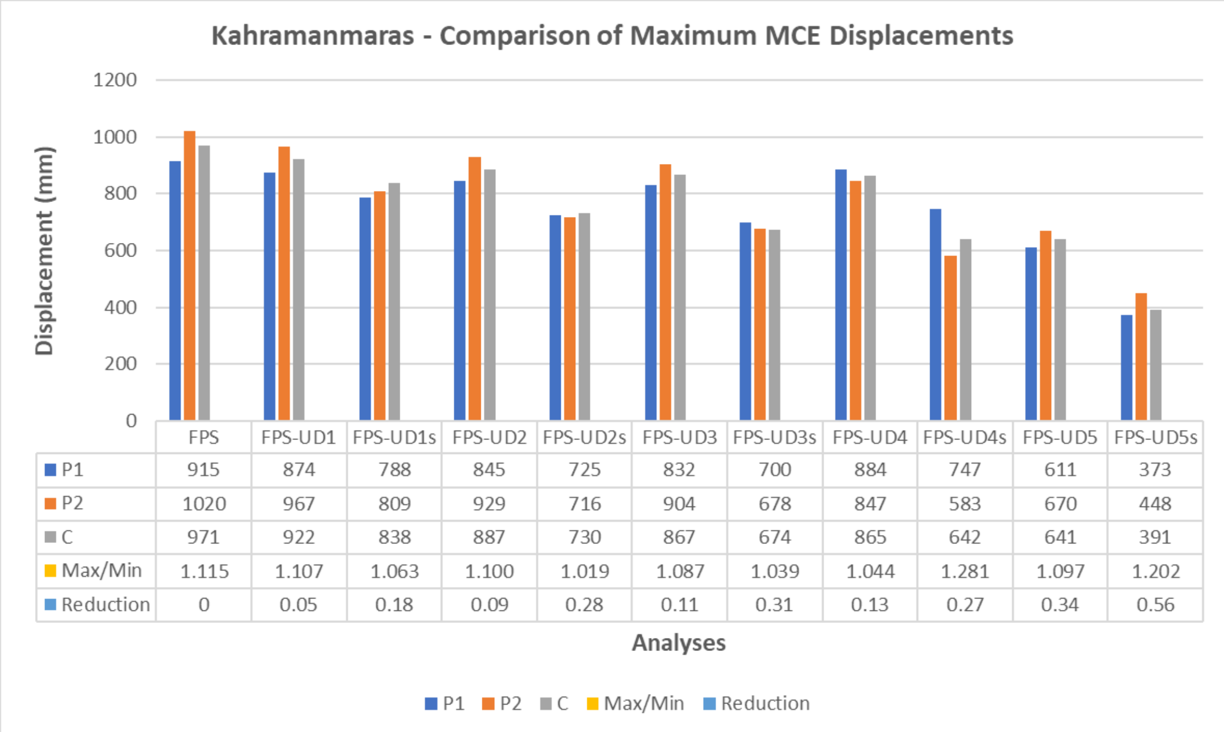

	FPS	FPS-UD1	FPS-UD1s	FPS-UD2	FPS-UD2s	FPS-UD3	FPS-UD3s	FPS-UD4	FPS-UD4s	FPS-UD5	FPS-UD5s
P1	915	874	788	845	725	832	700	884	747	611	373
P2	1020	967	809	929	716	904	678	847	583	670	448
C	971	922	838	887	730	867	674	865	642	641	391
Max/Min	1.115	1.107	1.063	1.100	1.019	1.087	1.039	1.044	1.281	1.097	1.202
Reduction	0	0.05	0.18	0.09	0.28	0.11	0.31	0.13	0.27	0.34	0.56

Figure 3.26 Comparison of maximum displacement demands – Kahramanmaraş (B1)

The last comparison graph is focused on the base shear to building weight ratio. The aim here is to observe changes in base shear with added dampers. According to these results, it can be evaluated as the second damper alternative is not a good option based on base shear. Since the second alternative is stiffer than isolators, the base shear ratio increases gradually. That's why it is an advantage to use less stiff dampers than isolators (Figure 3.22).

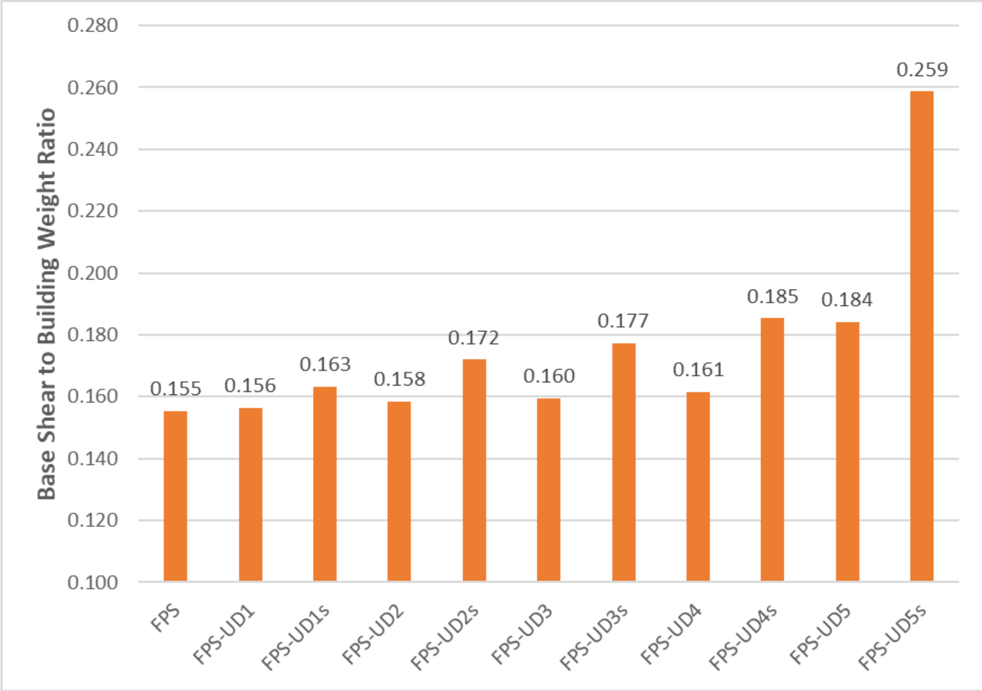

Figure 3.27 Comparison of base shear ratios – Kahramanmaraş (B1)

Based on all these comparisons, the UD4 option can be the most reasonable case. A comparison of the FPS model and the UD4 model is figured out below (Figure 3.23 - 3.25). Although story accelerations decrease significantly, the increase in interstorey drifts is very small and still within the limits (Table 3.8). Moreover, displacement demand is decreased as 13% and max/min value approached to 1.

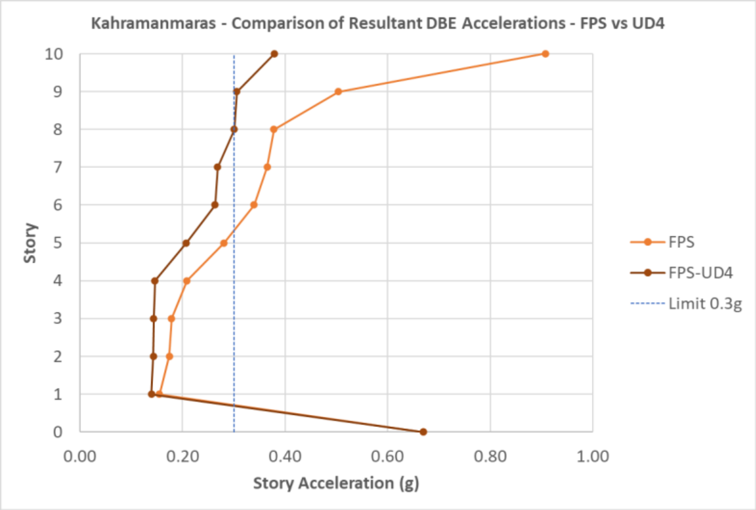

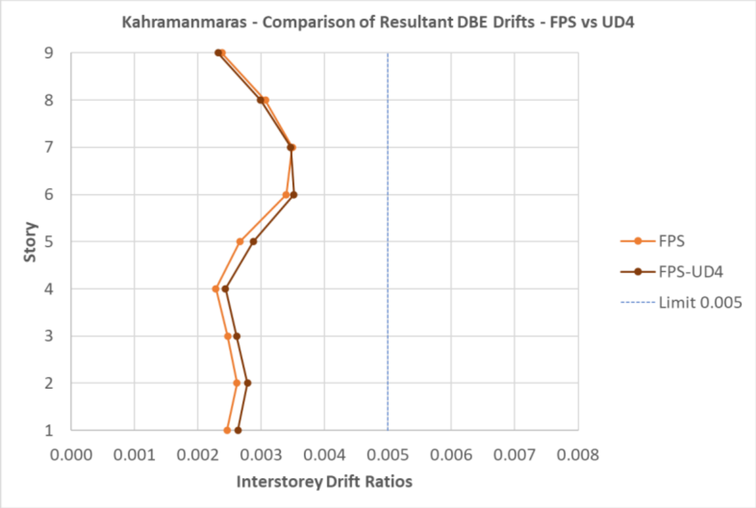

Figure 3.28 Comparison of accelerations and drifts for FPS and UD4 – Kahramanmaraş(B1)

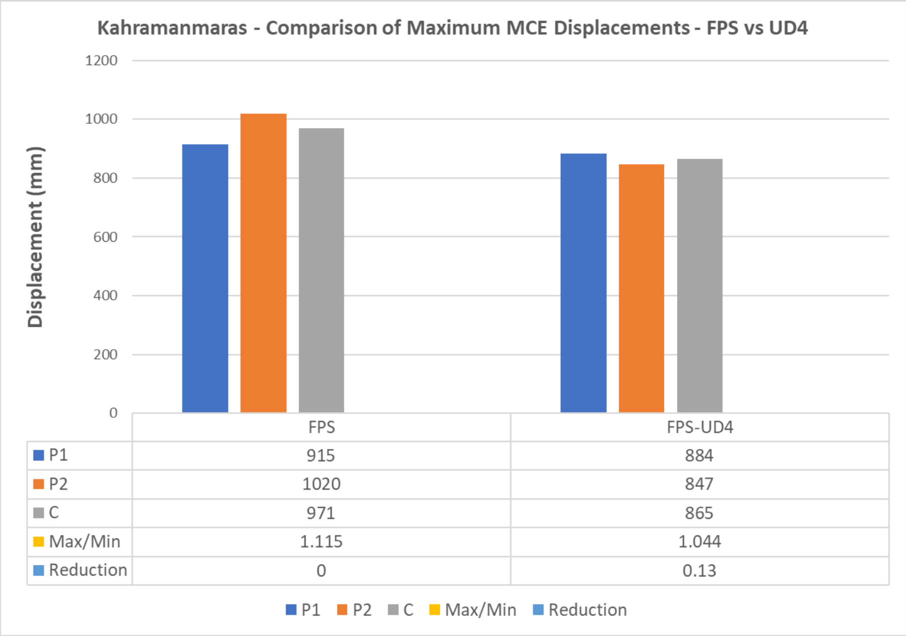

Figure 3.29 Comparison of maximum displacements for FPS and UD4 – Kahramanmaraş(B1)

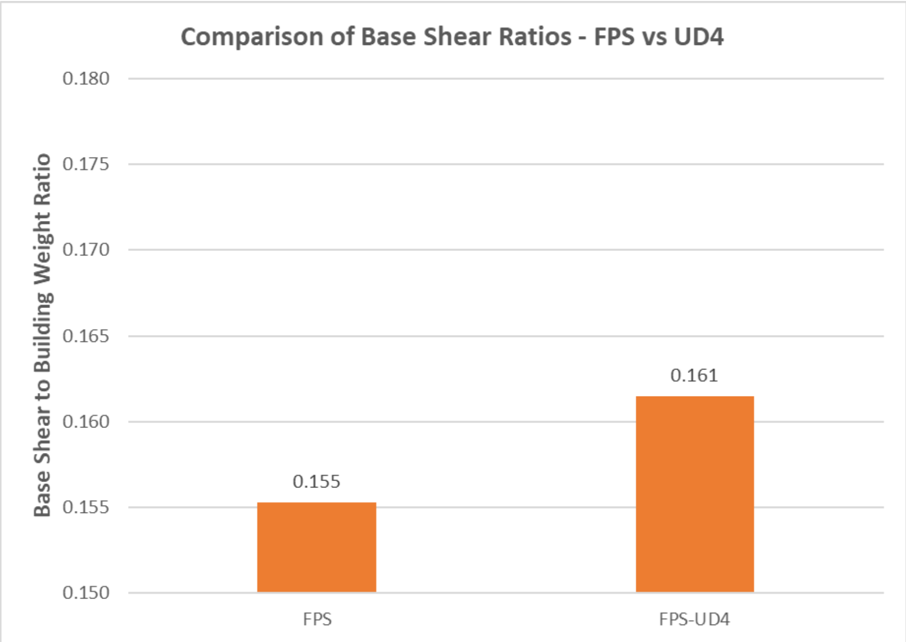

Figure 3.30 Comparison of base shear ratios for FPS and UD4 – Kahramanmaraş(B1)

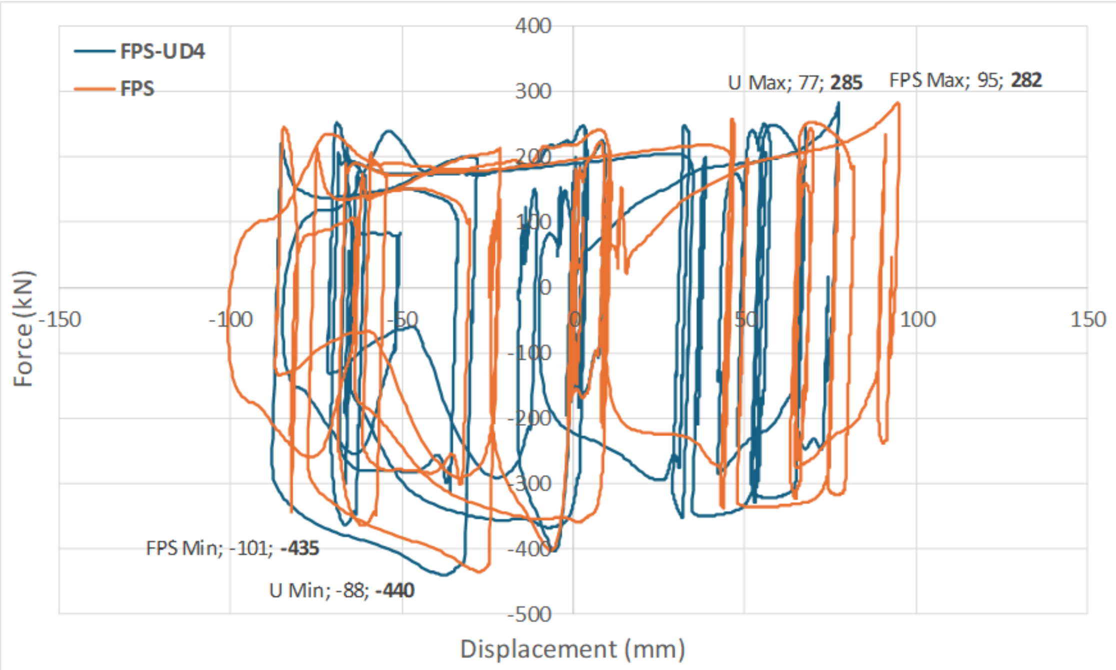

Figure 3.31 Comparison of Force-Displacement Behaviors for One Link – DBE UB

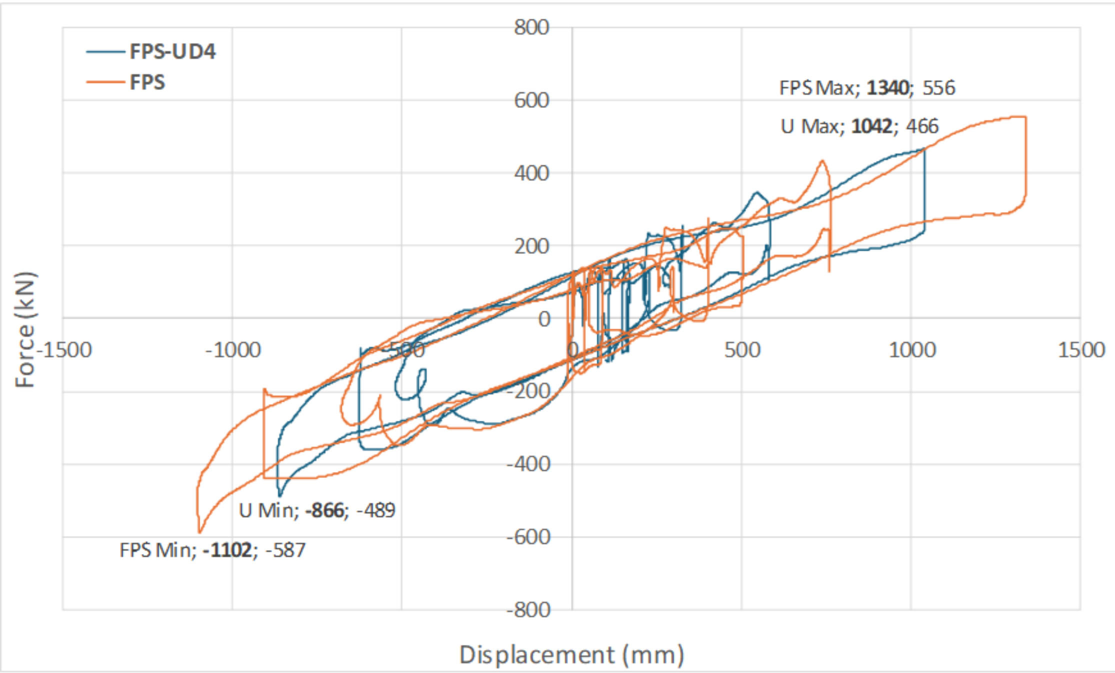

Figure 3.32 Comparison of Force-Displacement Behaviors for One Link – MCE LB

Force-Displacement behaviors of isolators shared in Figures 3.32 – 3.33. In the first figure, behaviors are compared for DBE UB and second figure represent MCE LB. Maximum horizontal link forces are increased a bit in FPS-UD4 like increased total base shear. Besides, maximum displacement demands can be examined in Figure 3.33. In FPS case, although maximum and minimum demands are 1340 and -1102 mm, in FPS-UD4 case, demands are 1042 and -866 mm. So, displacement demands have decreased significantly while horizontal forces did not increase much. Moreover, force-displacement curves are not smooth due to bi-directional analysis and these curves includes forces in one axis. This is the main reason of curves are not smooth.

Table 3.16 Comparison of all results for FPS and UD4 - Kahramanmaraş

	FPS 361 FPS	**UD4 361 FPS + 109 UD**	**Change (%)**
Max Acc (g)	0.91	0.38	-58.2
Max Drift Ratio	0.00349	0.00351	0.6
Max Displacement (mm)	1020	884	-13.3
Displacement Ratio	1.115	1.044	-6.4
Base Shear (W)	0.155	0.161	3.9
CoR - CoM Distance (m)	4.7	1.2	-74.5

3.4.2 Adıyaman Residential Building (B2)

As mentioned in the second chapter, metallic dampers were added to the Adıyaman Residential Building in addition to the curved surface sliders. The structure is in a highly active region, but it is not very close to the fault, that’s why the peak ground acceleration value is taken as 0.25g. It was observed that accelerations decreased slightly when a damper was added to the model. In the FPS model, limit values can be achieved; after the ninth-story acceleration values close to the limit value. With adding dampers, acceleration values are shifted.

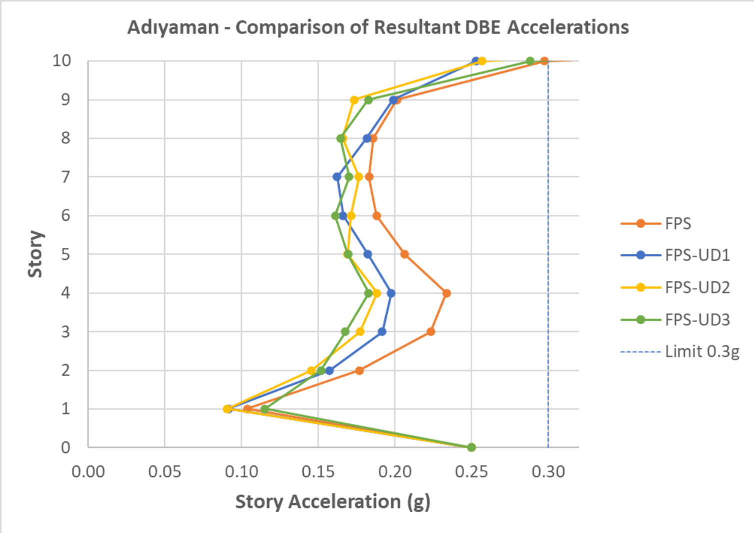

Figure 3.33 Comparison of story accelerations – Adıyaman UD

Table 3.17 Comparison of story accelerations for all stories – Adıyaman UD (g)

Case/Story	0	1	2	3	4	5	6	7	8	9	10
FPS	0.25	0.10	0.18	0.22	0.23	0.21	0.19	0.18	0.19	0.20	0.30
FPS-UD1	0.25	0.09	0.16	0.19	0.20	0.18	0.17	0.16	0.18	0.20	0.25
FPS-UD2	0.25	0.09	0.15	0.18	0.19	0.17	0.17	0.18	0.17	0.17	0.26
FPS-UD3	0.25	0.12	0.15	0.17	0.18	0.17	0.16	0.17	0.16	0.18	0.29

With stiffer dampers, the behavior of the structure is changed. After the ninth story, acceleration values started to increase.

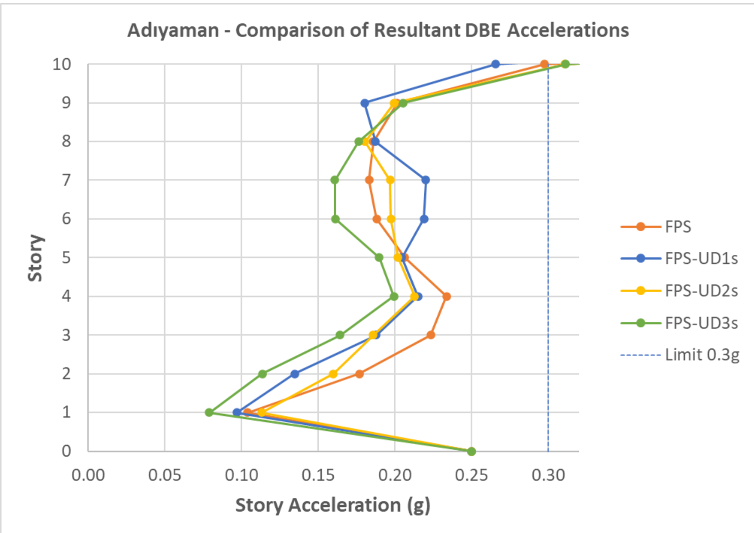

Figure 3.34 Comparison of story accelerations – Adıyaman UDs

Table 3.18 Comparison of story accelerations for all stories – Adıyaman UDs (g)

Case/Story	0	1	2	3	4	5	6	7	8	9	10
FPS	0.25	0.10	0.18	0.22	0.23	0.21	0.19	0.18	0.19	0.20	0.30
FPS-UD1s	0.25	0.10	0.13	0.19	0.22	0.20	0.22	0.22	0.19	0.18	0.27
FPS-UD2s	0.25	0.11	0.16	0.19	0.21	0.20	0.20	0.20	0.18	0.20	0.31
FPS-UD3s	0.25	0.08	0.11	0.16	0.20	0.19	0.16	0.16	0.18	0.21	0.31

It is seen that the use of additional dampers increased interstorey drifts. As the number of dampers increased, this rate of increase continued. A certain increase was observed for both damper types. As expected, the increase rate is much higher in the stiffer damper. It is important to keep the drifts at a certain rate and maintain the performance level of the structure. That's why values should be within the limits.

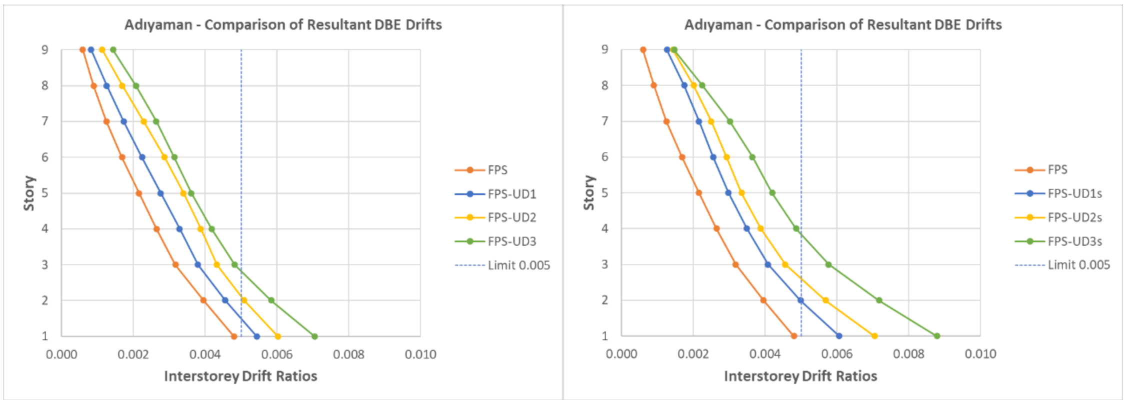

Figure 3.35 Comparison of interstorey drifts - Adıyaman

Table 3.19 Comparison of interstorey drifts for all story – Adıyaman U Damper (%)

Case/Story	1	2	3	4	5	6	7	8	9
FPS	0.005	0.004	0.003	0.003	0.002	0.002	0.001	0.001	0.001
FPS-UD1	0.005	0.005	0.004	0.003	0.003	0.002	0.002	0.001	0.001
FPS-UD2	0.006	0.005	0.004	0.004	0.003	0.003	0.002	0.002	0.001
FPS-UD3	0.007	0.006	0.005	0.004	0.004	0.003	0.003	0.002	0.001

Table 3.20 Comparison of interstorey drifts for all story – Adıyaman U Damper-Stiffer (%)

Case/Story	1	2	3	4	5	6	7	8	9
FPS	0.005	0.004	0.003	0.003	0.002	0.002	0.001	0.001	0.001
FPS-UD1s	0.006	0.005	0.004	0.003	0.003	0.003	0.002	0.002	0.001
FPS-UD2s	0.007	0.006	0.005	0.004	0.003	0.003	0.002	0.002	0.001
FPS-UD3s	0.009	0.007	0.006	0.005	0.004	0.004	0.003	0.002	0.001

In the Figure 3.29, maximum isolator displacements and reduction rates for every case are shown. In the current model, the displacement demand of the structure is around 200 mm, and it decreases at each step. The reduction rate is higher with the second damper alternative, and it could be reduced to 96 mm.

There is also a max/min value calculated. It is the ratio of the link with maximum demand and minimum demand. The aim of considering this value is to examine structure behavior. As this value approaches 1, all links have the same displacement demand.

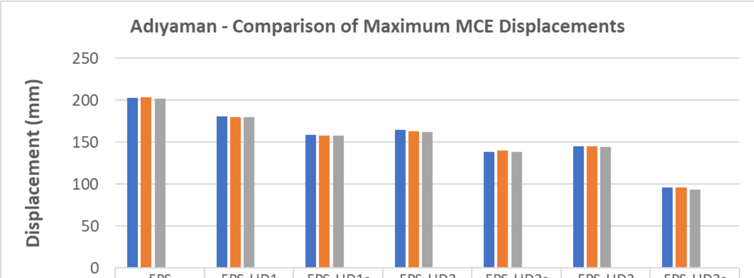

	FPS	FPS-UD1	FPS-UD1s	FPS-UD2	FPS-UD2s	FPS-UD3	FPS-UD3s
P1	203	181	159	164	138	145	96
P2	203	180	158	163	140	145	96
C	202	180	158	162	138	144	93
Max/Min	1.006	1.008	1.009	1.014	1.013	1.008	1.034
Reduction	0	0.11	0.22	0.19	0.31	0.29	0.53

P1 P2 C Max/Min Reduction

Figure 3.36 Comparison of maximum displacements – Adıyaman

The last comparison graph is focused on the base shear ratio of the structure. The aim here is to observe changes in base shear with added dampers and not to increase the base shear ratio. According to these results, it can be evaluated as a second damper alternative is not a good option based on base shear. Since the second alternative is stiffer than isolators, the base shear ratio increases significantly. That’s why it is an advantage to use fewer stiff dampers than isolators.

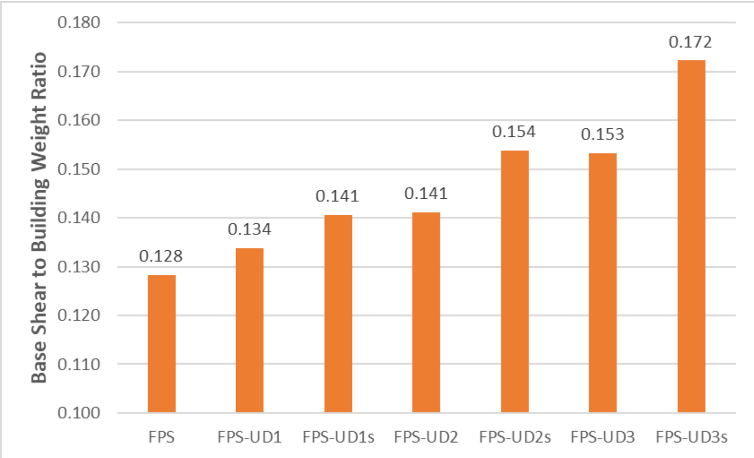

Figure 3.37 Comparison of base shear ratios – Adıyaman

Based on all these comparisons, the UD1 option can be the most reasonable case. A comparison of the FPS model and the UD1 model is figured out below in Figure 3.31.

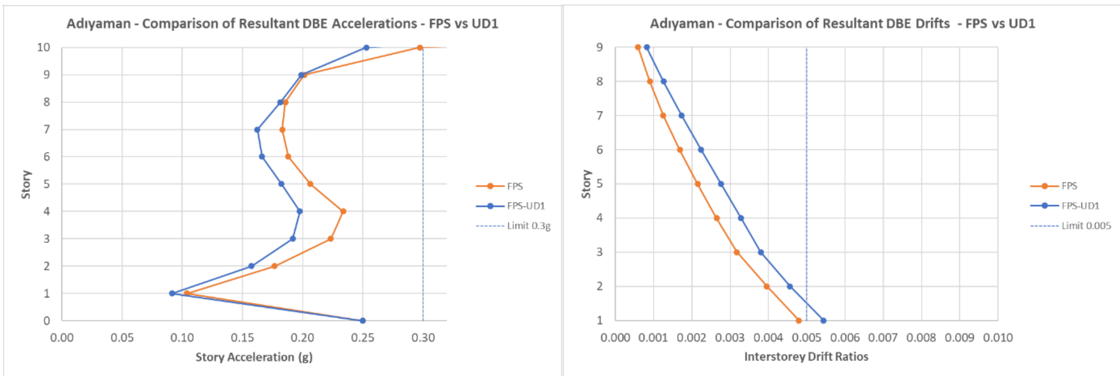

Figure 3.38 Comparison of accelerations and drifts of FPS and UD1 - Adıyaman

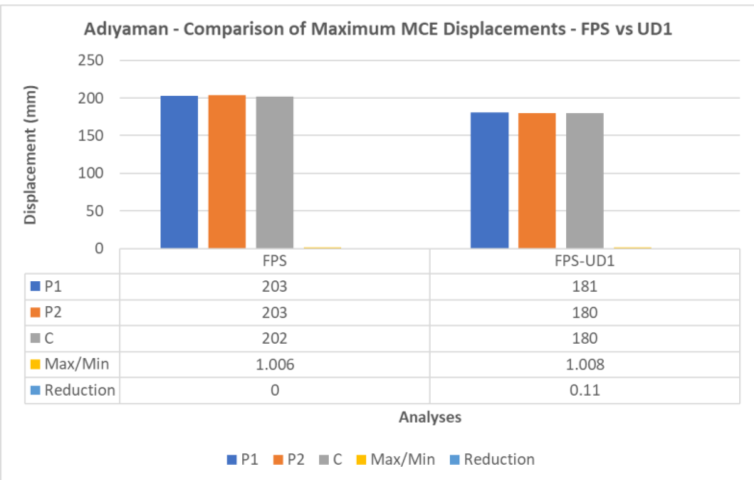

Figure 3.39 Comparison of maximum displacements of FPS and UD1 – Adıyaman

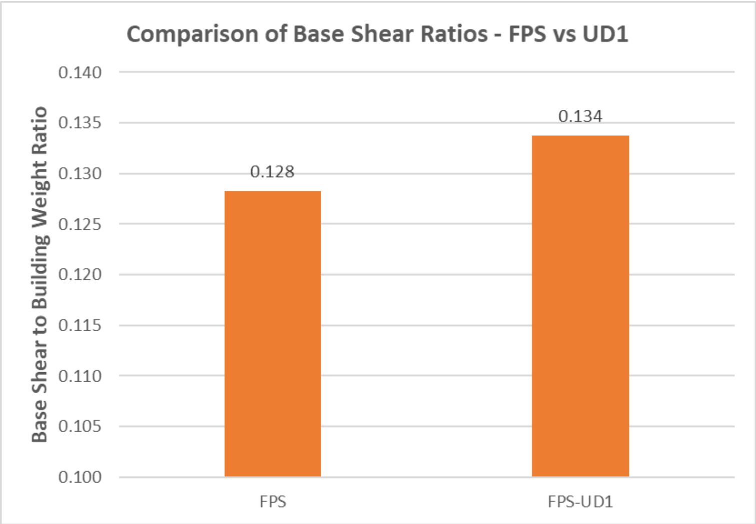

Figure 3.40 Comparison of base shear ratios of FPS and UD1 - Adıyaman

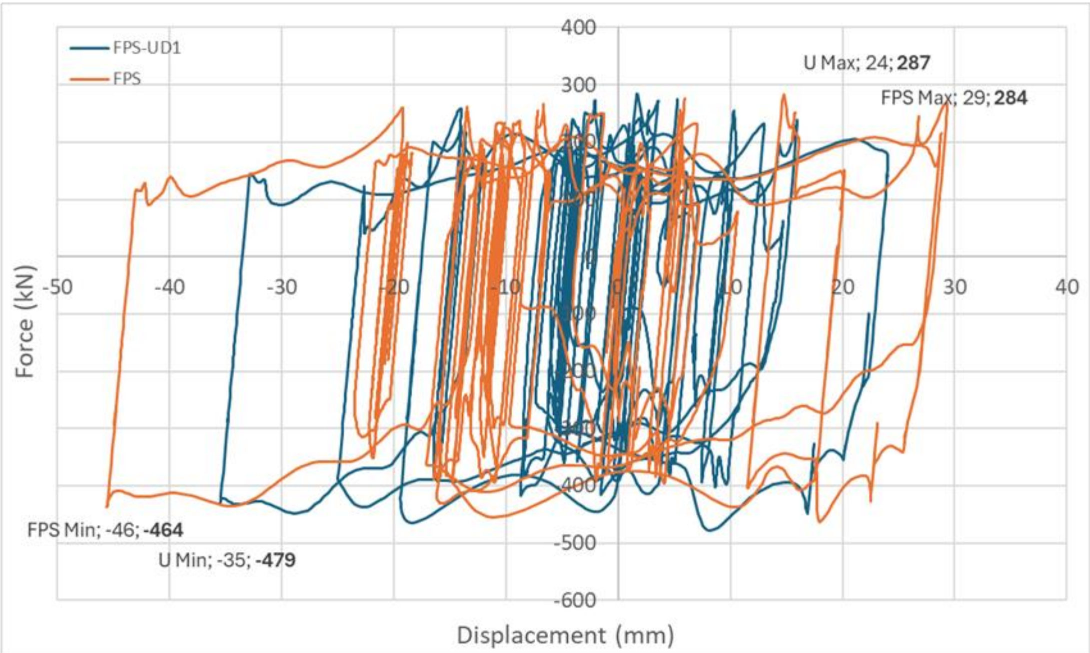

Figure 3.41 Comparison of Force-Displacement Behaviors for One Link – DBE UB

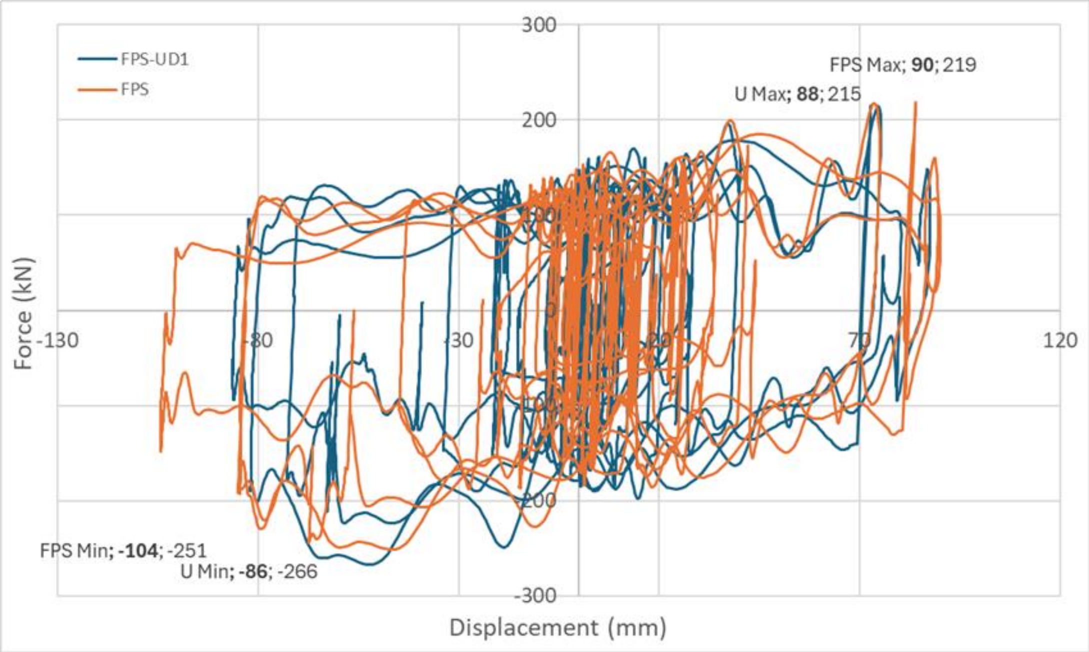

Figure 3.42 Comparison of Force-Displacement Behaviors for One Link – MCE LB

Table 3.21 Comparison of all results of FPS and UD1 – Adıyaman

	FPS 18 FPS	FPS-UD1 18 FPS + 4 UD	Change (%)
Max Acc (g)	0.3	0.25	-16.7
Max Drift Ratio	0.0048	0.00544	13.3
Max Displacement (mm)	203	181	-10.8
Displacement Ratio	1.006	1.008	0.2
Base Shear (W)	0.128	0.134	4.7
CoR - CoM Distance (m)	0.18	0.19	5.1

3.4.3 Bolu PMR Hospital (B3)

For Bolu PMR Hospital, due to high seismicity viscous dampers have been used to decrease isolator displacement demands. In addition to the FPS model, 4 different quantities of viscous dampers have been modeled, and all results have been mentioned in Chapter 3. In this part, these analyses will be discussed and compared.

Due to high seismicity, story accelerations could not be achieved within the limits even though it is a base-isolated model. It has been observed that as dampers were added to the model, accelerations started to decrease for the first 5 stories. But still, not all story acceleration values were within the limits: except for the first 2 stories, all accelerations are higher than 0.3g.

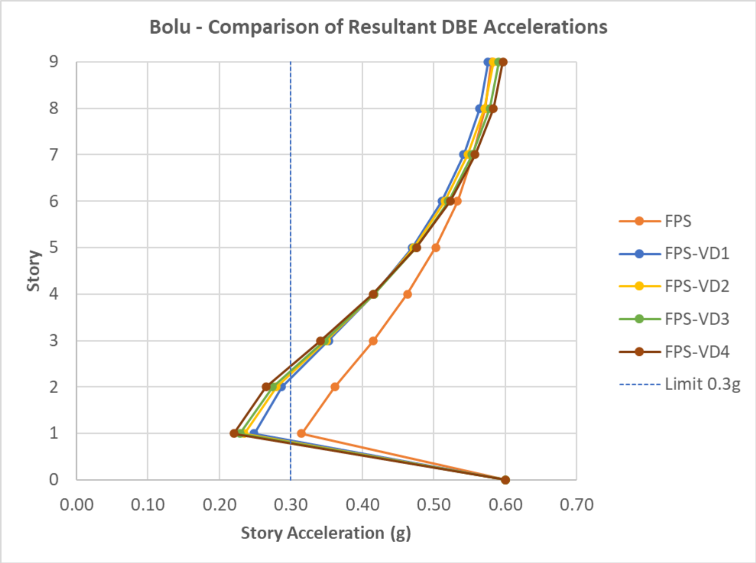

Figure 3.43 Comparison of story accelerations – Bolu

Table 3.22 Comparison of story accelerations for all stories – Bolu (g)

Case/Story	0	1	2	3	4	5	6	7	8	9
FPS	0.60	0.31	0.36	0.42	0.46	0.50	0.53	0.56	0.57	0.58
FPS-VD1	0.60	0.25	0.29	0.35	0.42	0.47	0.51	0.54	0.56	0.58
FPS-VD2	0.60	0.23	0.28	0.35	0.42	0.47	0.52	0.55	0.57	0.58
FPS-VD3	0.60	0.23	0.27	0.35	0.42	0.48	0.52	0.55	0.58	0.59
FPS-VD4	0.60	0.22	0.26	0.34	0.42	0.48	0.52	0.56	0.58	0.60

In the FPS model, even though acceleration values are not within the limits, all the drift ratios are within the limits. As dampers are added to the model, drift ratios tend to decrease.

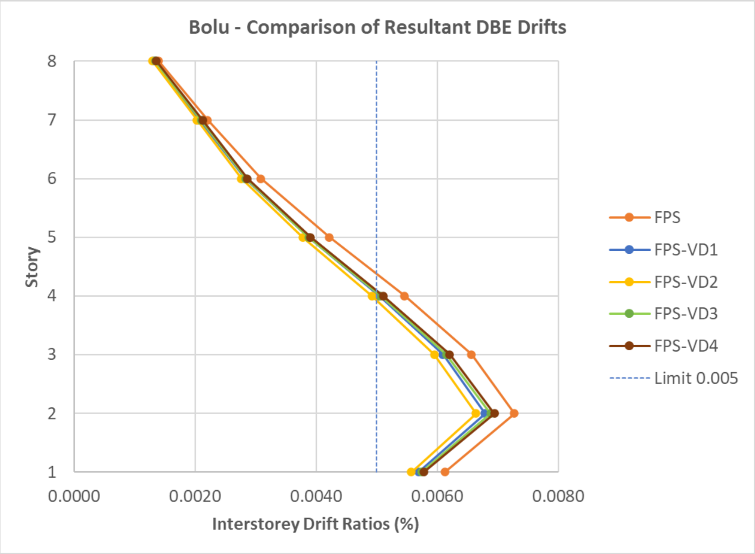

Figure 3.44 Comparison of interstorey drifts – Bolu

Table 3.23 Comparison of interstorey drifts for all story – Bolu (%)

Case/Story	1	2	3	4	5	6	7	8
FPS	0.0061	0.0073	0.0066	0.0055	0.0042	0.0031	0.0022	0.0014
FPS-UD1	0.0057	0.0068	0.0061	0.0050	0.0039	0.0028	0.0021	0.0013
FPS-UD2	0.0056	0.0066	0.0060	0.0049	0.0038	0.0028	0.0020	0.0013
FPS-UD3	0.0057	0.0069	0.0062	0.0051	0.0039	0.0028	0.0021	0.0013
FPS-UD4	0.0058	0.0069	0.0062	0.0051	0.0039	0.0029	0.0021	0.0014

In the FPS model, displacement demands were around 1800 mm, and the design and manufacture of an isolator with this displacement capacity is not possible. That's why in this graph, the reduction rate of displacement ratio will be focused. Displacement demands are approximately 1300, 1200, 1000, and 900 mm, respectively. The reduction rate can be up to 48% in the last case; FPS-VD4.

Maximum and minimum link displacements were also calculated to observe structure behavior, this value is 1.02 in the FPS model. It means that all links tend to have the same displacement demand and act the same. In VD4 model, is quite bigger than the FPS model due to architectural limitations. However, since the displacement reached the desired levels, this value was left as it is.

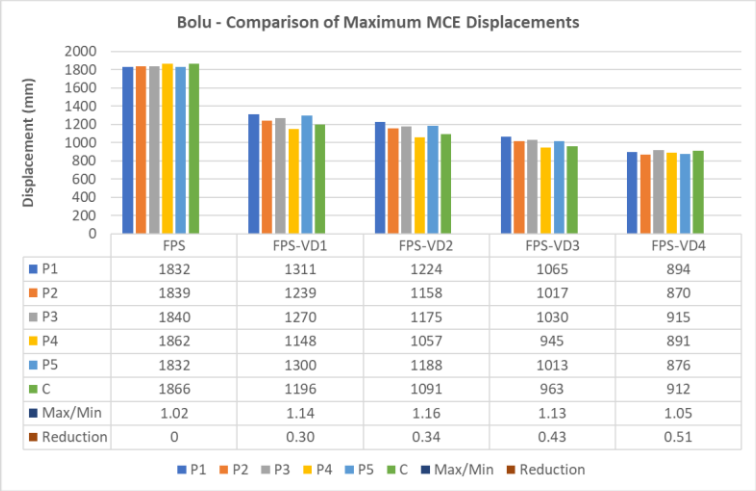

	FPS	FPS-VD1	FPS-VD2	FPS-VD3	FPS-VD4
P1	1832	1311	1224	1065	894
P2	1839	1239	1158	1017	870
P3	1840	1270	1175	1030	915
P4	1862	1148	1057	945	891
P5	1832	1300	1188	1013	876
C	1866	1196	1091	963	912
Max/Min	1.02	1.14	1.16	1.13	1.05
Reduction	0	0.30	0.34	0.43	0.51

Figure 3.45 Comparison of maximum displacements – Bolu

Base shear is one of the important parameters because this value will affect the design of the superstructure. In the FPS model, this value is around 0.116. Despite adding a damper to the system, this value has not increased significantly. It was noticed that this value was 0.12 in the last case named VD4.

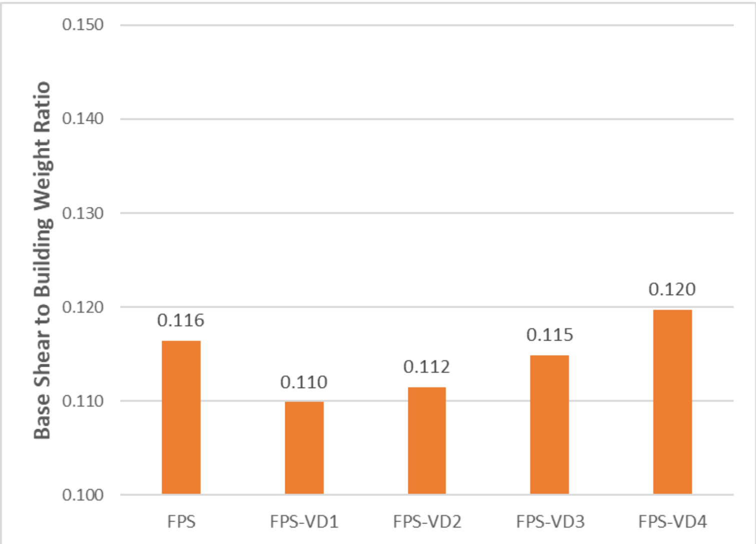

Figure 3.46 Comparison of base shear ratios – Bolu

According to all these comparisons of 5 different cases, it is observed that the most reasonable case is FPS-VD4 due to displacement limitations of an isolator.

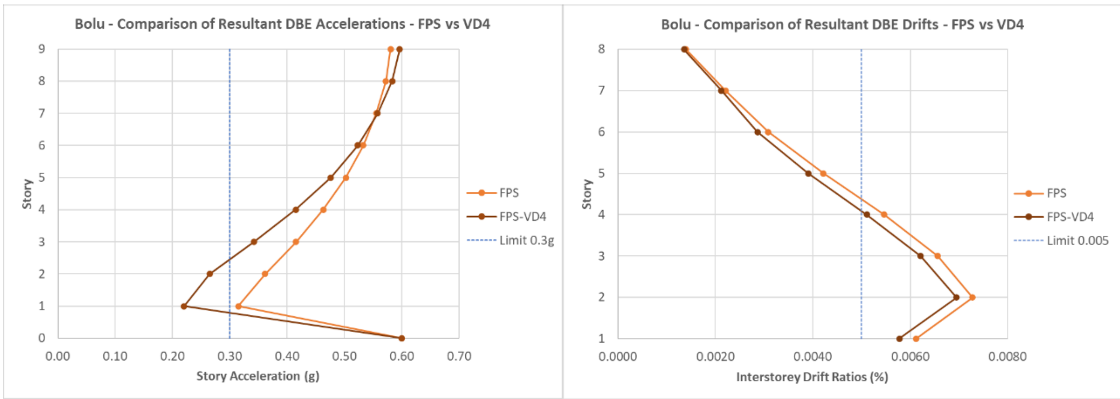

Figure 3.47 Comparison of accelerations and drifts for FPS and VD4 - Bolu

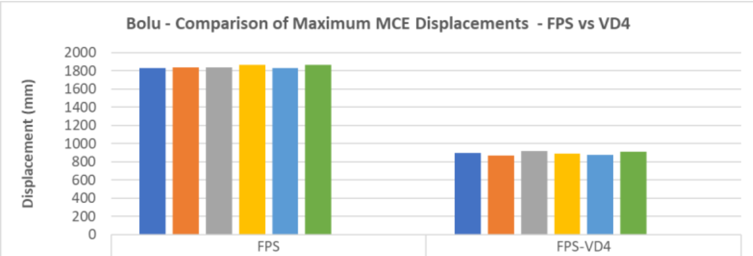

	FPS	FPS-VD4
P1	1832	894
P2	1839	870
P3	1840	915
P4	1862	891
P5	1832	876
C	1866	912
Max/Min	1.02	1.05
Reduction	0	0.51

P1 P2 P3 P4 P5 C Max/Min Reduction

Figure 3.48 Comparison of maximum displacements for FPS and VD4 – Bolu

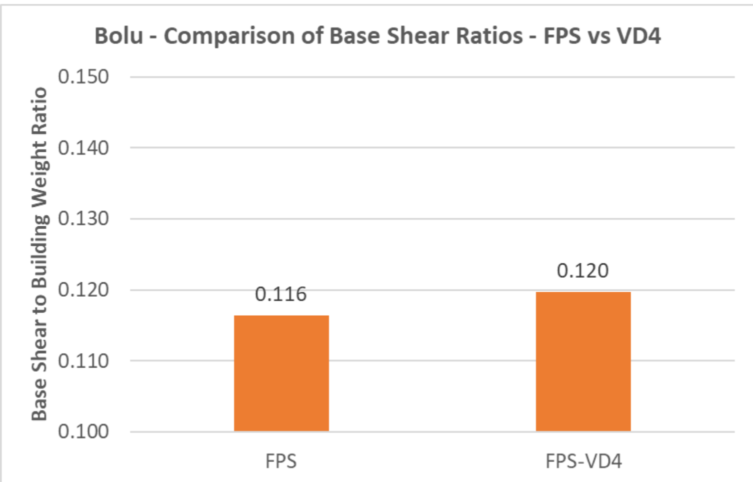

Figure 3.49 Comparison of base shear ratios for FPS and VD4 - Bolu

Story acceleration values tend to decrease for the first 5 stories and drift ratios are within the limits. Displacement demands are reduced to half; base shear increases very little.

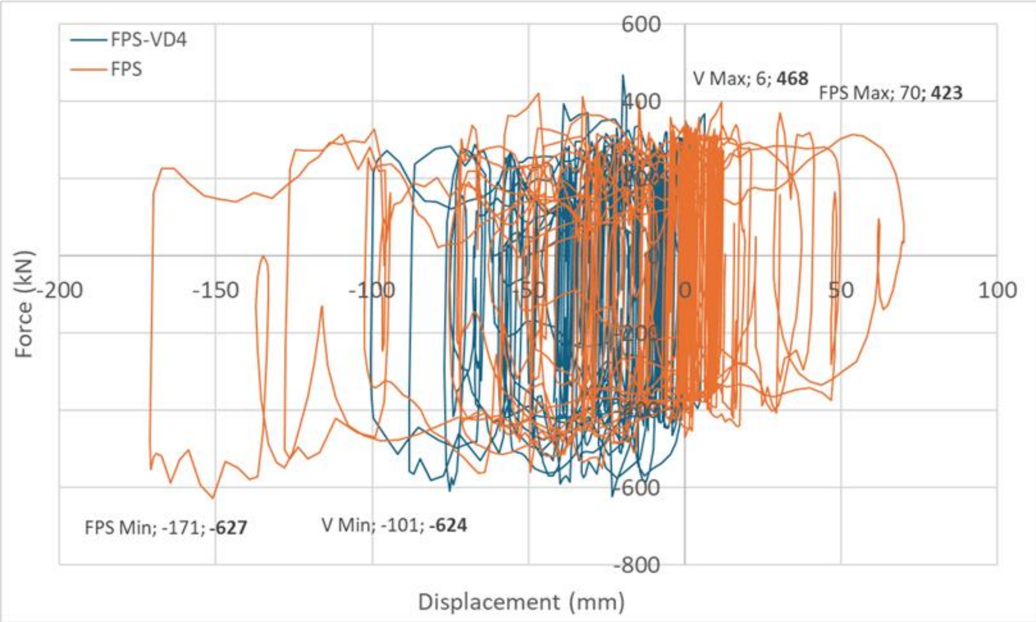

Figure 3.50 Comparison of Force-Displacement Behaviors for One Link – DBE UB

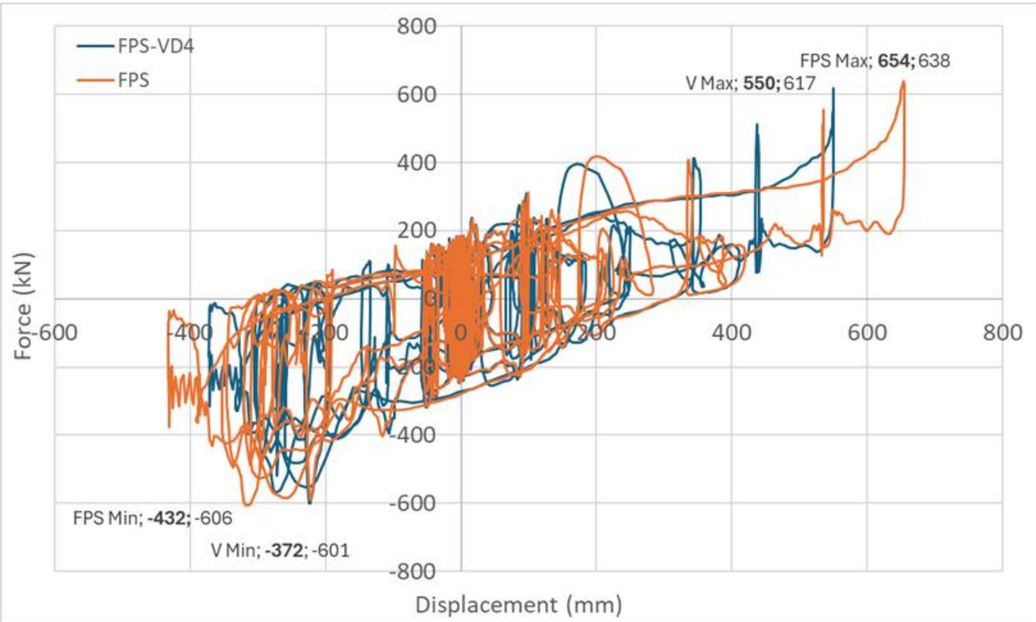

Figure 3.51 Comparison of Force-Displacement Behaviors for One Link – MCE LB

Table 3.24 Comparison of all results for FPS and VD4 - Bolu

	FPS **184 FPS**	**FPS-VD4** **184 FPS + 64 VD**	**Change (%)**
Max Acc (g)	0.58	0.6	3.45
Max Drift Ratio	0.0011	0.0011	0.00
Max Displacement (mm)	1862	912	-51.02
Displacement Ratio	1.02	1.05	2.94
Base Shear (W)	0.116	0.12	3.45

4. SUMMARY AND CONCLUSIONS

In this dissertation, three different base-isolated structures were considered; two of them are hospital buildings located in a highly seismic zone and one of them is a residential building. All three structures are designed with friction pendulum types of isolators. In addition to isolators, metallic dampers, and viscous dampers were added to the models. Modal analysis and non-linear time history analysis are performed, and all results are summarized in Chapter 3. Story accelerations, interstorey drifts, base shear ratios, and maximum isolator demands are examined and compared with original base-isolated structures, and an optimum case is selected. Based on the results, the following conclusions can be made to summarize the behavior of the structures with additional damping systems:

- In structures whose center of mass and center of gravity are not close, isolator displacement demands may differ from each other. Dampers added by paying attention to these centers can reduce the deviations in isolator displacement demands and ensure a more homogenous distribution of isolator displacement demands.
- Metallic dampers which are less stiff than isolators are more useful rather than stiffer ones. The fact that the damper has yielded before the isolator is activated provides a great advantage in base shear. It has been observed that the total base shear force is much higher in structures which have stiffer dampers and change in interstorey drift ratios will be higher with the structures have stiffer dampers.
- Adding dampers can cause the accelerations on the upper story to decrease. In connection with this, it may slightly increase story drifts but still structure can satisfy same performance level.
- Using dampers at certain positions instead of installing to all isolators placed in the structure will give the most effective results. If dampers are used in all isolators, shear force demands will increase largely and an economical design will not be possible. The ideal damper usage rate is around 20-30% of total isolators.
- By considering the same performance levels of the structure, it is possible to make a design that reduces the isolator displacement demands without affecting the superstructure by adding damper at isolation level.

- Adding a damper in addition to the isolator system is more suitable in projects with very large story areas, such as hospitals. Since the story area in residential type buildings is relatively small and sufficient rigidity cannot be provided, adding dampers can increase interstorey drifts much.

REFERENCES

AFAD (2018a) Turkish earthquake code for buildings. Disaster and Emergency Management Authority, Ankara, Turkey

Akyüz, U., Yakut, A., Çabuk, E., Sütçü, F., Murota, N., Suzuki, S., & Mori, T., Performance comparison of high-damping rubber isolators and friction pendulum isolators with different modelling approaches, METU/EERC 2020-02.

Atasever, K., Celik, O. C., & Yüksel, E. (2017, September 1). 11.50: Modelling hysteretic behaviour of U-shaped steel dampers. Ce/Papers. https://doi.org/10.1002/cepa.377

Alotta, G., Cavaleri, L., Paola, M. D., & Ferrotto, M. (2016, April 29). Solutions for the Design and Increasing of Efficiency of Viscous Dampers. The Open Construction and Building Technology Journal, 10(1), 106–121. https://doi.org/10.2174/1874836801610010106

Barrera-Vargas, C. A., Díaz, I. M., Soria, J. M. N., & García-Palacios, J. H. (2020, August 13). Enhancing Friction Pendulum Isolation Systems Using Passive and Semi-Active Dampers. Applied Sciences (Basel). https://doi.org/10.3390/app10165621

Buckle, I., Constantinou, M., Dicleli, M., & Ghasemi, H. (2006, August 1). Seismic isolation of highway bridges. https://hdl.handle.net/11511/81975

Castaldo, P. (2013, November 27). Passive Energy Dissipation Devices. Springer Tracts in Mechanical Engineering. https://doi.org/10.1007/978-3-319-02615-2_2

Cho, C. B., Kim, Y. J., Chin, W. J., & Lee, J. Y. (2020, November 20). Comparing Rubber Bearings and Eradi-Quake System for Seismic Isolation of Bridges. Materials (Basel). https://doi.org/10.3390/ma13225247

Christopoulos, C., & Montgomery, M. (2013, July 9). Viscoelastic coupling dampers (VCDs) for enhanced wind and seismic performance of high-rise buildings. Earthquake Engineering & Structural Dynamics, 42(15), 2217–2233. https://doi.org/10.1002/eqe.2321

Computers and Structures Inc. (2017). CSI Analysis Reference Manual.

Constantinou, M., & Whittaker, A. S. (2005, January 1). Building structures with damping systems: from research to design practice. www.academia.edu. https://www.academia.edu/15553228/Building_structures_with_damping_systems_from_research_to_design_practice

Constantinou, M. C., & Symans, M. D. (1993, June). Experimental study of seismic response of buildings with supplemental fluid dampers. The Structural Design of Tall Buildings, 2(2), 93–132. https://doi.org/10.1002/tal.4320020203

Ghobarah, A. (2001, August). Performance-based design in earthquake engineering: state of development. Engineering Structures, 23(8), 878–884. https://doi.org/10.1016/s0141-0296(01)00036-0

Hwang, J. S., Hung, C. F., Huang, Y., & Wang, S. J. (2010). DESIGN FORCE TRANSMITTED BY ISOLATION SYSTEM COMPOSED OF LEAD-RUBBER BEARINGS AND VISCOUS DAMPERS. International Journal of Structural Stability and Dynamics, 10(02), 287–298. https://doi.org/10.1142/s0219455410003440

Javanmardi, A., Ibrahim, Z., Ghaedi, K., Benisi Ghadim, H., & Hanif, M. U. (2019, March 1). State-of-the-Art Review of Metallic Dampers: Testing, Development and Implementation. Archives of Computational Methods in Engineering, 27(2), 455–478. https://doi.org/10.1007/s11831-019-09329-9

Jia J., A State of the Art Review Seismic Isolation Technology in Bridge Engineering, 2014

Joyner, W. B., & Boore, D. M. (1982). Estimation of response-spectral values as functions of magnitude, distance, and site conditions {abstract. Earthquake Notes, 53, 70.

Karimi M.R.B., Yaghin M.A., Nezhad R.M., Sadeghi V., Aghabalaie M., Seismic Behavior of Steel Structure with Buckling-Restrained Braces, International Journal of Civil and Environmental Engineering, 2015

Kelly, J. M. (1999). The role of damping in seismic isolation. Earthquake Engineering & Structural Dynamics (Print), 28(1), 3–20. https://doi.org/10.1002/(sici)1096-9845(199901)28:1

Li, H. N., Li, G., & Wang, S. Y. (2014, January 1). Study and application of metallic yielding energy dissipation devices in buildings. ResearchGate. https://doi.org/10.4231/D3FQ9Q593

Martinez-Rueda J.E., On the Evolution of Energy Dissipation Devices for Seismic Desing, Earthquake Spectra, Volume 18, No.2, pages 309-346, May 2002

MacKay-Lyons, R., & Christopoulos, C. (2012). ENHANCING THE SEISMIC PERFORMANCE OF RC COUPLED WALL HIGH-RISE BUILDINGS WITH VISCOELASTIC COUPLING DAMPERS.

Mokha, A., Constantinou, M., & Reinhorn, A. (1990). Teflon Bearings in Base Isolation I: Testing. Journal of Structural Engineering, 116(2), 438–454. https://doi.org/10.1061/(ASCE)0733-9445(1990)116:2(438)

Mualla, I. H. (2000). Experimental evaluation of new friction damper device. In 12th world conference on earthquake engineering, Auckland, New Zealand.

Mualla, I. H., & Jakupsson, E. (2010, January 1). A rotational friction damping system for buildings and structures. ResearchGate. https://www.researchgate.net/publication/288266253_A_rotational_friction_damping_system_for_buildings_and_structures

Murota, N., Suzuki, S., Mori, T., Wakishima, K., Sadan, B., Tuzun, C., Sutcu, F., & Erdik, M. (2021, April). Performance of high-damping rubber bearings for seismic isolation of residential buildings in Turkey. Soil Dynamics and Earthquake Engineering, 143, 106620. https://doi.org/10.1016/j.soildyn.2021.106620

Nakamura, Y., & Okada, K. (2019, June 3). Review on seismic isolation and response control methods of buildings in Japan. Geoenvironmental Disasters. https://doi.org/10.1186/s40677-019-0123-y

Naeim, F., & Kelly, J. M. (1999, March 5). Design of Seismic Isolated Structures. https://doi.org/10.1002/9780470172742

Nsengi, Nippon Steel Metallic Damper Specification

Nuraini S., Tambusay A., Suprobo P., A comparative study of base isolation devices in light rail transit structure featured with lead rubber bearing and friction pendulum system, MATEC Web of Conferences 195, 2018

Patil, S. J., & Reddy, G. R. (2012). State of art review-base isolation systems for structures. International journal of emerging technology and advanced engineering, 2(7), 438-453.

Soong T.T., Dargush G.F., Passive Energy Dissipation and Active Control, Structural Engineering Handbook, 1999

Soong T.T., Spencer Jr B.F., Supplemental energy dissipation:state of the art and state of the practice, Engineering Structures, 2002

Su L., Ahmadi G., Comparative Study of Base Isolation Systems, Journal of Engineering Mechanics, 1989

Symans, M. D., Charney, F. A., Whittaker, A. S., Constantinou, M. C., Kircher, C. A., Johnson, M. W., & McNamara, R. J. (2008, January). Energy Dissipation Systems for Seismic Applications: Current Practice and Recent Developments. Journal of Structural Engineering, 134(1), 3–21. https://doi.org/10.1061/(asce)0733-9445(2008)134:1(3)

Taylor Devices, Fluid Viscous Damper Specification

Xie, Q. (2005, June 1). State of the art of buckling-restrained braces in Asia. Journal of Constructional Steel Research. https://doi.org/10.1016/j.jcsr.2004.11.005